Phanerozoic cooling events in the continental rims of the Central Atlantic Ocean.

Rémi Charton, Delft University of Technology, Applied Geology, The Netherlands

Rémi Leprêtre, Geosciences Environment Cergy, CY Cergy Paris Université, France.

Keywords: Central Atlantic, cooling events, vertical movements, Low-Temperature Thermochronology, Time-Temperature Modelling

Appendix: An appendix is included at the end of this document

Contents

Abstract

In this review, we have digitized and georeferenced over 7000 Low-Temperature Thermochronology (LTT) data points and 750 Time-Temperature Modelling (TTM) results from 252 published works. The study area includes the continental crusts adjacent to the rifted margins (~Late Triassic to Early Jurassic) of the Central Atlantic Ocean and its direct neighbours.

Our main intention is to map out the thermal cooling events as recorded by LTT data and as illustrated by TTM results. The time interval targeted in this review is the Phanerozoic (i.e., 540 to 0Ma), which is possible thanks to LTT ages spanning this entire period in the study area. It allows us to investigate the thermal evolution of the continental rims of the Central Atlantic Ocean at an unprecedented scale. In rifted margins and their shoulders, a debate exists whether the LTT-recorded cooling is the results of post-rift erosional exhumation or post-heating thermal relaxation, especially for the area directly in the vicinity of the paleo-rift zone. We therefore devised a short workflow to examine these propositions by filtering out the LTT dataset and spatially plotting the LTT ages. Furthermore, we investigate the relationship between LTT ages and distance from the Continent-Ocean Boundary/Transition Zone.

LTT ages alone have often been described as bearing little geological meaning, thus requiring to run TTM in order to reconstruct the thermal/geological history, as several factors are to be taken into account in the thermal history reconstruction. Here, we examine whether a statistically significant LTT dataset can serve as a proxy in the reconstruction of cooling events. To this end, we compare peaks of LTT cooling ages and of TTM cooling event.

Our investigation reveals that i) generalised cooling occurred in the pre-, syn-, and post-rift phases of the Central Atlantic, ii) there is a clear LTT age oceanward youngening trend, iii) the lack of LTT age with a syn-rift signal within ~500km along the shorelines suggests erosional exhumation (i.e., vertical movements) as main driver of the cooling, and iv) large LTT datasets bear meaning on the cooling events and thus on vertical movements, at least in this case studies in the rims of the Central Atlantic Ocean.

1. Cooling and km-scale exhumation in passive margin shoulders

In the unstretched continental crusts adjacent to rifted passive margins (e.g., margins of the Atlantic, Indian, Southern, and Arctic Oceans), a wealth of Low-Temperature Thermochronology (LTT), sometimes associated with time-temperature modelling (TTM), have demonstrated the occurrence of substantial cooling in their pre-, syn- and early post-rift history, often accounted for in terms of km-scale vertical movements (i.e., exhumation and/or burial; e.g., Turner et al., 2008; Japsen et al., 2009; Japsen et al., 2012; Green and Machado, 2017; Leprêtre et al., 2017; Charton et al., 2021). LTT dating on apatite and zircon crystals potentially allows for the investigation of the cooling history of the upper part of the crust (e.g., Murray et al., 2018), which is the uppermost ~10km of the crust in regions characterised by a 'normal' geothermal gradient (***Fig. 1a;*** when considering apatite & zircon thermochronological systems). This characteristic helps geoscientists to unravel some complex geological histories from the Precambrian to the Present-Day. This tool, routinely used for more than two decades now, evidenced that the timing of the "vertical" movements in the can be unexpected or at odds with regional geodynamic events (e.g., Barbarand et al., 2001; Withjack and Schlische, 2005; Ghorbal et al., 2008).

In the case of the passive margins, the precise temporal relationship(s) between exhumation/cooling events as evidenced via LTT and TTM studies and the syn-/post-rift phases is key for determining and constraining the responsible mechanism(s). This is important for their associated thermal signature and erosional pattern(s) at the millions of years temporal scale, otherwise only accessible through numerical modelling, and that in both the thinned rifted crust and the "stable" adjacent continental crusts (***Fig. 1b*** and ***c***). To date, these vertical movements remain largely debated and/or enigmatic in passive margin shoulders, as exemplified with the 'anomalous' and 'unexpected' km-scale vertical movements in Mauritania (Gouiza et al., 2019). Many hypotheses have already been submitted that account for large-scale (e.g., dynamic topography, far-field stresses with crustal to lithospheric wavelength, climate variations, and eustasy) and regional/local-scale (e.g., orogeny, fault movements, fluvial/marine incisions, localised thermal doming, uplifted-shoulder, etc…) processes (e.g., Green et al., 2018; Amidon et al., 2016; Oukassou et al., 2013; Bertotti and Gouiza, 2012) Regarding these processes, we thus lack consensus about both the triggering mechanism(s) for and consequently what are the conditions maintaining or shutting of these "anomalous" vertical movements. For instance, in the rifted margins and their continental shoulders, a debate exists whether the LTT-recorded post-rift cooling is the results of post-rift erosional exhumation or post-rift thermal relaxation of the syn-rift heating signature (e.g., Green et al., 2018; Barbero et al., 2007, respectively).

A note on the terminology is necessary at this point. Exhumation is the removal of the rock column above any chosen buried surface (Ring et al., 1999). Denudation is the regional erosional process leading to the removal of rocks at the surface of the Earth. The investigation of exhumation includes tracking that surface (and its rocks) through their material path, typically until their present-day position at the surface of the Earth. It is therefore a relative vertical movement, as it only constraint the removal of overburden, and not an uplift of Earth's surface for instance, and is recorded by LTT measurements as cooling. Erosional exhumation cannot directly be translated into rock nor surface uplift (e.g., Malùsa and Fitzgerald, 2019), without prior knowledge of one or the other (England and Molnar (1990; equation 1).

$$\text{Surface uplift} = \text{uplift of rock} - [\text{erosional}]\ \text{exhumation}$$

Equation 1 | Uplift and exhumation relationship, modified after (England and Molnar, 1990).

It is commonly accepted that uplift will lead to erosional exhumation because of the generated topography. Nevertheless, there are cases where erosional exhumation will occur without uplift such as marine regression exposing new surfaces to erosion, or in the case of the footwall of a normal fault (tectonic exhumation for rocks under the exposed fault plane and erosional exhumation away from the fault plane because of the created topography). In LTT studies, authors combine geological and radiometric evidences - which are considered as 'constraints' - to interpret the cooling events recorded by the LTT data as linked to thermal relaxation, erosional exhumation, or tectonic exhumation (Malùsa and Fitzgerald, 2019).

Because these not-fully-understood relative vertical movements occurred 1) in the vicinity of the future rift valley (pre-rift), 2) adjacent to the rift zone (syn-rift), and 3) in the passive margin (post-rift), many authors have speculated and sometimes tested the relationship between the exhumation events and the rifting/drifting tectonics (e.g., Leroy et al., 2008; Amidon et al., 2016; Leprêtre et al., 2017; Charton et al., 2018; Gouiza et al., 2019; Malùsa and Fitzgerald, 2019). For instance, using AFT datasets collected near margins elsewhere than around the Central Atlantic, Gallagher and Brown (1997, 1999) observed, 1) a differential erosion rates from the coastal plain to the hinterland, 2) a break-up signature is superimposed/removed because of long-lasting erosion, 3) variability between the erosion and morphology across studied margins, and 4) pre-/syn-rift regional structural features reactivated in the post-rift phase, linked to large scale processes. They concluded that there are no simple models applicable to use directly these data in order to solve the problem of the erosional evolution of the margin from coastal plain to hinterland.

In the Central Atlantic Ocean (CAO) rims (***Figs. 1C*** and ***2***), as is documented locally in LTT/TTM studies reviewed in this contribution and sometimes synthetized for large regions (e.g., Ye et al., 2017; Charton et al., 2021), there is no consensus on the evolution of the unstretched continental crusts adjacent to rifted margins that are characterised by minor to substantial differences from their recorded pre- to/and post-rift cooling history. Many LTT/TTM studies conducted around the CAO evidenced syn- to post-rift cooling. Two studies proposed to explain the syn-rift cooling in terms of erosional exhumation linked to rift shoulder uplift (Ruiz et al., 2011 on the African side; Tremblay et al., 2013 on the American side). For early post-rift LTT cooling ages, some authors have argued that the rift thermal signature outreached its rift zone (e.g., Barbero et al., 2007; Gouiza et al., 2017a). This out-of-bounds thermal perturbation would have affected the geothermal gradient of the continental crust, resulting in a reset of the LTT ages followed by a post-rift thermal relaxation (Malùsa and Fitzgerald, 2019). Some other authors have proposed large-scale mechanisms, with intervening far-field/intra-plate stresses (e.g., Gouiza et al., 2017a), enhanced erosion by base level change/climatic/landmass position change (e.g., Amidon et al., 2016, Shorten and Fitzgerald, 2019), and/or dynamic topography (e.g., Taylor and Fitzgerald, 2011; Leprêtre et al., 2017), either superimposed to rifting thermal perturbation or simply as the sole responsible process for recorded early post-rift cooling event.

This review focuses on the rims of the CAO (***Fig. 2***) for several fundamental and practical reasons: a) it is the ocean with the oldest oceanic crust that has not been subducted, meaning unravelling the exhumation history for this ocean passive margins can prove an example for more recent settings and predict their future evolution; b) the mechanism(s) behind the exhumation/burial events, their timing, amplitude and wavelength, as well as their precise expression at the surface (landscape evolution, source-to-sink system) have not been well-constrained there regionally, let alone at the scale of each bordering country and c) there are over 3000 LTT data points on each side of the CAO, and in both sides, they are interestingly distributed up to 2000 km from the coasts, amounting to a dataset of over 6000 LTT and over 700 TTM data points, compiled for this study. Note that both datasets compiled for this work (LTT and TTM) thus relate to cooling and not depth.

For this review, we have compiled a LTT dataset, encompassing zircon and apatite helium and fission-tracks dating methods (i.e., ZHe, AHe, ZFT, and ZHe, respectively) for the rims of the CAO. Examples of similar database constructions have been published for Canada (AFT; Kohn et al., 2005; Pinet et al., 2020), Scandinavia (AFT and AHe; Hendriks et al., 2007), the World (ZHe, AHe, ZFT, and ZHe; Herman et al., 2013; lacking several thousand points in this work study area), Japan (ZHe, AHe, ZFT, and ZHe; Sueoka and Tagami, 2019), Iberia (AFT and ZFT; Rat et al., 2019), and Central America (ZHe, AHe, ZFT, and ZHe; Gray et al., 2020), to cite only a few. No similar TTM dataset of digitized curves is known to us, except for Charton et al. (2021).

This review treats first with the construction of this database and the way data are digitized when available, presented, and filtered. Second, with this wealth of data at hand, this review aims at 1) establishing the large-scale distribution of LTT ages in the continents that were joined prior to the Central Atlantic rifting (in early Triassic times), and were affected by the Triassic rift system, 2) evidencing potential relationships between LTT ages and the distance from the rift zone or the absence thereof, 3) answering whether LTT data alone (i.e., without TTM), when compiled in large datasets, can be used safely as a readable tool (qualitatively and/or quantitatively) for such long-lasting vertical motions around one main geodynamic event that is the CAO opening, and 4) illustrating the cooling events along the rims of the Central Atlantic Ocean through time starting in the pre-rift phase, for both LTT and TTM, in order to study their consistencies with geodynamic events at first order and then with higher precision for selected times and places.

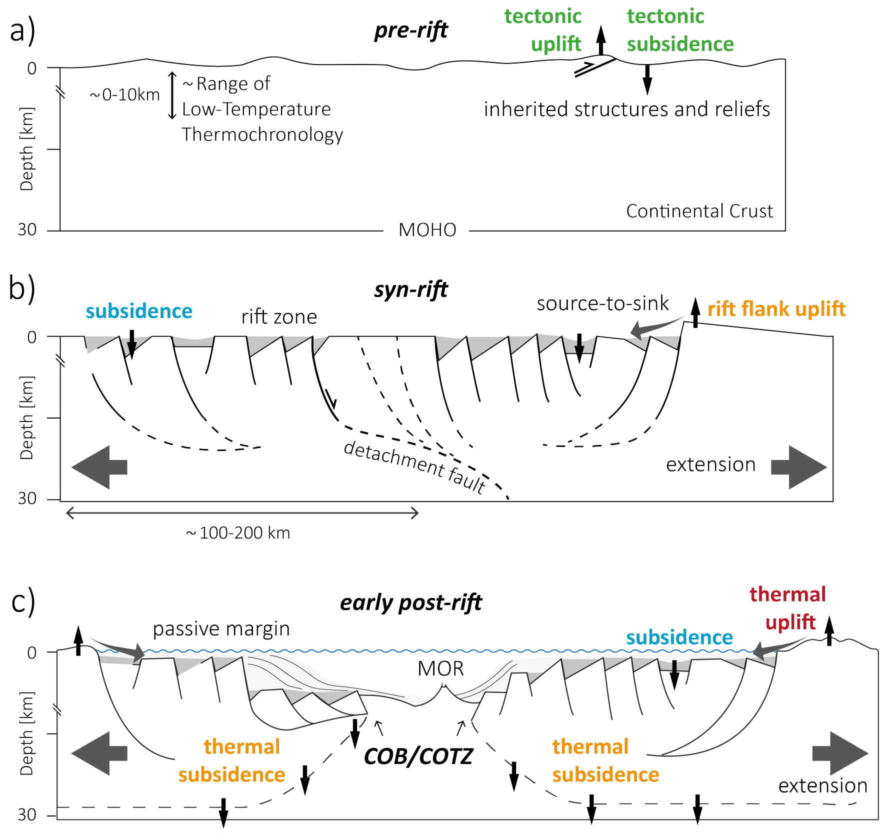

Figure 1 | Highly simplified cross-sections illustrating the development of an ocean (after Gouiza, 2011) for the **a)** pre-, **b)** syn-, and **c)** early post-rift phases. Expected thermal events and vertical movements after Leeder (2006; subsidence), Watts (2012; thermal subsidence), Leroy et al. (2008; thermal uplift), Olsen (1995; flank uplift), and Teixell et al., (2009; tectonic uplift/subsidence). *MOR* = Mid-Oceanic Ridge; COB/COTZ = Continent-Ocean Boundary/Transition Zone.

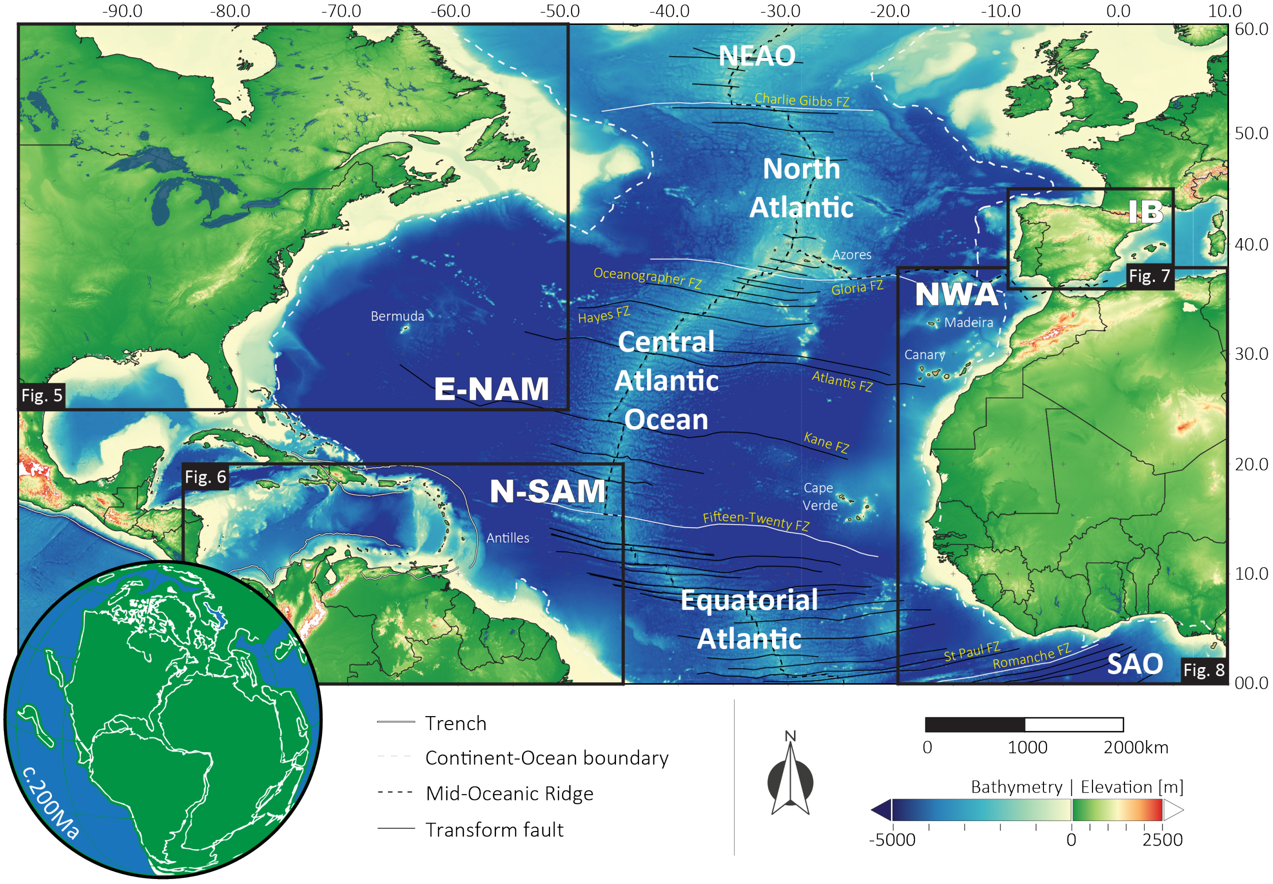

Figure 2 | Bathymetric map of the Central Atlantic Ocean, its conjugate margins, and adjacent oceanic and continental domains (geological Atlantic Ocean limits after Biari et al., 2021; elevation data GEBCO_2014_1D). *FZ* = Fault zone; *NEAO* = North East Atlantic Ocean; *SAO* = South Atlantic Ocean. Insert: Sketch of the Plate reconstruction at c. 200Ma (after Müller et al., 2016). The Continent Ocean Boundary illustrate the location of the continent-ocean transition zone. *E-NAM* = Eastern North America; *N-SAM* = North South America; *IB* = Iberia; *NWA* = North West Africa.

2. Central Atlantic geological history

This section draws the main lines of the evolution of the Central Atlantic Ocean (CAO) domain, from the Palaeozoic to the Cenozoic. Strictly speaking, in the present-day configuration (***Fig. 2***), the CAO represents the oceanic domain located between the Gibraltar-Azores-New Foundland (Gloria) fault zone in the north and the Guinea/Fifteen-Twenty fault zone in the south (e.g., Biari et al., 2021). These fault zones separate the CAO from the North and Equatorial Atlantic branches, respectively. On both passive margins of the CAO, remnants of various Palaeozoic orogenies are outcropping and complementary. They follow structural directions that are generally close to the main orientation of the oceanic ridge. Then, the Mesozoic witnessed the rifting and opening of the CAO, where the oldest oceanic rocks of a present-day existing ocean are recorded on earth.

2.1. Pre-rift: Variscan and older orogens

The building of the now stacked Palaeozoic orogenic system (***Fig. 3***) on both sides of the CAO is the consequence of two phenomena: the dismantling and subsequent squeezing of the extended Laurentian margin and the drifting away of Gondwana-related terranes that successively accreted to the Peri-Laurentian margin (van Staal et al., 2009; Hatcher et al., 2010). The interlocking of the different terranes along the US and Canadian passive margin thus reflects this succession of events. From west to east, the different terranes are the Peri-Laurentian terranes (Humber and related margins) on one hand, and the Ganderia, Avalonia/Carolinia and Meguma terranes on the other hand, that derived from Gondwana. Each one is characterized by sedimentary, metamorphic, and magmatic events that gave them their own characteristics and enable the reconstruction of a chronology of the orogenies (van Staal et al., 2009; Hatcher et al., 2010; Michard et al., 2010; van Staal and Barr, 2012). A succession of different orogenies thus happened, from the Ordovician to the Carboniferous, witnessing the growth of the Laurentian margin, at the expense of successive oceanic domains (e.g., Hibbard et al., 2010).

The westernmost collage along the Laurentia margin occurred during the Early to Middle Ordovician, with the closure of a narrow oceanic space between Laurentia and the ribbon-like microcontinent of Dashwoods, namely the Taconic seaway, thus developing the Taconic orogeny. After this first accretion event, the Gondwana-related terranes will collide against the Laurentia margin up to the Devono-Carboniferous and the final formation of the Pangaea. The two terranes of Ganderia and Avalonia were respectively accreted during the Early Silurian and Late Silurian-Early Devonian while consuming the Iapetus oceanic domain. The Meguma terrane was later incorporated within the system, bounded by the Laurentia composite margin and the Variscan-Alleghenian system developing at the time between Middle Devonian to Mississippian (i.e., to Early Carboniferous; Hibbard et al., 2010; van Staal and Barr, 2012). The final closure of the Rheic ocean between Laurentia and NW Gondwana (future Senegal-Mauritania-Morocco area) occurred later, probably during Pennsylvanian times, according to the ages of the earliest contractional events recorded in Morocco (e.g., Chopin et al., 2014; Wernert et al., 2016; Delchini et al., 2018; Martínez-Catalán et al., 2021).

Within the latest stages of the Alleghenian-Variscan orogeny, intense magmatic activity is recorded within NW Africa and Western Europe (e.g., in Morocco: Mrini et al., 1992; Gasquet et al., 1996; El Hadi et al., 2006; Chopin et al., minor revisions; e.g., in W. Europe: Gutierrez-Alonso et al., 2011; Vanderhaeghe et al., 2020). There, the latest Permian orogenic pulses occurrences are dated at c.265Ma in the Meseta domain (Leprêtre et al. 2022; Chopin et al., minor revisions), whereas slightly more recent magmatism has been recognized in the Anti-Atlas domain at c.260 Ma (Najih et al., 2019), attributed to indicative signs of Pangaea dislocation.

On the American side, a temporally widespread plutonic activity is recorded, spanning a similar time range from post-330Ma up to the Permian (Sinha and Zietz, 1982; Hatcher, 1989). In any cases, these magmatic activities ended well before the beginning of the Triassic rifting and long before the Central Atlantic Magmatic Province (CAMP) emplacement around the Triassic to Jurassic transition (***Fig. 4***). At present day, the Rheic suture position between N America and NW Africa is not known. Several recent geochronological studies pointed out that the CAO opened in between different Gondwana-derived terranes (Kuiper et al., 2017; 2021) and that the Variscan-Alleghenian suture lies westwards of the Mazagan escarpment. So far, no Rheic suture could be find within the Late Palaeozoic belts (Michard et al., 2010; Bea et al., 2020; Kuiper et al., 2021). Thus, the CAO probably opened while reworking the Alleghenian suture. This structural inheritance is likely not directly associated to thermal inheritance. As we wrote above, important plutonic activity on both future Atlantic sides occurred until Mid-Late Permian (270-255 Ma) and no more important magmatic event occurred before the volcanic CAMP event.

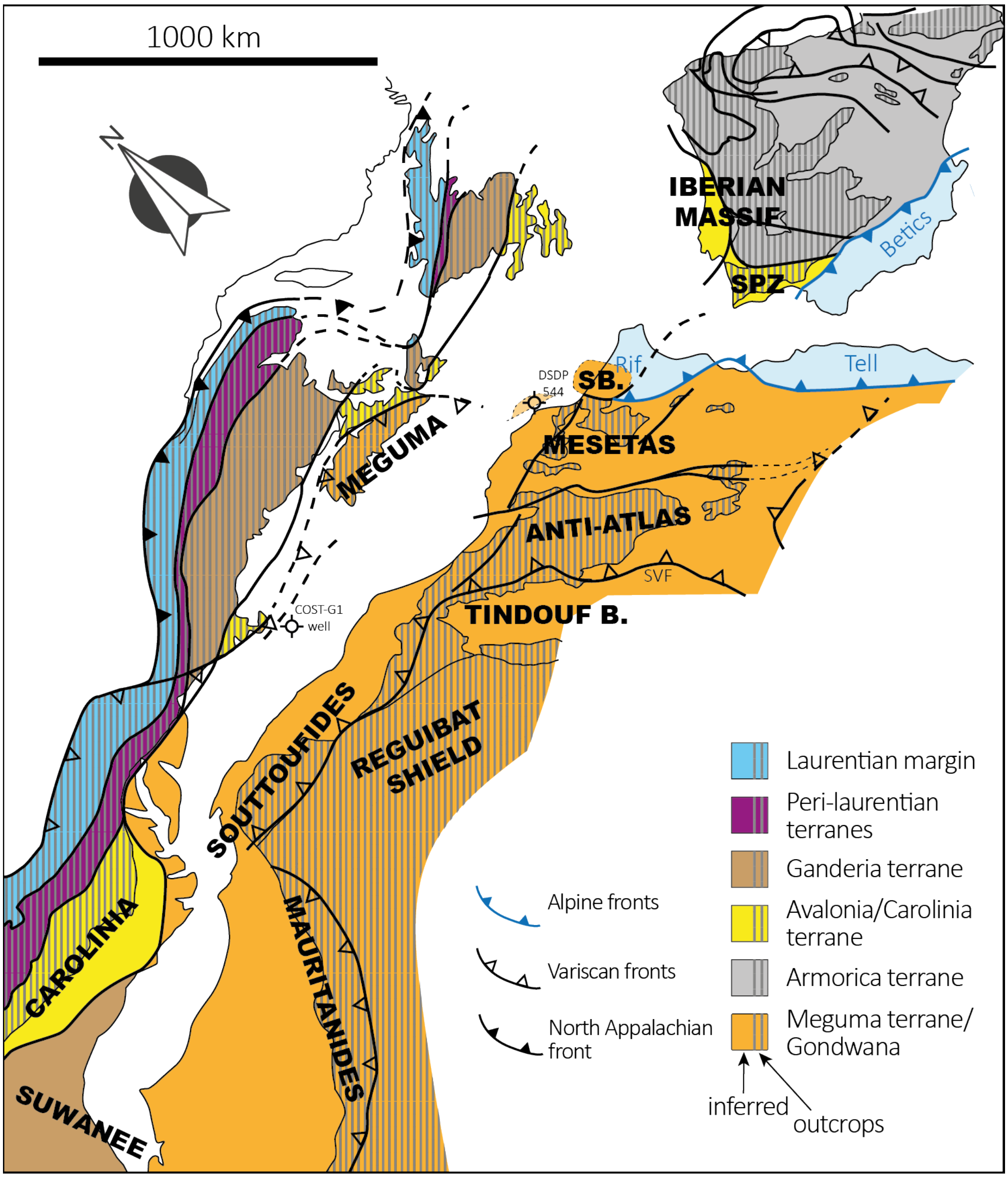

Figure 3 | Distribution of terranes around the Central Atlantic Ocean in the pre-rift phase after Martinez-Catalan et al. (2002), Simancas et al. (2005), Caby and Kienast (2009), Hibbard et al. (2010), Kuiper et al. (2017), and van Staal et al. (2020).

2.2. Syn-rift: Triassic to Early Jurassic

In short, the Mesozoic began first with a widespread and diffuse rifting event during the Triassic. This rifting event is topped by a short-lived mega-regional magmatic event before the occurrence of Pangaea break-up during the Early Jurassic.

2.2.1. Triassic rifting and CAMP

The overall Triassic rift system has been reviewed by Leleu et al. (2016) specifically for the Central Atlantic system. The Triassic rifting events, that allowed the development of continental fluvial to lacustrine paleo-environments, occurred through a protracted 35 Myr period, between the Ladinian to the Rhaetian. The final sedimentary sequences are showing significant salt deposition within restricted paleo-environments that will have important halokinetic activity later on (e.g., Tari and Jabour, 2013; Pichel et al., 2019; Uranga et al., 2022). The salt basins are widely developed in the northern CAO, offshore Nova Scotia and Morocco (***Fig. 4***). These rift basins extended from Florida (USA) to Newfoundland (Canada) with the segment between Nova Scotia (Canada) and north Morocco developing first as soon as the Anisian (Middle Triassic), whereas other branches developed from the Ladinian (Middle Triassic) onwards. They developed laterally to up to few hundred km-wide rifts across both North America and West Africa (e.g., in N. America: Schlische, 1993; Withjack et al., 1998; 2020; e.g., in NW. Africa: Hafid, 2000; Le Roy and Piqué, 2001; Escosa et al., 2021). The significant width of this rift system was only locally controlled by bounding faults, reactivating former structures, but is probably more the expression of a mega-regional subsidence that stems from lower crustal-flow within a high heat-flow regime at the time. This kind of wide rift architecture detailed by Leleu et al. (2016) is in agreement with models involving a weak crust, preventing the location of the deformation in narrow rifts (e.g., Huismans and Beaumont, 2014).

Around the CAO - across South America, Africa, North America and Western Europe - Triassic and older rocks are either cross-cut or capped by basalt flow, dykes or sills of the Central Atlantic Magmatic Province (CAMP; ***Fig. 4***), which belongs to the LIPs (Large Igneous Provinces). This short-lived magmatic event occurred within a restricted time-window around 200 Ma (Marzoli et al., 1999; Nomade et al., 2007), with a peak activity around 200 ± 1 Ma and a time span that could last c.10 Myr (Marzoli et al., 2017). This magmatism event is showing geochemical characteristics close to the MORB-types, and points out toward an upper depleted mantle source (e.g., Callegaro et al., 2014; Marzoli et al., 2017; Gimeno-Vives et al., 2019), involving a low fusion rate and a subsequent relatively low crustal contamination (< 10%), while asthenospheric contributions are expected for certain regions (Merle et al., 2011). The CAMP magmatism occurred in the final stages of the rifting events and is either on top of the salt deposits or being interbedded with them (Tari and Jabour, 2013). Let us add here that, at a first order, the CAMP does not seem to follow a clear pattern along the different rims of the future CAO (***Fig. 4***). The CAMP appears widely distributed over a geographical area that exceeded the future CAO passive margins domains, which would make it unlikely to be explain assumed differential vertical motions along strike of the passive margins. Yet, Boscaini et al. (2022), who worked on the CAMP sub-province of West Africa, suggested that the cratonic keels could play a role in the localization of the magmatism, mainly along the cratonic borders. Following this observation, it could bear significant implications for the modifications it had on the crust and lithosphere compositions, and thus thermal structure, for the future passive margins of the CAO.

The occurrence of the CAMP at the end of the Central Atlantic Triassic rifting must be underlined here. Indeed, following Frizon de Lamotte et al. (2015) line of thoughts, the temporal relationship between the CAMP and the Triassic rifting could be suggestive of a passive rifting where the magmatism was initiated thanks to the long-protracted extension, in turns leading to a lithospheric thinning. The resulting CAMP-related regional doming, in places, could thus explain the erosional unconformity that developed in many Triassic basins (e.g., Withjack et al., 1998; Leleu et al., 2016).

2.2.2. Early Jurassic and the breakup of Pangaea

The uppermost rift-related deposits, together with the CAMP magmatic rocks, are overlain by an important unconformity that is recorded on both sides of the CAO, often put in relation with the CAO opening in regional studies (e.g., Frizon de Lamotte et al., 2008; Tari and Jabour, 2013; Withjack et al., 2020). While this surface has been recognised and studied, the precise timing of the onset for the CAO opening remains, to date, an open question.

The CAO opening age estimations range between 195 and 170 Ma (see review in Labails et al., 2010). The precise timing of the break-up is problematic because the age of the oldest magnetic isochron in the CAO is the M25 anomaly, which is dated at 154.5 Ma (Gradstein et al., 2004; Bird et al., 2007 and references therein). Toward the Eastern America passive margin, two additional magnetic lineaments are known for a long time, namely the Black Spur Magnetic Anomaly (BSMA; ***Fig. 4d***) and the East Coast Magnetic Anomaly (ECMA). The age of the BSMA, of oceanic nature, is suggested to be c.170 Ma (Early Bajocian, Middle Jurassic) obtained from a time constraint down the DSDP 534 scientific well (Sheridan, 1974; 1983; Sheridan et al., 1993), whereas the ECMA is not dated. On the West African side, the precise recognition of time-equivalent magnetic anomalies that could be fit with the BSMA and ECMA have been debated for several decades already (reviewed in Labails et al., 2010). The tracking of African time-equivalent of BSMA and ECMA magnetic anomalies is crucial here since they could be used in plate tectonic reconstructions to determine the closure position of the continental masses at the time of break-up.

The changing interpretations of the magnetic anomalies on the African side conditioned the proposed kinematic models since the paper of Klitgord and Schouten (1986). There, the ECMA and West African Coast Magnetic Anomaly (WACMA) were modelled to, after a first low-spreading stage from 175 to 170 Ma, form a proto-Atlantic oceanic crust that is preserved between the ECMA and BSMA, and where a ridge jump occurred around 170 Ma. This view has been also defended by Schettino and Turco (2009) more recently. Criticisms on this model have been given by Sahabi et al. (2004) and Labails et al. (2010) who reinterpreted the geophysical record to propose the existence of a consistent WACMA anomaly and an equivalent to the BSMA on the African side, respectively. The use of these reinterpretations led them to suggest that break-up was much older, occurring at around 190 Ma, with a first stage of low-spreading rate and asymmetrical formation of oceanic crust up to the Early Bajocian (Middle Jurassic). Apart from geophysical arguments, geological observations from the two margins suggest that syn-rift activity was over by the end of Triassic-Early Jurassic (e.g., Klitgord et al., 1988; Welsink et al., 1989; Withjack et al., 1998; Hafid, 2000; Le Roy and Piqué, 2001;

Sibuet et al., 2012), suggesting that plate-distributed extensional stresses stopped, possibly due to break-up. The absence of good-quality and reliable borehole-calibrated seismic profiles in the deep offshore of the African and American margins at the Ocean-Continent Transition still impedes a precise conclusion on the age of the break-up. In the following, we will keep in mind the wide range of 190 to 175 Ma for break-up, although – for us – the interpretations of Labails et al. (2010), in addition to the geological field and seismic evidence are in favour of the "older" model with a 190-185 Ma break-up age.

2.3. Early Post-rift: Middle Jurassic to Early Cretaceous

The post-rift period is characterized on the offshore passive margin by important sedimentary accumulations whose nature changed in the end of Jurassic/Early Cretaceous in the northern CAO. Good syntheses of the compared offshore records of conjugate margins were realized by Jansa and Wiedmann (1982) or Sheridan and Grow (1988). An update on the African side can be found in Davison (2005) and on the American side in Miall et al. (2008). For the considered stratigraphic record on both passive margins, significant N-S sedimentary differences must be noted (e.g., Jansa and Wiedmann, 1982). For most of the post-break-up Jurassic series, the offshore margins are generally witnessing carbonate build-ups at least up to the end of Middles Jurassic. Some clastic influences can be detected in the northern segment of NE America, with proximal deposits on the margin being clastic and laterally evolving toward the carbonate platform (Jansa and Wiedmann, 1982). After more and more clastic influences during the Late Jurassic, the northern CAO passive margins (north of Blake Plateau and north of Senegal Basin) are showing a significant transition toward a clastic sedimentation on both sides that largely by-passed the former platform edge. It is exemplified by the setting of km-thick Lower Cretaceous deltaic systems on the northernmost parts (Morocco and Nova Scotia) as shown by Heyman (1989) or Wade and McLean (1990). By contrast, the southern CAO passive margins witnessed a generally continuous carbonate sedimentation up to the Aptian (e.g., in W. Africa: Davison, 2005; Brownfield and Charpentier, 2003; e.g., in E. America: Jansa, 1981; Poag, 1991).

In terms of tectonic setting, the CAO post-rift period witnessed some important geodynamic changes. To the north of the Gibraltar-Azores-Newfoundland Fault zone, kinematic studies suggest slow rates of extension since the Early Jurassic between Newfoundland and Iberia, accelerating at the Late Jurassic-Early Cretaceous transition (c.145 Ma; see Nirrengarten et al., 2018 for a review). At the time, the cessation of oceanic accretion in the Maghrebian Tethys between Iberia and north Africa made them move subsequently together eastward. At the same time, the CAO continue to open and the southern North Atlantic Ocean experienced a northward propagation of hyper-extension, mantle exhumation and beginning of oceanic accretion before Albian (Nirrengarten et al., 2018). To the south, toward the future site of the Equatorial Atlantic Ocean, Ye et al. (2017) proposed that rifting-related crustal thinning and normal faulting progressed eastward, from the Valanginian to the Aptian (Lower Cretaceous), before connexion with South Atlantic branch was made. Within this extensional context, several rifted branches opened through Equatorial Africa from the Neocomian to the Albian (Lower Cretaceous; Guiraud and Morin, 1992; Frizon de Lamotte et al., 2015). In western Africa, these rifted branches often re-used former inherited structural directions, mainly from the Pan African cycle (Guiraud and Morin, 1992). Tectonic activities have been documented to reach as far as the Hoggar Mountains, re-using the West African Craton/Tuareg Shield limit and some Tuareg Shield fault zones.

During the Middle Jurassic-Early Cretaceous post-rift period, the onshore NW Africa and NE America are now known to have experienced post-rift uplifts (e.g., in NW Africa: Ghorbal et al., 2008; Saddiqi et al., 2009; Ruiz et al., 2011; Oukassou et al., 2013; Leprêtre et al., 2015, 2017; Sehrt et al., 2017, 2018; Charton et al., 2018; Gouiza et al., 2017a, b, 2019; e.g., in NE America: Wang et al., 1994; Roden-Tice et al., 2000;Spotila et al., 2004; Reed et al., 2005; McKeon et al., 2013; Shorten and Fitzgerald, 2019; Withjack et al., 2020). Post-rift cooling – generally attributed to erosional exhumation and/or uplift – occurred from the Mid-Late Jurassic to the Neocomian (Cretaceous), with varying rates, more or less at the time of sedimentation changes from a carbonate-dominated to siliciclastic-dominated type in the northern CAO. This is well-exemplified within the interior of the northern West African Craton (WAC)/Tuareg Shield where a general hiatus exists from the Late Palaeozoic up to the Early Cretaceous (Fabre, 2005; Leprêtre et al., 2017; Ye et al., 2017). By contrast, the southern WAC is mainly considered as having behaved as a paleohigh (Ye et al., 2017), characterised by very slow denudation since the onset of CAO rifting, enabling the continuous development of Jurassic-Early Cretaceous carbonate platforms on the African side.

North of the WAC, in Morocco, this uplift/erosional event is also well-recorded with a general sedimentary hiatus between the Middle to Late Jurassic and the Aptian-Turonian (Lower to Upper Cretaceous; Charrière and Haddoumi, 2016) and the establishment of deltaic system feeding both the Atlantic rifted margin but also the NE Maghreb (Delfaud, 1974; Vila, 1980). This N-S duality at the WAC scale is not so well-detailed on the eastern North American side in the onshore record, nor in the presently offshore one. Still, exposure of onshore geology shows unconformable mid-Late Cretaceous rocks, on top of the deformed Palaeozoic deposits overlain by remnants of Triassic rifted basins (Reed et al., 2004). Unfortunately, these rocks are mainly localized in the SE of the United States and does not extend northward where mainly Palaeozoic rocks are accessible as outcrops. Precise paleo-environmental maps of the near offshore with relationship with the onshore record are crucially lacking along the eastern North America passive margin.

2.4. Post-rift: Late Cretaceous to Present-Day

The major event recorded in the Mid-Late Cretaceous times, while the CAO accretion continued, is the eustatic maximum of the Cenomanian-Turonian (early Late Cretaceous) that is well-expressed in NW Africa all along the margin (Jansa and Wiedmann, 1982; Davison, 2005) but also along East America (e.g., Jansa and Wiedmann, 1982; Poag and Valentine, 1988). In NW Africa, particularly north of the WAC and W Maghreb, the Cenomanian-Turonian transgression penetrated very far within the continent interior (Vila, 1980; Frizon de Lamotte et al., 2008; Leprêtre et al., 2015; Ye et al., 2017; Abioui et al., 2019). By contrast, in NE America, the transgression from CAO did not extend west to northwestward within the continent interior (e.g., Ford and Golonka, 2002), and was more expressed toward the south, in the future Gulf of Mexico (Snedden et al., 2016). In a general way, the sedimentation remained relatively shaly for the Late Cretaceous, with for instance some exceptional source rocks along the NW Africa margin (Davison, 2005). In Ye et al. (2017) maps, a net difference is visible and persisted between the north and the south African margins, with a more continental-dominated sedimentation in northern Mauritania throughout the Late Cretaceous. In NE America, by contrast, marine carbonate sedimentation expanded southwards, down to Florida, whereas along the northern segments, sedimentation remained generally siliciclastic (Poag & Valentine, 1988; Gradstein et al., 1994).

In general, the Late Cretaceous deposits on both passive margins were related to the high-stand sea-level during this period with different transgressive pulses (Miller et al., 2005). On the American side, an important unconformity is often recognised between the Paleogene and Cretaceous deposits and numerous hiatuses are present within the Cenozoic stratigraphy, generally related to the sea-level variations (Poag and Valentine, 1988). Along the NE America margin, a Miocene-onwards rejuvenation of the Appalachian Mountains is attested by geomorphology, low-temperature thermochronology, and the mass balance between offshore/onshore domains (Poag and Sevon, 1989; Pazzaglia & Brandon, 1996; Gallen et al., 2013; Miller et al., 2013; McKeon et al., 2013; Amidon et al., 2016; Shorten and Fitzgerald, 2019). The origin of this rejuvenation that fed the margin is still debated.

On the NW African side, in the offshore domain of northern Morocco, Hafid et al. (2006) showed truncated portions of the inverted Mesozoic structures through erosion from the Late Cretaceous to the Neogene, in relationship with the Atlas Orogeny. Offshore southern Morocco, an erosional episode cut through the Paleogene down to the Early Cretaceous (Wiedmann et al., 1982; Hafid et al., 2008) that might be assigned to far-field stress effects of the Atlas orogeny (Leprêtre et al., 2015).

Around Senegal and Guinea, a general unconformity is recorded at the Late Cretaceous/Paleogene transition mostly during the Maastrichtian, for its low-stand sea-level (Davison, 2005; Miller et al., 2005). Later on, the Oligocene-Miocene is generally observed resting unconformably on top of the older series, also because of low-stand sea-level, whereas transgressive trends during Palaeocene and Eocene times stimulated the deposition of sediments along the eastern CAO margin (Davison, 2005).

2.5. Alongshore crustal structure of the passive margin segments

The along strike evolution of the margin structure (***Fig. 4***) is relevant in the frame of this review. For instance, changes in the amount of stretching during rifting, the volcanic or non-volcanic character, presence of mantle bodies or volcanic accumulations in the crust/lithosphere could have had importance in the subsequent mechanical behaviour of the rifted and continental margins. As such, we considered it as one of the prime parameters to discuss.

Results of wide-angle seismic data along the northern CAO passive margins have been presented in Biari et al. (2021), and geophysical surveys are relatively well-distributed along the two conjugate passive margins of the CAO, with the exception of the southern eastern margin, from Mauritania to Senegal, where we lack such results. A cartographic summary is given in figure ***4***, picturing the main differences between both conjugate margins. The most striking difference is the largely volcanic character of the eastern North America passive margin (***Fig. 2***) showing many Seaward Dipping Reflectors (SDRs) down to the Florida offshore Bahamas Bank (Funck et al., 2004; Louden et al., 2010, 2013). Northward, the SDRs are disappearing along the Nova Scotia segment (Louden et al., 2013; Lau et al., 2018) where the ocean-continent transition zone would show serpentinized mantle on the American side, but not on the Moroccan one (Biari et al., 2015). Although we lack deep seismic imaging on the Mauritanian-Senegal segment of NW Africa, SDRs are not recognized on this portion (Davison, 2005), with the noticeable exception of southern Senegal and Guinea. There, conjugate Guinea and Demerara Plateaux (***Fig. 4***), in the eastern and western margins, respectively, are showing structures on seismic data that have been interpreted as SDRs by Reuber et al. (2016). These SDRs have been proposed to represent the expression of a hotspot volcanic activity during the Middle Jurassic (Basile et al., 2020 and references therein). The architecture of this southernmost part (Guinea and Demerara Plateaux) of the CAO is complex (e.g., Casson et al., 2020; 2021), given its position adjacent to the Equatorial Atlantic Ocean. This complexity, as observed on seismic data, is partly inherited from the successive drifting phases of the CAO in the Jurassic and of the Equatorial Atlantic in the Cretaceous, which likely induced a complex erosional pattern at the intersection (e.g., Labails et al., 2010; Reuber et al., 2016 and references therein).

In the Nova Scotia-north Morocco segment, the estimated amount of stretching is similar to its conjugate counterpart (Biari et al., 2021), thinning a 35-38 km-thick crust in along a 150-200 km distance. Southward, the North American and south Morocco segment are showing the volcanic/non-volcanic contrast between conjugate margins. The comparison between the DAKHLA (Klingelhoefer et al., 2009; Biari et al., 2017) and the LASE profiles on the US side (LASE Study Group, 1986) shows

i) an amount of stretching similar on both sides of the CAO, ii) a significant difference in crustal thickness (US part: 40 km; Dakhla part: 27-28 km), iii) the large SDRs presence on the US side against few magmatic intrusions in the Moroccan crust, and iv) the occurrence of an underplated dense body at the ocean-continent transition on the US side. From a crustal point of view, the rifting is generally considered as relatively symmetrical (Biari et al., 2021), with potential asymmetry between Nova Scotia and northern Morocco (Maillard et al., 2006). South of Western Sahara, no comparison could be realized between the margins of Mauritania-Senegal and southern United States (Biari et al., 2021). The passive margin of northwest Africa is a rifted, mature, fairly narrow, sediment-nourished margin (e.g., Michard et al., 2008). It is considered as non-volcanic, or magma-poor, as the continental margin lacks seaward dipping reflectors (e.g., Contrucci et al., 2004; Biari et al., 2017).

On both conjugate margins, remnants of the Palaeozoic orogenies have been reworked during the CAO rifting, with a more continuous Alleghenian system along the eastern American margin (Hatcher et al., 2010), whereas the Variscan front appears more sinuous along the NW Africa counterpart (***Fig. 3***). For instance, the cratonic Reguibat Shield (northern WAC) deviated the Variscan thrust fronts, which extend southward towards the Leo Shield (southern WAC), and where the front is following the WAC boundaries (Peucat et al., 2005; Villeneuve, 2008; Caby & Kienast, 2009; Villeneuve et al., 2015). As such, it illustrates how the lithospheric nature is significantly variable along strike on the NW African side. Instead, alongside on the NE American side, the Appalachian-Alleghenian orogeny consists in stacked crustal strips somehow parallel to the future CAO rift, where less variabilities is expected among the different stacked crustal domains compared to the duality cratonic vs. “classical” lithosphere of the African counterpart (e.g., Boscaini et al., 2022).

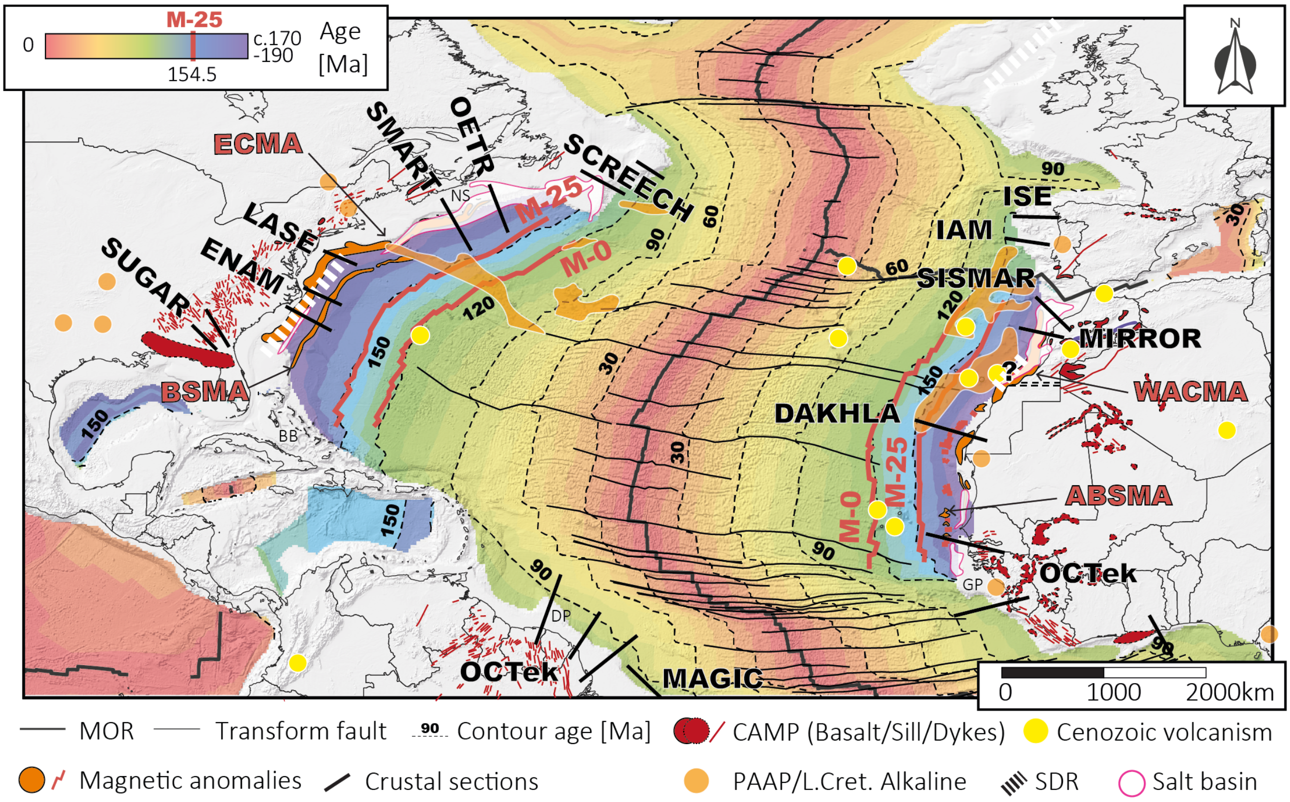

Figure 4 | Central Atlantic Oceanic floor age (data from Muller et al. 2008; *MOR* = Mid Oceanic Ridge), overlaid with Magnetic anomalies (after Biari et al., 2017) and selection of crustal profile locations after the review in the Central Atlantic from Biari et al. (2021; references therein), in the North Atlantic from Fernandez (2019; references therein), Kuznir et al. (2020; OCTek), Marzen et al. (2020; SUGAR), and Moulin et al. (2021; MAGIC), overlaid with of magmatism, volcanism, and evaporite occurrences (CAMP occurrences after Marzoli et al., 2017; PAAP/Late Cretaceous Alkaline event occurrences after Matton and Jébrak, 2009 and Merle et al., 2019, respectively; Cenozoic volcanism, see ***figure 11***; Seaward Dipping Reflectors (SDRs) after Geoffroy, 2005; salt basins after Biari et al., 2017). DP = Demara Plateau; GP = Guinea Plateau; BB = Bahamas Banks; NS = Nova Scotia.

3. LTT and TTM datasets

3.1. LTT and TTM principles

LTT provides time and temperature constraints when apatite or zircon crystals cooled down through specific closure temperatures between c.300 and 40°C (equivalent with normal geotherm to 1 to 10 km of crustal depths). The methods are well established today and the number of LTT refereed articles has steadily increased the last two decades and has been extensively described (based Google Scholar search results of August 2022; e.g., Reiners and Ehlers, 2005; Malùsa and Fitzgerald, 2019). It has several limitations, one of which is that rock samples must contain zircon and/or apatite crystals, limiting the investigations to crystalline basement, most magmatic/plutonic bodies, and their eroded products (e.g., conglomerates, sandstones). The dataset compiled for this review is composed of the results of four LTT methods (***Table 1***), from lowest to highest temperatures of application: i) (U-Th-Sm)/He on apatites (AHe; ~40-100ºC; Shuster et al., 2006), ii) Fission tracks on apatites (AFT; ~60 to 120ºC; Green et al., 1989); iii) (U-Th-Sm)/He on zircons (ZHe; ~160-200ºC; Reiners et al., 2005; Guenthner et al., 2013), and iv) Fission tracks on zircons (ZFT; ~210 to 270ºC; Brandon et al., 1998).

Furthermore, single LTT age alone generally does not hold geological meaning, as several other parameters need to be taken into account when deriving the thermal history in both forward and inverse modelling (e.g., Ketcham et al., 2005; Gallagher, 2012; Ketcham et al., 2018). In the vast majority of recent studies, elaborated thermal histories are described after the results of inverse Time-Temperature Modelling (TTM), which is achieved mostly using either HeFTy or QtQT programs (Ketcham et al., 2005 and Gallagher, 2012, respectively; other codes and programs are listed in the ***appendix***). Such modelling has several advantages over qualitative interpretation of raw LTT data: 1) different geological constraints (time-temperature 'boxes') can be tested in short modelling time with statistical insights over the realisations, 2) it provides visual representation of the thermal history within a temperature range, and 3) it enables the comparison within and between geological domains (e.g., Charton et al., 2021).

Low-Temperature Thermochronology Analyses			Temperature [°C] (30–270)
Apatite	(U-Th)/He (AHe)	Shuster et al. 2006	He-PRZ
	Fission Tracks (AFT)	Green et al., 1989	APAZ
Zircon	(U-Th)/He (ZHe)	Reiners et al., 2005	He-PRZ
	Fission Tracks (ZFT)	Brandon et al., 1998	ZPAZ

Table 1 | LTT methods and their temperature of application ('closure temperatures'), see references therein. *He-PRZ* = Partial Retention Zone; *APAZ*, *ZPAZ* = Apatite and Zircon Partial Annealing Zones. See also Guenthner et al. (2013) for the ZHe method.

3.2. LTT/TTM Datasets

The 252 references from which data was digitised, sometimes georeferenced, and organised into this database are listed in ***tables 2*** to ***5***. In total, 2221 AHe, 3013 AFT, 888 ZHe, and 768 ZFT data point compose the LTT dataset, amounting to 6890 LTT data, spread over 15 countries. For the TTM dataset, cooling events were digitized from 749 time-temperature models or histories (**Appendix**), as exemplified for Morocco in Charton et al. (2021). Statistically representative ages for the AHe and ZHe replicates (or aliquots) are not always provided in the reviewed articles. Therein, the number of replicates varies between 1 (e.g., Ruiz et al., 2011) and 20 (e.g.Flowers and Kelley, 2011). In order to perform comparison and interpolation of the (U-Th)/He ages, we have calculated median ages (e.g., Vermeesh, 2008; Ketcham et al., 2018). This work dataset is divided into four regions (***Fig. 2***): eastern North America (henceforth referred to as E-NAM; ***Fig. 5***; references in ***table 2***), northern South America (henceforth referred to as N-SAM; ***Fig. 6***; references in ***table 3***), Iberia (referred to as IB in figures; ***Fig. 7***; references in ***table 4***), and Northwest Africa (henceforth referred to as NWA; ***Fig. 8***; references in ***table 5***).

The figures of maps illustrating the sample locations in articles without precise GPS coordinates were georeferenced using QGIS and a polynomial method of interpolation. Between 6 and 10 points visible on the figure and for which the GPS location was known (e.g., cities, villages, river bends, road intersections, shoreline, and country/state borders) were required as data input in the georeferencing interpolation.

The entire LTT dataset compiles ages between 0 Ma, from well samples, to several billion years for the Precambrian basement the USA. ***Figure 9*** illustrate the raw temporal distribution of the LTT ages for the four methods in the four regions.

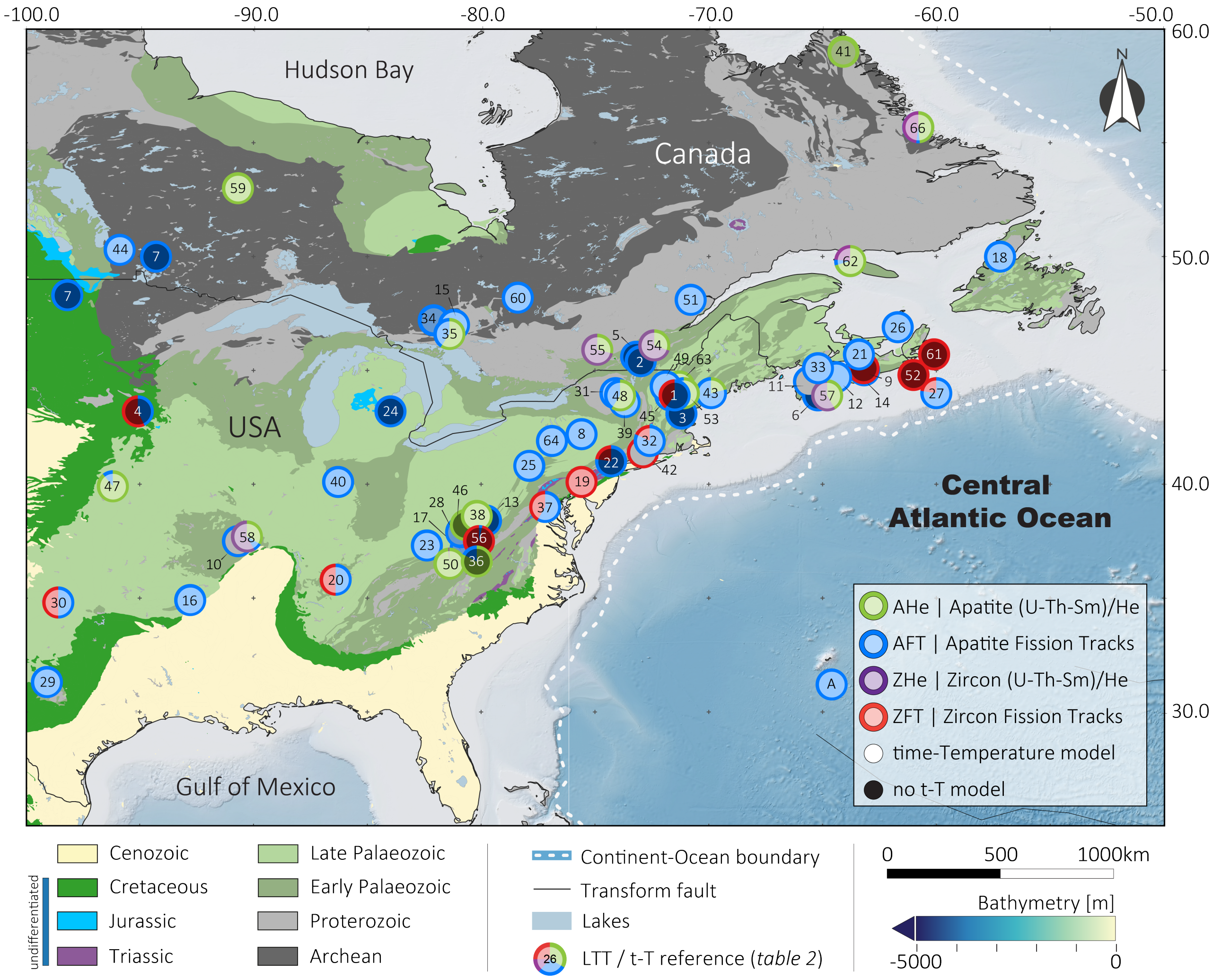

Figure 5 | Eastern North America geology and LTT/TTM studies carried out since 1980. Geological map after USGS and bathymetry data from GEBCO_2014_1D. Note that the pie diagrams depict the proportion of LTT ages from each method for each reference. The proportions between fission track and (U-Th)/He methods are established with 1 fission track data point equals 1 sample (i.e., all crystals measured for the fission track age) and 1 (U-Th)/He data point equals 1 replicate (or aliquot; i.e., 1 dated crystal), thus over-representing (U-Th)/He ages. See ***table 2*** for references.

ID_{REF}	Reference [-]	Country [-]	AHe [count]	AFT [count]	ZHe [count]	ZFT [count]	t-T [-]
1	Doherty and Lyons, 1980	USA	0	9	0	6	no
2	Eby et al., 1985*	Canada	0	4	0	0	no
3	Eby et al., 1985*	USA	0	1	0	0	no
4	Crowley et al., 1986	USA	0	9	0	12	no
5	Currie et al., 1986	Canada	0	4	0	0	no
6	Reynolds et al., 1987	Canada	0	4	0	0	no
7	Crowley and Kuhlman, 1988*	Canada	0	27	0	0	no
7	Crowley and Kuhlman, 1988*	USA	0	5	0	0	no
8	Miller and Duddy, 1989	USA	0	114	0	0	yes
9	Ravenhurst et al., 1989	Canada	0	0	0	3	no
10	Arne et al., 1990a	USA	0	13	0	0	no
11	MacKillop, 1990	Canada	0	5	0	0	NoData
12	Ravenhurst et al., 1990	Canada	0	8	0	0	yes
13	Roden, 1991	USA	0	26	0	0	no
14	Arne et al., 1990b	Canada	0	12	0	0	no
15	Crowley, 1991	Canada	0	43	0	0	yes
16	Arne, 1992	USA	0	14	0	0	yes
17	Blackmer, 1992	USA	0	18	0	0	NoData
18	Hendriks et al., 1993	Canada	0	31	0	0	yes
19	Kohn et al., 1993	USA	0	0	0	42	yes
20	Roden et al., 1993	USA	0	6	0	6	yes
21	Ryan, 1993	Canada	0	24	0	0	yes
22	Steckler et al., 1993	USA	0	34	0	10	no
23	Boettcher and Milliken, 1994	USA	0	10	0	0	yes
24	Wang et al., 1994	USA	0	5	0	0	no
25	Blackmer et al., 1994	USA	0	29	0	0	yes
26	Grist et al., 1995	Canada	0	15	0	0	yes
27	Li et al., 1995	Canada	0	41	0	12	yes
28	Hulver, 1997	USA	0	9	0	0	NoData
29	Corrigan et al., 1998	USA	0	20	0	0	yes
30	Winkler et al., 1999	USA	0	8	0	8	yes
31	Roden-Tice et al., 2000	USA	0	43	0	0	yes
32	Roden-Tice and Wintsch, 2002	USA	0	32	0	7	yes
33	Grist and Zentilli, 2003	Canada	0	17	0	0	yes
34	Lorencak, 2003	Canada	0	51	0	0	NoData
35	Lorencak et al., 2004	Canada	32	22	0	0	yes
36	Spotila et al., 2004	USA	33	7	0	0	no
37	Kunk et al., 2005	USA	0	7	0	5	yes
38	Reed et al., 2005	USA	15	0	0	0	yes
39	Roden-Tice and Tice, 2005	USA	10	112	0	0	yes
40	Weber et al., 2005	USA	0	16	0	0	yes
41	Centeno, 2005	Canada	52	0	0	0	NoData
A	Spiegel et al., 2007 *	Central Atlantic	0	2	0	0	yes
42	Bernet, 2008	USA	0	0	0	3	NoData
43	West et al., 2008	USA	11	41	0	0	yes
44	Feinstein et al., 2009	USA	0	10	0	0	yes
45	Roden-Tice et al, 2009	USA	0	132	0	0	yes
46	Littlefield, 2010	USA	30	0	0	0	no
47	Flowers and Kelley, 2011	USA	41	5	0	0	yes
48	Taylor and Fitzgerald, 2011	USA	26	18	0	0	yes
49	Roden-Tice et al, 2012	USA	0	9	0	0	yes
50	McKeon et al, 2013	USA	160	0	2	0	yes
51	Tremblay et al., 2013	Canada	0	54	0	0	yes
52	Willner et al., 2015	Canada	0	0	0	6	no
53	Amidon et al., 2016	USA	30	3	0	0	yes
54	Emberley, 2016	Canada	40	0	102	0	yes
55	Hardie, 2016	Canada	34	0	84	0	yes
56	Naeser et al., 2016	USA	0	5	0	137	no
57	Chang, 2017	Canada	10	0	14	0	yes
58	DeLucia et al., 2018	USA	12	3	21	0	yes
59	McDannell et al., 2018	Canada	1	0	0	0	yes
60	Pinet, 2018	Canada	0	8	0	0	yes
61	Willner et al., 2018	Canada	0	0	0	6	no
62	Powell et al., 2018	Canada	12	1	4	0	yes
63	Fame et al., 2019	USA	20	0	0	0	yes
64	Shorten and Fitzgerald., 2019	USA	0	38	0	0	yes
65	McDannell et al., 2019	Canada	0	13	0	0	no
66	Vogler, 2021	Canada	134	16	135	0	yes

Table 2 (previous page) | Eastern North America LTT/TTM references compiled in this review (***Fig. 4***). Rows highlighted in grey: LTT data available but not the article itself (compilation from Herman et al., 2013). * Same study with sampling in two countries. A*: Spiegel et al. (2007) have collected ages from wells in three of the four study areas from this work.

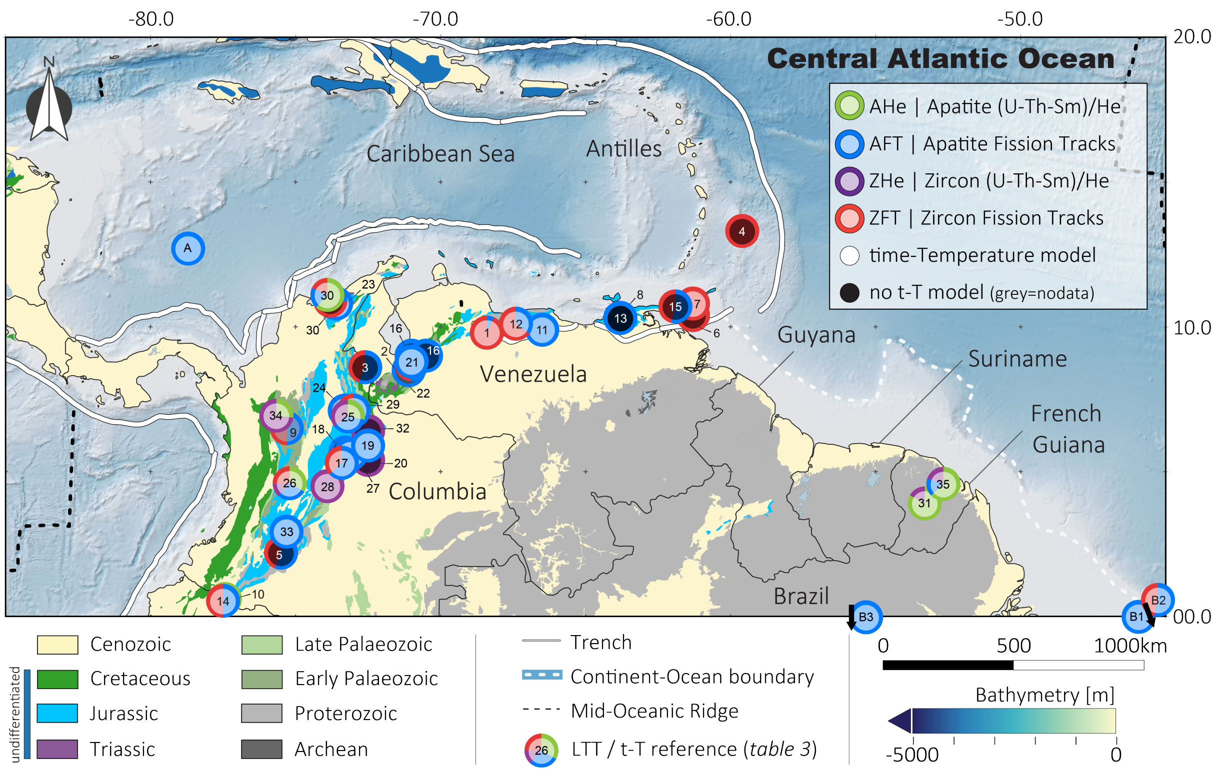

Figure 6 | Northern South America geology and LTT/TTM studies carried out since 1984. Geological map of South America after CGMW and bathymetry data from GEBCO_2014_1D. See the notes on the proportion of LTT data in the caption of ***figure 5***. See ***table 3*** for references.

ID_{REF}	Reference [-]	Country [-]	AHe [count]	AFT [count]	ZHe [count]	ZFT [count]	t-T [-]
1	Kohn et al., 1984a	Venezuela	0	1	0	14	yes
2	Kohn et al., 1984b	Venezuela	0	22	0	21	no
3	Shagam et al., 1984	Venezuela	0	30	0	23	no
4	Baldwin et al., 1986	Barbados	0	0	0	89	no
5	van der Wiel and Andriessen, 1991	Colombia	0	14	0	11	no
6	Algar, 1993	Trinidad	0	0	0	7	no
7	Algar et al., 1998	Trinidad	0	0	0	25	yes
B1	Harman et al., 1998	Brazil	0	20	0	0	yes
8	Locke, 2001	Venezuela	0	20	0	0	no
9	Saenz, 2003	Colombia	0	15	0	15	NoData
10	Spikings et al., 2004	Ecuador	7	0	0	0	yes
11	Perez de Armas, 2005	Colombia	0	56	0	0	yes
12	Sisson et al., 2005	Venezuela	0	6	0	11	yes
13	Locke et al., 2005	Venezuela	0	20	0	0	no
14	Spikings et al., 2005	Ecuador	0	4	0	4	yes
A	Spiegel et al., 2007 *	Caribbean Sea	0	3	0	0	yes
15	Cruz et al., 2007	Venezuela	0	7	0	6	no
16	Bermudez et al., 2009a	Venezuela	0	30	0	0	yes
16	Bermudez et al., 2009b	Venezuela	0	13	0	0	yes
16	Bermudez et al., 2009c	Venezuela	0	8	0	0	no
16	Bermudez et al., 2009d	Venezuela	0	15	0	0	no
B2	Morais Neto et al., 2009	Brazil	0	5	0	4	yes
17	Parra et al., 2009	Colombia	0	29	0	17	yes
18	Mora et al., 2010a	Colombia	0	4	0	0	no
19	Mora et al., 2010b	Colombia	0	43	0	0	yes
20	Horton et al., 2010	Colombia	0	0	55	0	no
21	Bermudez et al., 2010	Venezuela	0	47	0	0	yes
22	Bermudez et al., 2011	Venezuela	0	13	0	0	no
23	Villagomez et al., 2011	Colombia	0	29	0	1	yes
24	Parra et al., 2012	Colombia	0	21	0	0	yes
25	Caballero et al., 2013	Colombia	16	21	20	0	yes
26	Villagomez et al., 2013	Colombia	45	38	18	34	yes
27	Silva et al., 2013	Colombia	0	46	0	0	yes
B3	De Pina et al., 2014	Brazil	0	12	0	0	yes
28	Mora et al., 2015	Colombia	0	0	22	0	yes
29	van der Lelij et al., 2016	Colombia	0	12	0	11	yes
30	Piraquive, 2017a	Venezuela	37	12	0	11	yes
30	Piraquive, 2017b	Venezuela	0	9	0	26	no
31	Derycke et al., 2018	French Guiana	39	0	8	0	yes
32	Sivaro et al., 2018	Colombia	0	0	38	0	no
33	Bonilla et al., 2019	Colombia	0	1	0	0	yes
34	Noriega-Londono et al., 2019	Colombia	7	0	19	0	yes
35	Derycke et al., 2021	French Guyana	18	4	5	0	yes

Table 3 | Northern South America LTT/TTM references compiled in this review (***Fig. 5***). Rows highlighted in grey: LTT data available but not the article itself (compilation from Herman et al., 2013). Rows highlighted in green: we compiled AFT ages from northern Brazil, just outside of the study area to provide constrain in the SE of N-SAM, as very few studies exist for the Guyana Shield. A*: Spiegel et al. (2007) have collected ages from wells in three of the four study areas from this work.

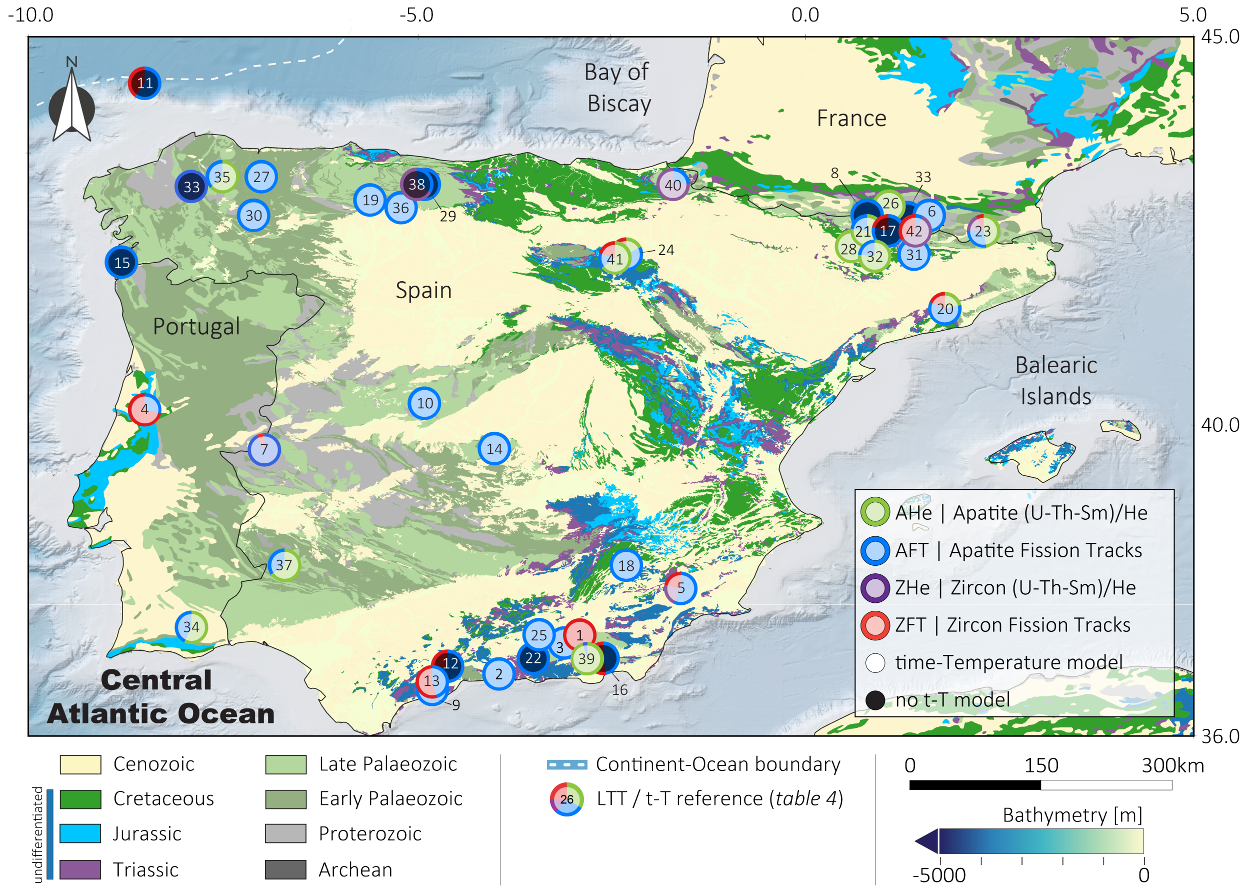

Figure 7 | Iberia geology and LTT/TTM studies carried out since 1995. Geological map after Rodríguez Fernández et al. (2015; IGME geological map of Spain) and the geological map of Europe (BGR/CGMW; 2003) and bathymetry data from GEBCO_2014_1D. See the notes on the proportion of LTT data in the caption of ***figure 5***. See ***table 4*** for references.

ID_{REF}	Reference [-]	Country [-]	AHe [count]	AFT [count]	ZHe [count]	ZFT [count]	t-T [-]
1	Johnson, 1995*	Spain	0	0	0	12	yes
2	Andriessen and Zeck, 1996	Spain	0	8	0	0	yes
3	Johnson, 1997	Spain	0	16	0	0	yes
4	Pereira et al., 1998	Portugal	0	6	0	15	yes
5	Lonergan and Johnson, 1998	Spain	0	8	3	3	yes
6	Morris et al., 1998	Spain	0	21	0	0	yes
7	Stapel, 1999	Portugal	0	56	0	5	yes
8	Fitzgerald et al., 1999	Spain	0	27	0	0	no
9	Sosson et al., 1999	Spain	0	9	0	0	yes
10	De Bruijn and Andriessen, 2001	Spain	0	56	0	0	yes
11	Fugenschuh et al., 2003	Central Atlantic	0	6	0	4	no
12	Platt et al., 2003	Spain	0	15	0	6	no
13	Esteban et al., 2004	Spain	0	10	0	12	yes
14	Barbero et al., 2005	Spain	0	13	0	0	yes
15	Perez-Arlucea et al., 2005	Spain	0	5	0	0	no
16	Platt et al., 2005	Spain	0	7	0	8	no
17	Sinclair et al., 2005	Spain	0	15	0	4	no
18	Barbero and Lopez-Garrido, 2006	Spain	0	14	0	0	yes
19	Carriere, 2006	Spain	0	32	0	0	yes
20	Juez-Larre and Andriessen, 2006	Spain	21	59	0	18	yes
21	Gibson et al., 2007	Spain	30	9	0	0	yes
22	Reinhardt et al., 2007	Spain	0	4	0	0	no
23	Maurel et al., 2008	France	19	11	7	3	yes
24	Del Rio et al., 2009	Spain	3	12	0	2	yes
25	Clark and Dempster, 2009	Spain	0	26	0	0	yes
26	Metcalf et al., 2009	Spain/France	17	0	0	0	yes
27	Grobe et al., 2010	Spain	0	21	0	0	yes
28	Filleaudeau et al., 2012	Spain	73	0	0	0	yes
29	Fillon et al., 2012	Spain	0	10	6	0	no
30	Martin-Gonzalez et al., 2012	Spain	0	17	0	0	yes
31	Rushlow et al., 2013	Spain	0	18	0	0	yes
32	Fillon et al., 2013	Spain	13	4	0	0	yes
33	Herman et al., 2013**	Spain	0	52	0	0	no
33	Herman et al., 2013**	Spain/France	0	28	0	0	no
34	Rodrigues, 2014	Portugal	20	15	0	0	yes
35	Grobe et al., 2014	Spain	24	14	0	0	yes
36	Botor and Anczkiewicz, 2015	Spain	0	6	0	0	yes
37	Vasquez-Vilchez et al., 2015	Spain	17	9	0	0	yes
38	Fillon et al., 2016	Spain	0	9	18	0	no
39	Janowski et al., 2016	Spain	20	1	0	0	yes
40	DeFelipe et al., 2019	Spain	0	9	28	0	yes
41	Rat et al., 2019	Spain	22	5	0	7	yes
42	Waldner et al., 2021	Spain/France	0	3	32	19	yes

Table 4 | Iberia LTT/TTM references compiled in this review (***Fig. 6***). Black reference: no TTM; White reference: TTM model(s) available; * Not all data were digitized (some ages <66Ma were excluded). **Same study, different countries (original data from the world LTT compilation).

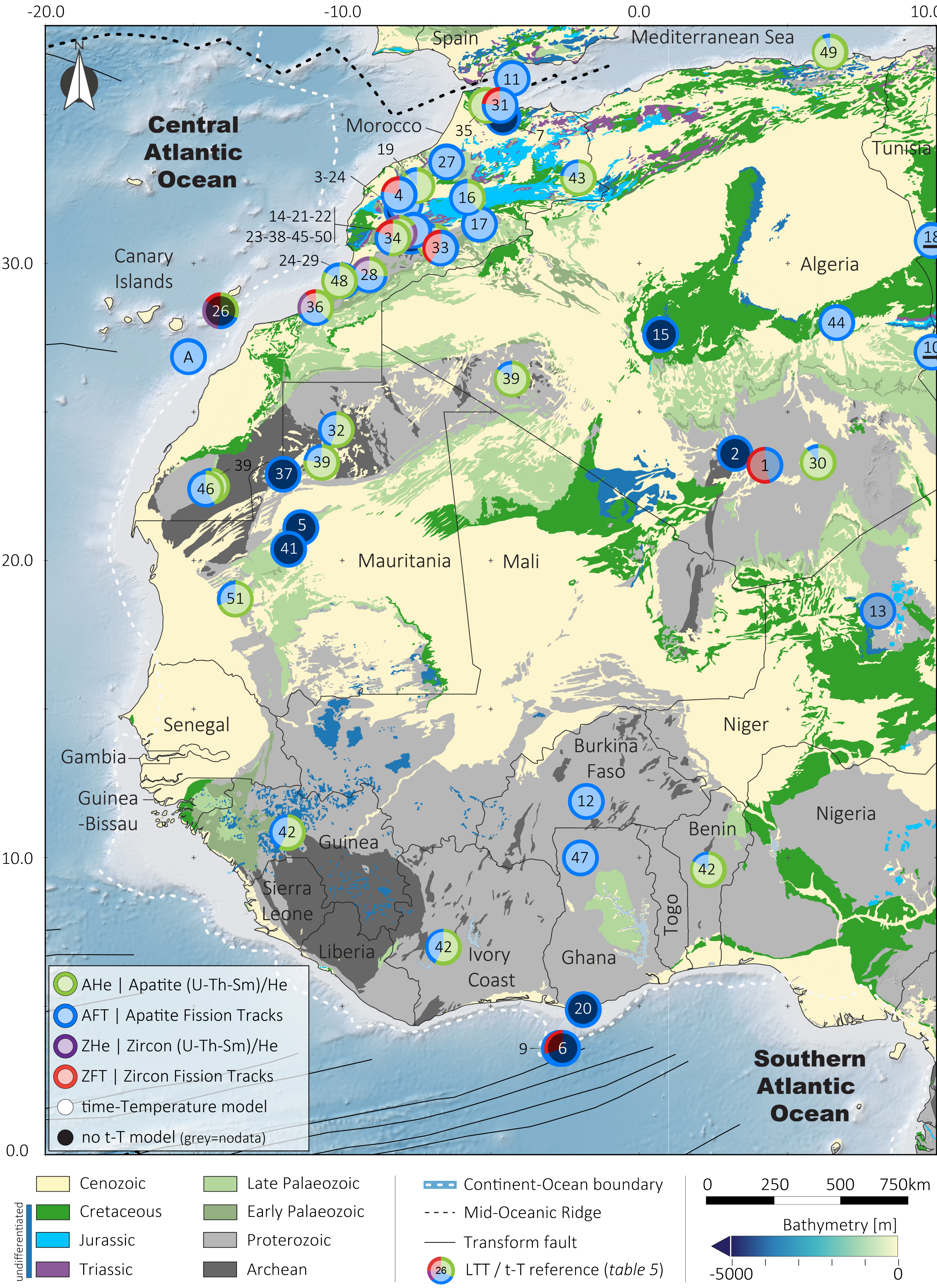
-20.0
-10.0
0.0
10.0
30.0
20.0
10.0
0.0
Central Atlantic Ocean
Southern Atlantic Ocean
Mediterranean Sea
Spain
Morocco
Tunisia
Algeria
Canary Islands
Mauritania
Mali
Senegal
Gambia
Guinea -Bissau
Guinea
Sierra Leone
Liberia
Ivory Coast
Ghana
Togo
Benin
Burkina Faso
Niger
Nigeria
AHe | Apatite (U-Th-Sm)/He
AFT | Apatite Fission Tracks
ZHe | Zircon (U-Th-Sm)/He
ZFT | Zircon Fission Tracks
time-Temperature model
no t-T model (grey=nodata)
Cenozoic
Cretaceous
Jurassic
Triassic
undifferentiated
Late Palaeozoic
Early Palaeozoic
Proterozoic
Archean
Continent-Ocean boundary
Mid-Oceanic Ridge
Transform fault
LTT / t-T reference (table 5)
0 250 500 750km
Bathymetry [m]
-5000
0

Figure 8 | North-West Africa geology and LTT/TTM studies carried out since 1982. Geological map after UNESCO, 1990 and bathymetry data from GEBCO_2014_1D. See the notes on the proportion of LTT data in the caption of ***figure 5***. See ***table 5*** for references.

ID_{REF}	Reference [-]	Country [-]	AHe [count]	AFT [count]	ZHe [count]	ZFT [count]	t-T [-]
1	Carpena, 1982	Algeria	0	5	0	6	NoData
2	Carpena et al., 1988	Algeria	0	6	0	0	no
3	Mansour, 1991	Morocco	0	7	0	0	no
4	Sabil, 1995	Morocco	0	21	0	6	yes
5	Poupeau et al., 1996	Mauritania	0	3	0	0	no
6	Bouillin et al., 1997	Central Atlantic	0	7	0	3	no
7	Azdimousa et al., 1998	Morocco	0	5	0	0	no
8	Clift et al., 1998	Central Atlantic	0	4	0	0	yes
10	Glover, 1999	Libya	0	6	0	0	yes
11	Hurford et al., 1999	Mediterranean	0	11	0	0	yes
12	Gunnell, 2003	Burkina Faso	0	6	0	0	yes
13	Cavellec, 2006	Algeria	0	3	0	0	NoData
14	Missenard, 2006	Morocco	0	6	0	0	no
15	Akkouche, 2007	Algeria	0	19	0	0	no
16	Barbero et al., 2007	Morocco	5	8	0	0	yes
17	Malusà et al., 2007	Morocco	0	10	0	0	yes
18	Underdown et al., 2007	Libya - Algeria	0	3	0	0	yes
A	Spiegel et al., 2007 *	Central Atlantic	0	2	0	0	yes
19	Ghorbal et al., 2008	Morocco	30	4	0	0	yes
20	Hayford et al., 2008	Ghana	0	6	0	0	no
21	Missenard et al., 2008	Morocco	0	14	0	0	no
22	Balestrieri et al., 2009	Morocco	0	11	0	0	yes
23	Ghorbal, 2009	Morocco	122	23	0	0	yes
24	Saddiqi et al., 2009	Morocco	0	10	0	0	yes
25	Sebti et al., 2009	Morocco	0	0	0	10	yes
26	Wipf et al., 2010	Canary Islands	6	4	6	3	no
27	Barbero et al., 2011	Morocco	0	7	0	0	yes
28	Ruiz et al., 2011	Morocco	5	10	4	0	yes
29	Sebti, 2011	Morocco	0	5	0	0	yes
30	Rougier, 2012	Algeria	104	13	0	0	yes
31	Azdimousa et al., 2013	Morocco	0	13	0	4	yes
32	Leprêtre et al., 2013	Mauritania	5	4	0	0	yes
33	Oukassou et al., 2013	Morocco	0	9	0	6	yes
34	Elhaimer, 2014	Morocco	14	7	0	5	yes
35	Romagny et al., 2014	Morocco	45	0	0	0	yes
36	Sehrt, 2014 **	Morocco	91	76	52	25	yes
37	Bradley et al., 2015	Mauritania	0	1	0	0	no
38	Domenech Verdaguer, 2015 **	Morocco	33	0	165	0	yes
39	Leprêtre, 2015 **	Algeria	38	7	0	0	yes
39	Leprêtre, 2015 **	Mauritania	30	9	0	0	yes
39	Leprêtre, 2015 **	Morocco	51	9	0	0	yes
40	Girard et al., 2015	Mauritania	0	10	20	0	yes
41	Martin-Monge et al., 2016	Mauritania	0	5	0	0	no
42	Ye, 2016 **	Benin	88	18	0	0	yes
42	Ye, 2016	Guinea	35	26	0	0	yes
42	Ye, 2016	Ivory coast	15	11	0	0	yes
43	Lafforgue, 2016	Morocco	18	5	0	0	yes
44	English et al., 2017	Algeria	0	7	0	0	yes
45	Gouiza et al., 2017a	Morocco	31	11	0	0	yes
46	Gouiza et al., 2017b	Morocco	12	17	0	0	yes
47	Fernie et al., 2018	Ghana	0	17	0	0	yes
48	Charton et al., 2018	Morocco	10	2	0	0	yes
49	Recanati et al., 2018	Algeria	50	4	0	0	yes
50	Leprêtre et al., 2018	Morocco	79	10	0	0	yes
51	Gouiza et al., 2019	Mauritania	32	14	0	0	yes
52	Lanari et al., 2020	Morocco	92	24	0	0	yes
53	Gimeno-Vives et al., 2020	Morocco	15	1	0	0	yes

Table 5 (previous page) | Northwest Africa LTT/TTM references compiled in this review (***Fig. 8***). Rows highlighted in grey: LTT data available but not the article itself (compilation from Herman et al., 2013). Rows highlighted in green: we compiled AFT ages from northern Libya, just outside of the study area to provide constrain in the NE of NWA. ** PhD thesis containing ages later presented in refereed articles (Sehrt et al., 2017; 2018; Domenech et al., 2016; Wildman et al., 2019; Leprêtre et al., 2015; 2017).

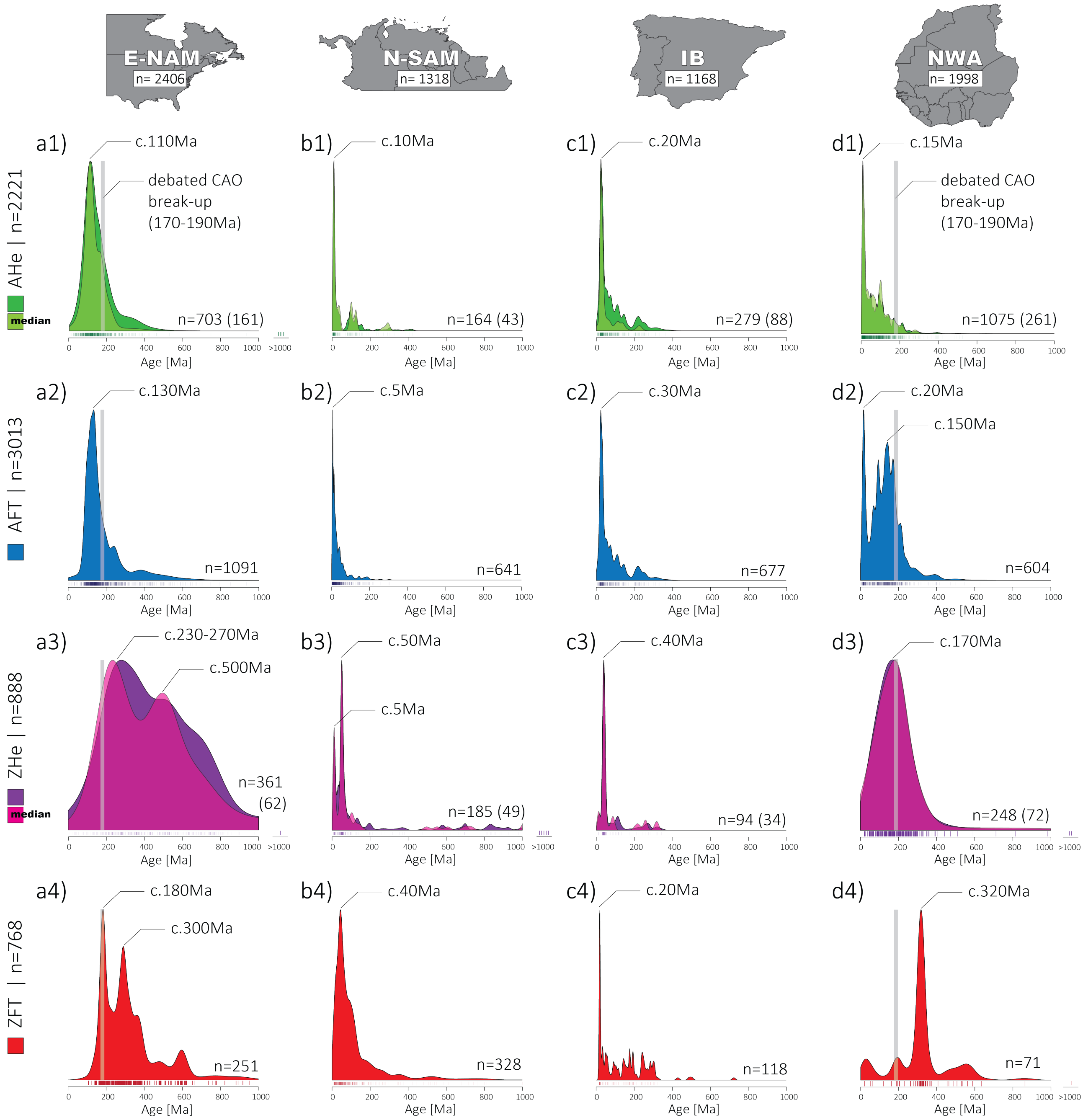

Figure 9 | Kernel Density Estimate (KDE) plots for the four investigated areas (a: E-NAM, b: N-SAM, c: IB, and d: NWA) and four LTT systems (1: AHe, 2: AFT, 3: ZHe, and 4: ZFT). The entire dataset is shown here (n=6890). Median ages are also shown for (U-Th)/He dating (the total amount of samples - and not of the single dated crystals - is given in brackets), representing the median age of all aliquots for each sample and were generated for this study. These plots were done using IsoplotR (isoplotr.es.ucl.ac.uk) with the following options enabled: 'Auto kernel bandwidth' and 'Adaptive KDE'.

3.3. Filtering the LTT dataset – Cenozoic LTT ages

Given our main target for investigation is the CAO and its rifting/break-up/early post-rift evolution, the time range involved for this can be somehow restricted to the 100 Myrs after rifting, meaning that we encompass a large time range from Early Jurassic up to the Late Cretaceous. In addition, in the case of the LTT & TTM results that are evidencing clear Cenozoic events (***Fig. 10***), in general, the geoscience community has a clear idea of the responsible process(es). Hence, we have filtered out LTT ages with a Cenozoic signal (i.e., if LTT ages <66Ma then remove from dataset). The filtered datasets for the different areas are plotted in ***figure 11***.

For instance, the recent orogens such as the Alpes, Atlas, Pyrenees, and Andes (depicted in ***Fig. 10a***) will result in cooling because of erosional tectonic exhumation (higher topography leading to enhanced erosion) with rates of up to 1 km/Myr (e.g., Guerit et al., 2016; Gemignani et al., 2017). The same reasoning can be followed for known Cenozoic magmatism occurrences. It can lead to the warming up of host rocks, resetting the LTT ages, and thermal relaxation leading to a new start of the thermo-chronometers. C'est peut-etre ici qu'il faudrait dire que cet effet depend du magmatisme entre manifestations regionales versus manifestations plus locales sans réelle modifications des structures thermiques de la croute et/ou de la lithosphere. Les exemples Canaries + Zguid l'illustreraient bien dans ce cas. The Canary Islands are a good example of this processes, with Cenozoic LTT cooling ages much younger than their sample stratigraphic ages, due to a significant regional thermal impact of the Canary plume on the very crustal thermal structure (Duggen et al., 2009). For the Cenozoic, however, recent magmatism/volcanism seems well-correlated with also younger LTT ages (***Fig. 10b***). These events clearly affected the post-rift history *sensus stricto* of the margin, and some cooling ages may have been rejuvenated by residing in the partial annealing/retention zones, thus also potentially impacting syn- and early post-rift signal.

In most cases of Cenozoic ages, the mechanisms can be ascribed to known processes and are unrelated, or at least indirectly related, to the passive margin evolution (e.g., the Hoggar Swell, the Andes orogens, etc…). In other areas unrelated to magmatic or known active tectonic processes at the time, (e.g., USA, West African Craton, Portugal), authors have argued, for instance, for exhumation linked to surface uplift and maintained by far field stresses (e.g., limit Morocco/Mauritania; Gouiza et al., 2017b), or climatic change leading to enhanced erosion (e.g., in Morocco, Westaway et al., 2009).

In the case of LTT ages with a Cenozoic signal but lacking a regional tectonic event such as an orogeny or magmatism, such as all the points in the USA and Canada (***Fig. 10b***), it is likely that the LTT ages are either a result of i) localised erosional exhumation, ii) tectonic exhumation by a fault, iii) "worldwide acceleration of mountain erosion under a cooling climate" (article title; Herman et al., 2013), and/or iv) an analytical error. Additionally, it is worth mentioning that part of the Cenozoic sub-dataset are the results of samples collected down boreholes at depth greater than ~2-3km where the LTT ages may have been reset or rejuvenated (e.g., Tarfaya Basin, Morocco; Sehrt et al., 2017).

Filtering the statistically representative Cenozoic LTT cooling ages (i.e., pooled and central fission track ages; median (U-Th)-He ages) results in removing some of the pre-Cenozoic signal. However, in most cases along the investigated margins the lost signal is that of Late Cretaceous and Paleogene cooling, and thus not linked to the syn-, and early post-rift signals and related unconstrained process(es) that we are reviewing here.

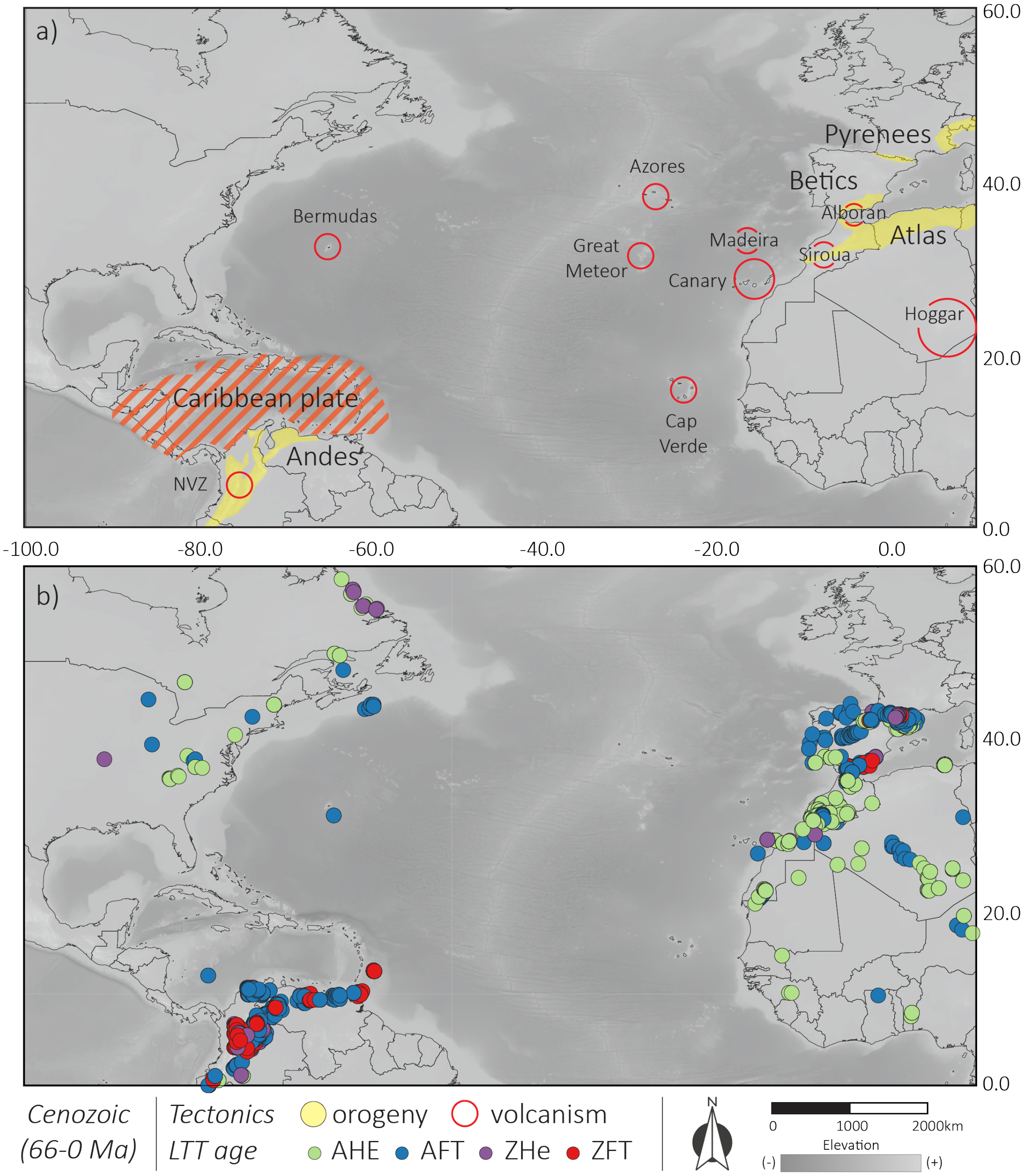

Figure 10 | Cenozoic **a)** volcanic and orogenic events, and **b)** LTT ages in the study areas. LTT references are listed in ***tables 2*** to ***5***.

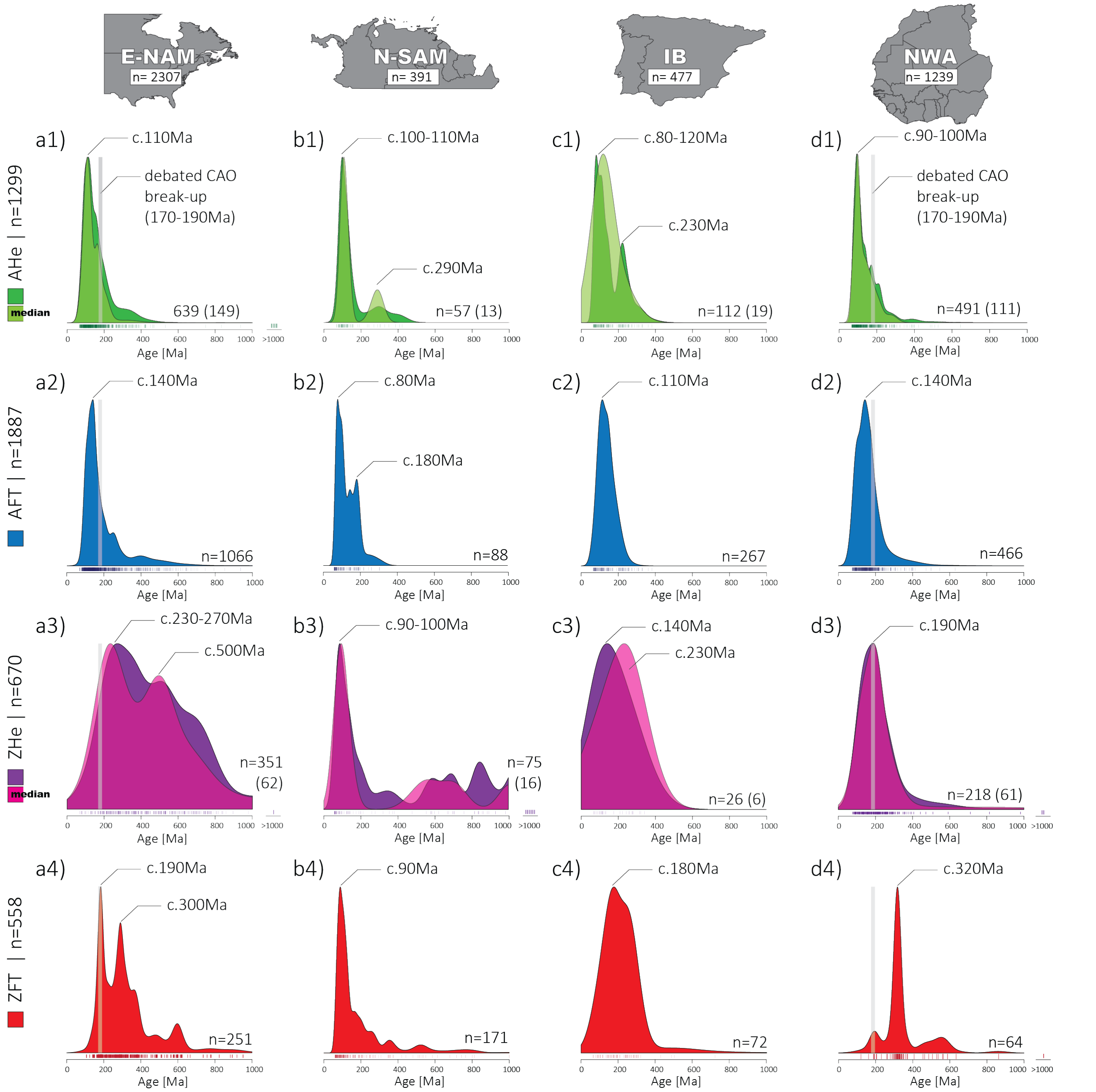

Figure 11 | Kernel Density Estimate (KDE) plots for the four investigated areas. The dataset has been filtered out ($n_{filtered}$=4414) from LTT ages younger than 66Ma (i.e., Cenozoic; ***Fig. 10***). See details in the caption of ***figure 9***.

3.4. Filtering the LTT dataset – Detrital ages

Another filter is applied to the LTT dataset in order to discriminate between rock samples that were already in place (deposited/emplaced) at the onset of the syn-rift phase in the Triassic, and those which were not (for instance a Cretaceous magmatic intrusion). The LTT dataset is thus divided into three categories, labelled as 'Basement', 'Cover', and 'Detrital' (***Fig. 12***). The 'Basement' and 'Cover' labels are used for LTT ages that are younger than the absolute age of their sample (either absolute dating or stratigraphical age). In short, rock samples from Permian or older strata are 'basement' and Triassic or younger stratigraphic ages are 'cover'. These two categories have in common that their LTT signal is that of the present-day geospatial position of the samples, meaning that the LTT age can be displayed on a map, while retaining geological meaning about its location.

In the case of sedimentary units, if the LTT age is older than the rock stratigraphic age, the LTT data are labelled as 'detrital'. This is to reflect that such rock samples have kept a pre- or syn-depositional signal. This signal is that of the sedimentary source area for instance, and that we therefore cannot constrain spatially, at least in the absence of excellent coverage of sedimentary provenance analysis studies (e.g., Accotto et al., 2022**)**. This should not be the case for plutonic and magmatic rock samples, yet very rare occurrences are present in the compiled dataset.

Stratigraphic ages attributed to each data point are based on the youngest possible age. For instance, a 175±10 Ma AFT age from a 'Late Triassic' sedimentary rock sample would be attributed with '201 Ma' as its stratigraphic age. The LTT age is here younger than the youngest possible stratigraphic age, and is then categorised as 'Cover', as the LTT age likely records the cooling that occurred after the Permian/Triassic boundary and after the deposition of the Triassic sediments.

Finally, note that the distinction between 'basement' and 'cover' is relative to the scope of this study, as we consider here the pre-"Triassic rift" rocks as the 'Basement'. The maps, issued from this filtering (***Figs. 13*** and ***14***), use two different circle symbols, one with a continuous black line for 'Basement' and dashed for 'Cover', for visualisation purposes (the 'Detrital' LTT data have been filtered out).

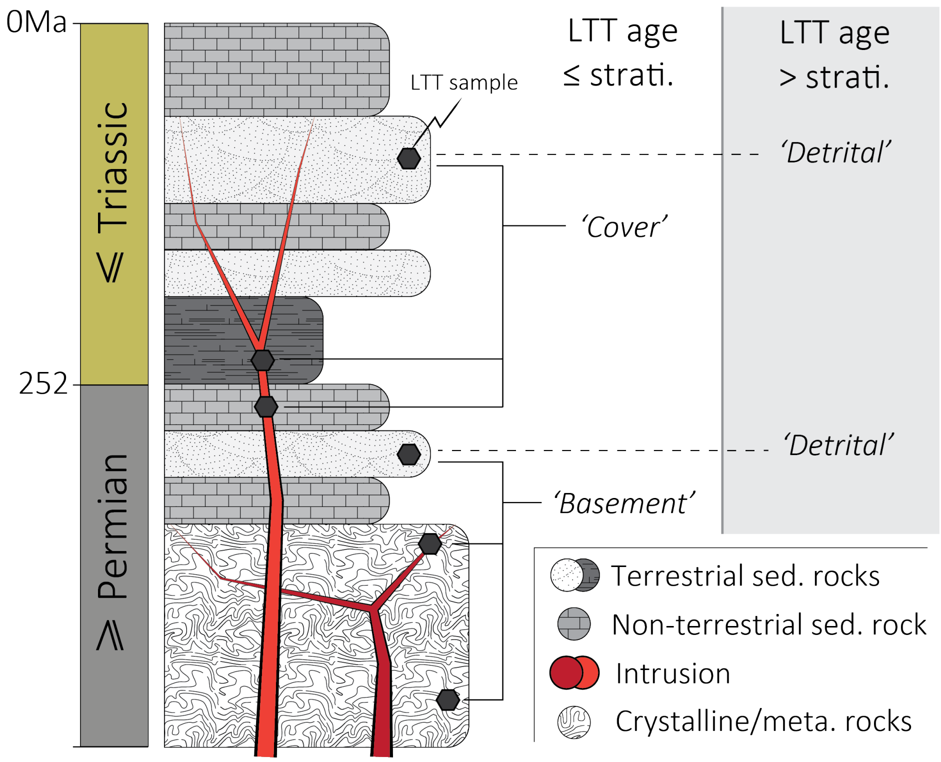

Figure 12 | LTT data categories based on the stratigraphic age and the LTT age of each data point. This distinction is necessary in order to have the geographical coordinates reflecting the thermal history location as opposed to of an unknown source location. Here, Permian-or-older and Triassic-or-younger rock samples bearing an LTT age younger than the stratigraphy are categorised as 'Basement' and 'Cover', respectively. Conversely, a sedimentary rock sample bearing an LTT age older than its stratigraphy is referred to as 'Detrital'.

4. Recorded signal and patterns

4.1. LTT age temporal pattern: LTT peaks *vs.* geodynamics

The Kernel Density Estimate (KDE) plots presented in the previous part (***Figs. 9 and 11***) illustrate the importance of the Cenozoic cooling signal in all parts of the study area, except for North America. Overall, about 60% of the data remains after applying a filter for "Cenozoic" LTT ages. The most impacted region is North SAM with up to 85% of filtered data, whereas in the eastern North America datasets, only 0 to 9% of the data were removed. Once filtered (***Fig. 11***), we assume that of the KDE plots reveal the timing of the cooling of tectonic events unrelated to presently or recently occurring ones (for the most part, as the Andes and the Pyrenees orogenies had contractional events as early as the Late Cretaceous). Hence, for LTT ages that fall within the syn- to post-rifting time windows (of the CAO, North Atlantic, or Equatorial Atlantic rifts), the cooling signals will now be interpreted as either thermal relaxation and/or erosional exhumation following, and related to, the establishment of the different Atlantic rift branches. Here, in the case of the CAO (E-NAM and NWA regions), the KDE plots for the apatite systems show peaks in the early post-rift. For zircon-based systems, we observe that while north South America datasets are, on average, younger than the CAO syn-/post-rift transition, the KDE peaks for ZFT and ZHe datasets are compatible with the syn-rift stage of the Equatorial Atlantic. Moreover, a dominant syn-rift signal is present in North America, Africa, and Iberia for the zircon LTT systems.

Eastern North America Phanerozoic tectonics are characterised by the Caledonian (~450-420Ma) and Alleghenian (~320-260Ma) orogenies, the Central Atlantic rifting (~230-180Ma), the CAMP (~200-190Ma) and PAAP (~100MA) LIPs, and the North Atlantic rifting (~100-50Ma) for its northern part (see the geological setting of this review and references therein). There, KDE plots revealed peaks at ~110, 140, 190, 230-270, 300 and 500 Ma (***Fig. 11a***). It is likely that the ZHe and most of the ZFT records the syn- or post-Alleghenian orogenic tectonic/erosional exhumations at ~300 and ~230-270Ma. The ZFT peak at 190 Ma is somewhat puzzling, since it reveals a younger peak than the main ZHe KDE peak. This could be due to spatial bias and the over-representation with 3 studies that published an important number of LTT data (Kohn et al., 1993; Steckler et al., 1993; Roden-Tice & Wintsch, 2002). In these cases, the authors proposed this to be related to the post-CAMP thermal relaxation and/or to the Central Atlantic syn-rift thermal signature. Instead, AFT and AHe dataset peaks (at ~140 and 110 Ma) are unexpected and unrelated to any tectonic events. As already submitted by several authors and investigated here, they may illustrate the thermal and/or surface evolution of the margin during its post-rift period.

In the studied part of South America, the last 550 Myr were marked by the Alleghenian (c.f., previous paragraph) and Andes (~90-0 Ma) orogenies, the Central and Equatorial (~150-100 Ma) Atlantic riftings, and the CAMP and PAAP LIPs (200 Ma and 125-80 Ma, respectively). Filtered LTT age peaks in northern South America (***Fig. 11b***) are centred at ~80, 90-110, 180, and 290 Ma. Thus, LTT datasets may have recorded the Alleghenian collapse, the onset of Central Atlantic drifting, and, coinciding around 100 Ma, i) the PAAP, ii) the end of syn-rift phase of the equatorial Atlantic, and iii) early tectonic phase(s) of the Andes. The tectonic/erosional exhumation linked to the Andes orogeny starting in the Late Cretaceous is well recorded in this region, with KDE peaks at ~90 and 80Ma and 50, 40, 10, and 5Ma for the filtered and unfiltered datasets.

Iberia known Phanerozoic tectonic events are the Variscan (~400-280Ma) and Alpine/Pyrenean (~100-0 Ma) orogenies, the Neo-Tethys rifting (~220-150Ma), the Central and North Atlantic rifting, and the CAMP and PAAP LIPs (200 Ma and 125-80 Ma, respectively). The KDE plots of the filtered LTT data show peaks at ~80-120, 140, 180, and 230 Ma (***Fig. 11c***), which can then be compared to the timing of tectonics events. While the peaks do not directly account for the syn- and post-Variscan signals (orogenic building and collapse), a large part of the 'spread' encompass the 250 to 400 Ma time range and is likely to illustrate the Iberian late Palaeozoic orogenic story. Given the complex evolution of the Iberia plate since the start of the Mesozoic, it is not surprising to find a wide mixture of ages with this initial 'raw' approach that does not take into account the spatial distribution of the compiled datasets (Triassic rifting; 230-180 Ma; Maghrebian Tethys and Columbrets Basins openings; 180 to 130-125 Ma; southern North Atlantic opening; 145-110 Ma; Central Iberian and Pyrenees basins opening, Early Cretaceous, and inversion, Late Cretaceous to Miocene, and West Mediterranean opening; 30-18 Ma; e.g., Bessière et al., 2021; Ethève et al., 2018; Leprêtre et al., 2018; Nirrengarten et al., 2018). Hence, it is difficult to discriminate between the Mesozoic signals when looking at the global KDE peak signatures.

In NW Africa, Cambrian to Present tectonic events preserved by the geological records are the Hirnantian Glaciation (~450-430 Ma), the Rheic Ocean rifting (~550-450 Ma), its subduction (~420-300 Ma), the Variscan orogeny (between Late Carboniferous and Cisuralian, 320-280 Ma), the Central Atlantic Ocean rifting (230-180 Ma), the CAMP and PAAP LIPs (200 Ma and 125-80 Ma, respectively), the Equatorial Atlantic Ocean rifting (for the southernmost part of NW Africa, 150-100 Ma), the Atlas orogeny (~80-0 Ma), and the Cenozoic magmatism and volcanism. Statistically significant LTT ages, as illustrated by the KDE plots (***Fig. 11d***), are centred around peaks at 90-100, 140, 190, and 320 Ma. ZFT, ZHe, and AHe ages coincide with the Variscan orogeny, the late syn-rift/possible break-up and post-rift, and both the PAAP and the onset of the South/Equatorial Ocean drifting phase, respectively. Compiled AFT ages from the African continent show a marked peak at 140 Ma. Although this does not coincide with a known tectonic event, this discrepancy has been investigated in Morocco and Mauritania (e.g., Ghorbal et al., 2008; Leprêtre et al., 2014, 2017; Gouiza et al., 2019), and appears coeval to the deposition of detritic material in the passive margin. One can notice here that a similar 140 Ma LTT signal is nicely recorded on the conjugate American continental margin (see above). Finally, note that the Cenozoic events (Atlas systems and magmatism/volcanism occurrences) are well recorded in the complete datasets (***Fig. 9d***).

The main limitations of using such an approach are the mixture of ages at the scale of continental blocks that are considered here, which record various tectonic events at their different and possibly opposite boundaries. Therefore, a spatial deconvolution of the LTT signal is necessary, which we carry in the following section. A peculiar signal is nonetheless singular to E-NAM and NW-A areas where, seemingly unrelated to tectonic events, both record a significant cooling signal at ~140 Ma that calls for explanation(s).

4.2. LTT age spatial and temporal patterns

4.2.1. LTT ages *vs.* geographic maps

The spatial distribution of the LTT ages is presented here through a series of eight maps (**Figs. 13** and **14**), for which the simplified base layer consists of the outcrop maps categorised either into 'Basement' rocks and their 'Cover', as defined in the previous part (section 3.4). Our first observation gained from these maps is the striking difference in the spatial coverage of apatite and zircon datasets. Apatite-based LTT data show a relatively homogeneous coverage (***Fig. 13***), especially for the AFT, whereas zircon-based methods show results in concentrated and very localized areas, in the four considered areas (***Fig. 14***). As such, the use of compilation of zircon-based LTT methods alone to draw general conclusions on the CAO evolution is disputable. We consider three exceptions here: 1) the ZFT ages along the Appalachian-Alleghanian belt in E-NAM region that shows Late Paleozoic to Cretaceous ages, 2) the ZFT ages of N-SAM that appears restricted to samples from the Andes showing Palaeozoic to Cretaceous ages (explained by complex relationships with Variscan inheritance and Mesozoic ages mixtures difficult to discriminate at the investigated spatial scale), and 3) the ZFT ages recorded along the Moroccan Atlas system, accounting only for a portion of the African CAO margin, but that can be compared with E-NAM dataset.

In particular, the spatial distribution of AFT and AHe ages (***Fig. 13***) bears a striking and consistent first order trend, namely a youngening towards the CAO crust, which is exemplified by the northern NWA area and even more nicely in the E-NAM area. Indeed, not a single Precambrian apatite-based LTT cooling ages is reported along the coastline, and only a few Palaeozoic ages are, located near French Guyana (AHe), Ghana (AFT), and in the Canadian provinces of Newfoundland and Labrador (AFT). The vast majority of data are otherwise Cenozoic (***Fig. 10***), Cretaceous, and Jurassic in age. This trend however is not visible in north South America, most likely due to a lack of data in the cratonic domain and because of the rejuvenation linked to the Andes orogeny. Contrary to the northern NWA, this trend seems unexistent in southern NWA, with distributed Triassic-Cretaceous AFT ages, probably in relationship with the later Equatorial Atlantic opening, rather than the CAO one.

Within the cases of E-NAM and northern NWA, local trends are difficult to evidence at the presented scale, however there are regional exceptions to the above-mentioned youngening. For instance, the Hoggar Massif (south of Algeria, see ***Fig. 10***), where a Cenozoic swell seem to have had an effect on the AHe and AFT ages, show younger ages than its western counterpart the Eastern Anti-Atlas. Indeed, in these maps, the Cenozoic LTT ages are not displayed, but the rejuvenating effect that the Cenozoic events may have had on older LTT ages was not accounted for and may still be superimposed to some of the displayed, unfiltered, ages. Finally, AFT ages sampled along the Labrador Sea are not following this trend when compared to their distance with respect to the CAO oceanic crust (i.e., they should be older). This is probably explained by the influence of the opening of this oceanic branch younger than the CAO, as submitted by Vogler (2021), who published these ages. Additionaly, the Andes and Pyrenees, which orogenic cycle started in the Cretaceous, are characterized by Cretaceous LTT cooling ages.

Unexpectedly, it is difficult to discuss the 'patchy' distributions of the E-NAM and NWA ZHe datasets (***Fig. 14a***). On both margins, they are strongly localized, showing in majority Paleozoic and some Mesozoic ages that are broadly consistent with the AFT datasets of the same areas. Instead, regarding the ZFT dataset, the E-NAM (***Fig. 14b***) shows a north-eastward youngening trend from Late Paleozoic to Cretaceous ages, that appears relatively oblique to the above-mentioned east to southeastward AFT/AHe youngening trend. Yet, the oldest ages are also the ones that are the farthest from the CAO oceanic crust in this dataset. The NWA ZFT dataset is less homogeneous and bears a consistent and dominantly Late Paleozoic cooling signal, which has been linked to the Variscan evolution (e.g., Sebti et al., 2009). Only few ZFT ages bear Jurassic and Cretaceous ages, namely 1) in the cratonic western Reguibat (Gouiza et al., 2017a) and 2) in the western Meseta (Sabil, 1995). Both datasets might thus confirm significant cooling events at the time, emphasizing the Mesozoic AFT and AHe results collected there.

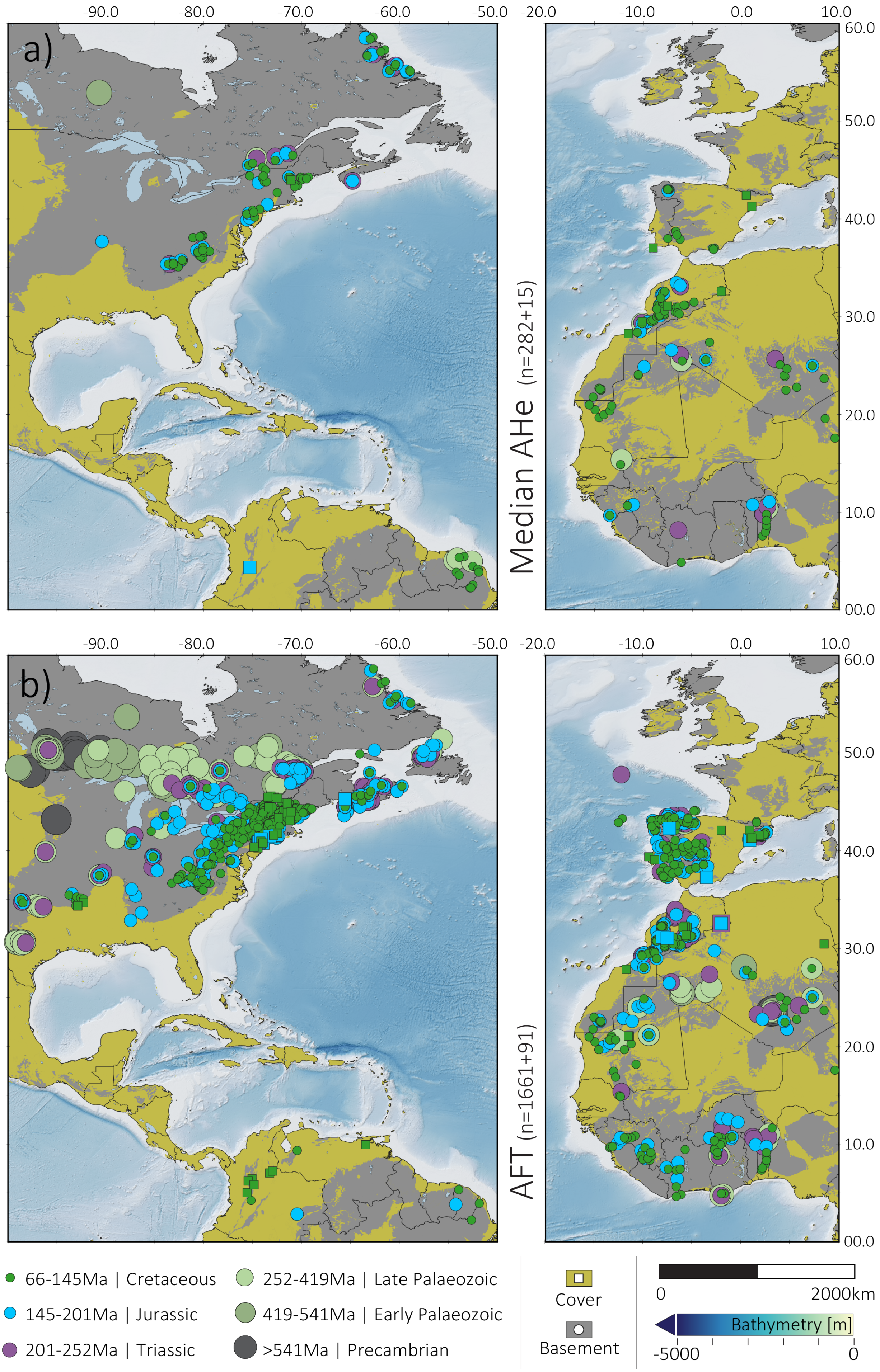
a)
Median AHe (n=282+15)
b)
AFT (n=1661+91)
-90.0
-80.0
-70.0
-60.0
-50.0
-20.0
-10.0
0.0
10.0
60.0
50.0
40.0
30.0
20.0
10.0
00.0
66-145Ma | Cretaceous
145-201Ma | Jurassic
201-252Ma | Triassic
252-419Ma | Late Palaeozoic
419-541Ma | Early Palaeozoic
>541Ma | Precambrian
Cover
Basement
0
2000km
Bathymetry [m]
-5000
0

Figure 13 (previous page) | Apatite LTT dating for **a)** median AHe and **b)** AFT datasets. Median ages younger than 66Ma were filtered out, not the aliquots. Number of samples is n = basement samples + cover samples. Cover and Basement as defined in ***figure 12***. LTT references are listed in ***tables 2*** to ***5***.

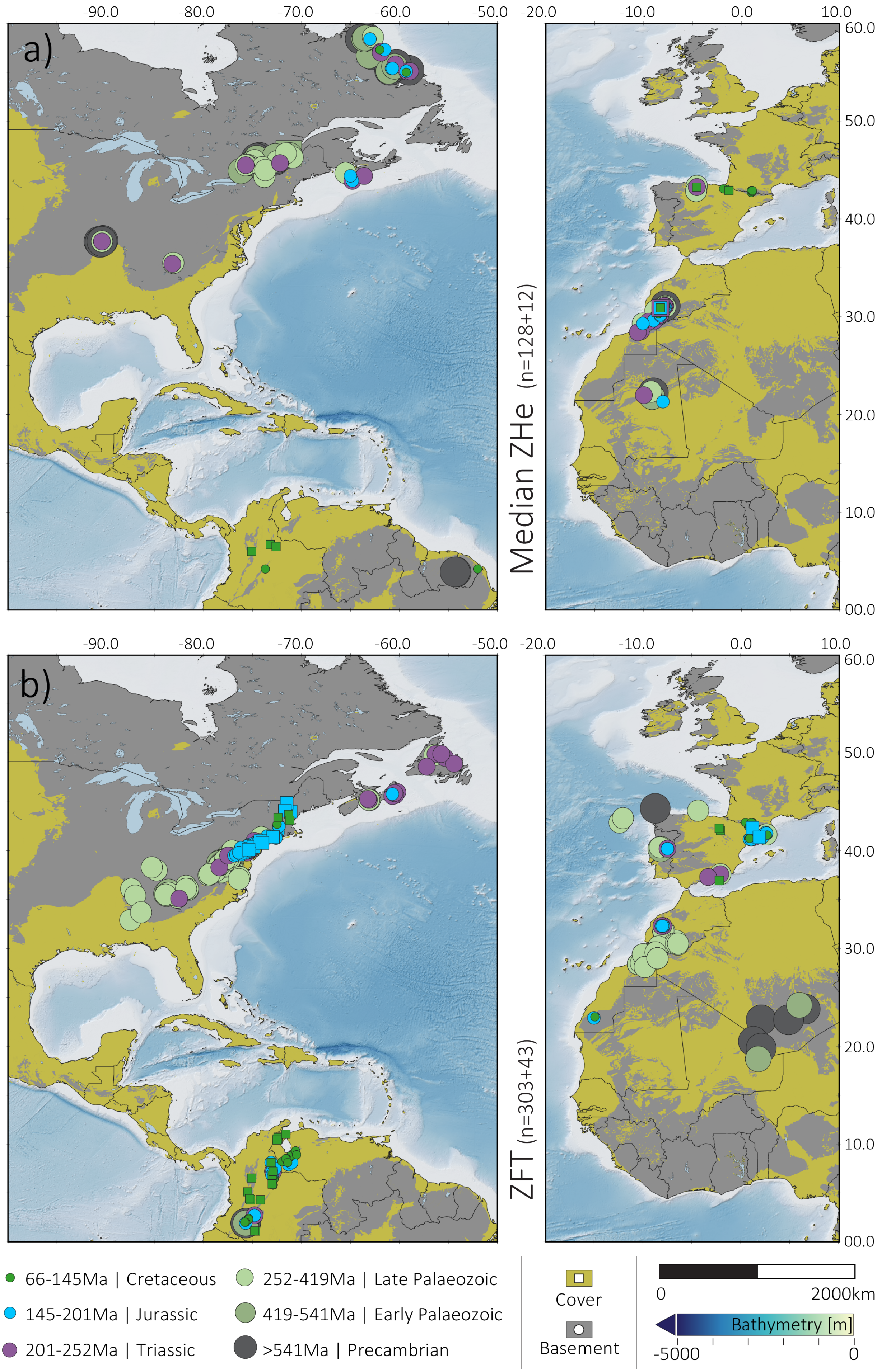
a)
b)
-90.0
-80.0
-70.0
-60.0
-50.0
-20.0
-10.0
0.0
10.0
60.0
50.0
40.0
30.0
20.0
10.0
00.0
Median ZHe (n=128+12)
ZFT (n=303+43)
66-145Ma | Cretaceous
145-201Ma | Jurassic
201-252Ma | Triassic
252-419Ma | Late Palaeozoic
419-541Ma | Early Palaeozoic
>541Ma | Precambrian
Cover
Basement
0
2000km
Bathymetry [m]
-5000
0

822

Figure 14 (previous page) | Zircon LTT dating for **a)** Median ZHe and **b)** ZFT datasets. Median ages younger than 66Ma were filtered out, not the aliquots. Number of samples is n= basement samples + cover samples. Cover and Basement as defined in ***figure 12***. LTT references are listed in ***tables 2*** to ***5***.

4.2.2 LTT ages *vs.* distance to Continent Ocean Boundary

As abovementioned, E-NAM AFT dataset offers the clearest youngening trend, with Precambrian to Late Palaeozoic ages to the west (around 100ºW) toward Jurassic/Cretaceous ages along the Atlantic coast (***Fig. 13b***). The illustrated trend is covering a distance of c.2000 km, ruling out directly short wavelength processes such as local/regional faulting, folding, and rift flanks. Despite showing Jurassic and Early Cretaceous superimposed ages, the youngest AFT ages appear concentrated along the coast from Canada to the USA. Instead, this pattern is more difficult to identify in the opposite margin.

Bearing in mind this first order trend, we check the possible link between the COB and the distribution of LTT along the continental margins. The shortest distance between each point and the Continental Ocean Boundary (COB) was calculated using QGIS (***fig. 15***). The COB data used for the distance computations is from Müller et al. (2016) and is available as a shapefile at this URL: https://www.earthbyte.org/gplates-2-1-software-and-data-sets/. LTT data are then plotted as a function of the distance from the COB for the four studied regions (***Figs. 16, 17, 18,*** and ***19***). The data compiled for this review is located between ~0 and 2000 km away from the COB.

Additionally, it has been demonstrated for the AFT system that Mean Track Length (MTL) vs. AFT age plots can potentially yield insights into the cooling history of the onshore domain of passive margins (e.g., Gallagher and Brown, 1997). There, cooling events evidenced with this method (cluster of long MTL) may display a temporal link to the rifting (i.e., longer tracks for AFT ages coeval to rifting period), as exemplified in the Brazilian and Indian rifted margins (Cogné et al., 2011; Campanile, 2007; respectively). Similar to the 'boomerang plot' present in MTL vs. AFT ages of some margin, the perturbations to the thermal field during the rifting phase is expected to leave its mark on the LTT record (e.g., Moore et al., 1986; Rohrman et al., 1994). In the Moroccan dataset however (Charton, 2018), there is no apparent 'boomerang' curve nor a clear temporal link between long MTL (ca. 13-15 µm) and the timing of CAO rifting.

In the case of important syn-rift thermal pertubations, the subsequent thermal relaxation (e.g., thermal subsidence) would likely result in a higher density of syn-rift or early post-rift LTT ages in the first 100s of kilometres away from the COB, i.e., in the rift zone, in the transition zone, and perhaps in the ajacent unstretch continental crust. While some of these 'expected' LTT age exist within the first 200 km (e.g., in America; ***Fig. 16a*** and ***b***), this does not appear to be the general rule (***Figs. 17, 18, and 19***).

Far away from the fossil rift zone, one may expect to see the LTT age record unaffected by the rift thermal overprint. Here, we use distance of ~1000km from the COB to investigate the relation between the LTT ages and their approximate distance from the oceanic crust. The distance of 1000km corresponds to the 'zoomed-in' domain on ***figures 16, 17, 18,*** and ***19***, which corresponds to the apparition of Palaeozoic AFT ages for E-NAM, and is 7 to 1.5 times greater than what literature has shown as the potentially affected distance by rifting thermal signature; e.g., Moore et al., 1986, Gallagher et al., 1998; Hendriks et al., 2007; Burke and Gunnell, 2008; Malusà et al., 2016; Leprêtre et al., 2017; Malusà and Fitzgerald, 2019a, b).

For the four methods, across the four areas, the post-rift cooling ages constitute an important component of the dataset (***Figs. 16*** to ***19***). By definition, post-rift periods are always closer to the Present-day than their related pre- and syn-rift ones. Thus, in any given geological area, the older the rifting, the more likely it is that a geological event, with a thermal expression, occurs and overprints the rifting signal. In that sense, a significant population of post-rift ages does not necessarily relate to a remarkable trans-continental geological event. What is clearly depicted for several regions, however, is that beyond ~1000km, LTT ages have retained an older cooling signal (***fig. 16***; exemplified in AFT and ZHE of North America datasets). The ZFT dataset for North America follows this trend already from 300-400km with more ages bearing a pre-rift (if related) cooling signal. There, the entire AHe dataset shows a rather flat age trend around 150Ma.

In South America (N-SAM), LTT data are sparce near the COB, and dense between one and two thousand kilometres, as this covers the northern Andes (***fig. 17b***). Overall, AHe, AFT, and ZHe ages decrease away from the COB and towards the Andes. The ZFT dataset, there, is composed of ages with an opposite trend, with Cenozoic cooling signal near the COB and older ones in the Andes.

In Iberia (***fig.18***; note the x-axis has been inverted compared to ***figures 16*** and ***17***), most LTT ages record a syn- and mainly post-rift (for the CAO) cooling signal, as far as ~1500km away from the North Atlantic COB (***fig. 15***; no compiled data further than the Eastern Pyrenees). Let us recall here that the two rifting events are here 1) Triassic (no break-up) and 2) Early Cretaceous (break-up) in age (Nirrengarten et al., 2018). In fact, no clear ages trends can be associated with the distance to the COB in the first thousand kilometres in Iberia (***fig. 18a***) and full mixture of Triassic to Cretaceous ages is observed with overlapping Triassic, Jurassic and Cretaceous ages. The age mixtures are resulting here from many superposed events, with many rifting events affecting the Central Iberian ranges (Angrand & Mouthereau, 2021) during the Mesozoic, the southern North Atlantic rifting during Early Cretaceous and inversions as soon as the Late Cretaceous. Furthermore, the Variscan structural inheritance is expressed in a very faulted crust that enables invididual block behaviour during the Meso-Cenozoic rifting and inversion story (e.g., Barbarand et al., 2021 for the Portuguese margin). Beyond 1500 km from the COB, the LTT ages get younger (***fig. 18b***), when reaching the Pyrenean domain.

In the first one thousand kilometres from the COB on the Africa continent (***fig. 19***), LTT ages decrease ocean-wards. In details, ages with recorded pre-rift cooling signals are statistically present beyond ~500-600km, syn-rift ones are well represented in the area between ~200 to 1200km (already evidenced in ***fig. 11d*** for the ZHe dataset) and early post-rift AFT ages show the strongest density and are present over all of the investigated crustal domain, and well over 1000km for the AHe and AFT datasets (***fig. 19b***). Given that the precise timing of both onset of rifting and continental break-up is approximative and debated, the distances of this paragraph are prone to a substantial error bar (of up to ~100km in NWA).

There is a lack of similar spatio-temporal recognizable pattern across all four LTT systems and four studied regions. However, we do observe one general trend: youngening towards the spatial occurrence of the most-recent and large-scale geological event. In the E-NAM and in the northern NWA LTT datasets, this event appears to be the post-rift phase located between the COB and ~600-800 km, while in South America and Iberia, this youngest event corresponds to the Andes and Pyrenees orogeneses, respectively.

One of our original questions thus remains: was the syn-rift thermal signature fully or partially recorded in the LTT located in the onshore continental margin and if so, how far in the interior of the plate? Zones on the plots characterised solely by pre-rift LTT ages are few. This is the case for the North American AFT and ZFT datasets after ~1700 and between ~600 and 1100km (no ZFT data further away from the COB), respectively, and for the NWA ZFT dataset beyond 1000km away from the COB. These areas have, a priori, not been affected by a syn-rift thermal signature hot enough to reset the ZFT system (~210-270°C). On the other hand, it is possible that a syn-rift thermal perturbation (increasing host rock temperature between 210 and 60°C) reached up to ~1700km, resetting some pre-rift AFT ages. As a last observation, the thermal perturbation of the African Hoggar swell (>90% of LTT ages beyond 1500km) has a clear impact on the apatite datasets with strong rejuvenation deep into the continent interior, unrelated to the CAO story.

The qualitative global distribution of the data has shown us that 1) the best datasets (spatial coverage, homogeneity) are the apatite-based ones, whereas zircon-based ones are generally very localized and 2) these same apatite datasets are also tightly associated with the margins of the CAO *sensu stricto*, i.e. E-NAM and NWA. The study of the CAO margins *s.s.* (NWA and E-NAM) thus appears relatively favourable, for the purpose of this review.

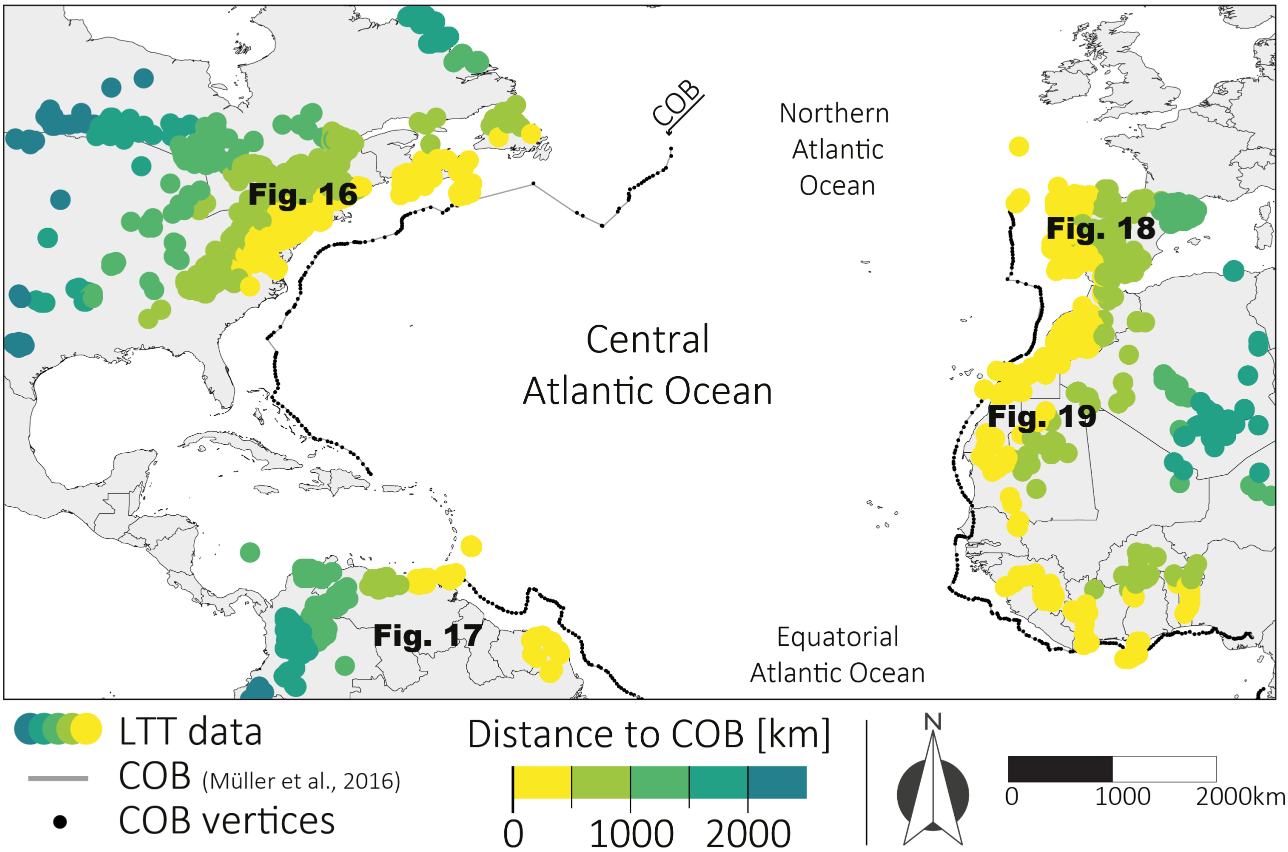

923

924 ***Figure 15*** | Filtered LTT data points (ages labelled 'detrital' have been removed) with distance to
925 closest vector from the Continent-Ocean Boundary. Calculation is done using QGIS tool 'Distance to
926 Hub', using the vertices of the COB data by Müller et al. (2016).

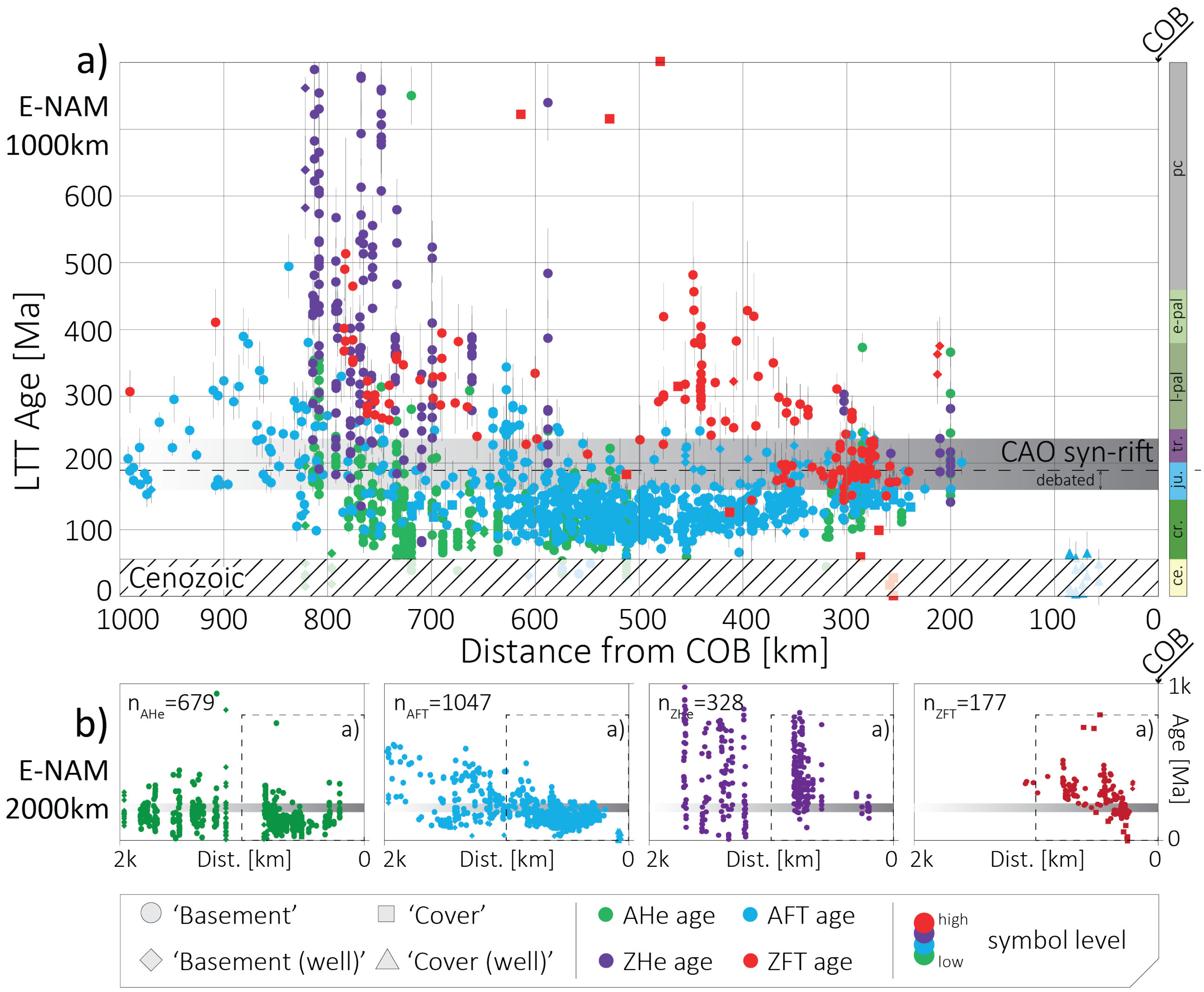

Figure 16 | LTT ages vs Distance to Continent-Ocean Boundary (*COB* on the right; data from Muller et al., 2016) for **E. North America** (E-NAM). a) is 1000kmx800Myr while the plots in b) are 2000kmx1000Myr. Calculation of distance to COB are detailed in the caption of ***figure 15***. The box grey-white is the syn-rift period for the Central Atlantic (CA). LTT references are listed in ***table 2***.

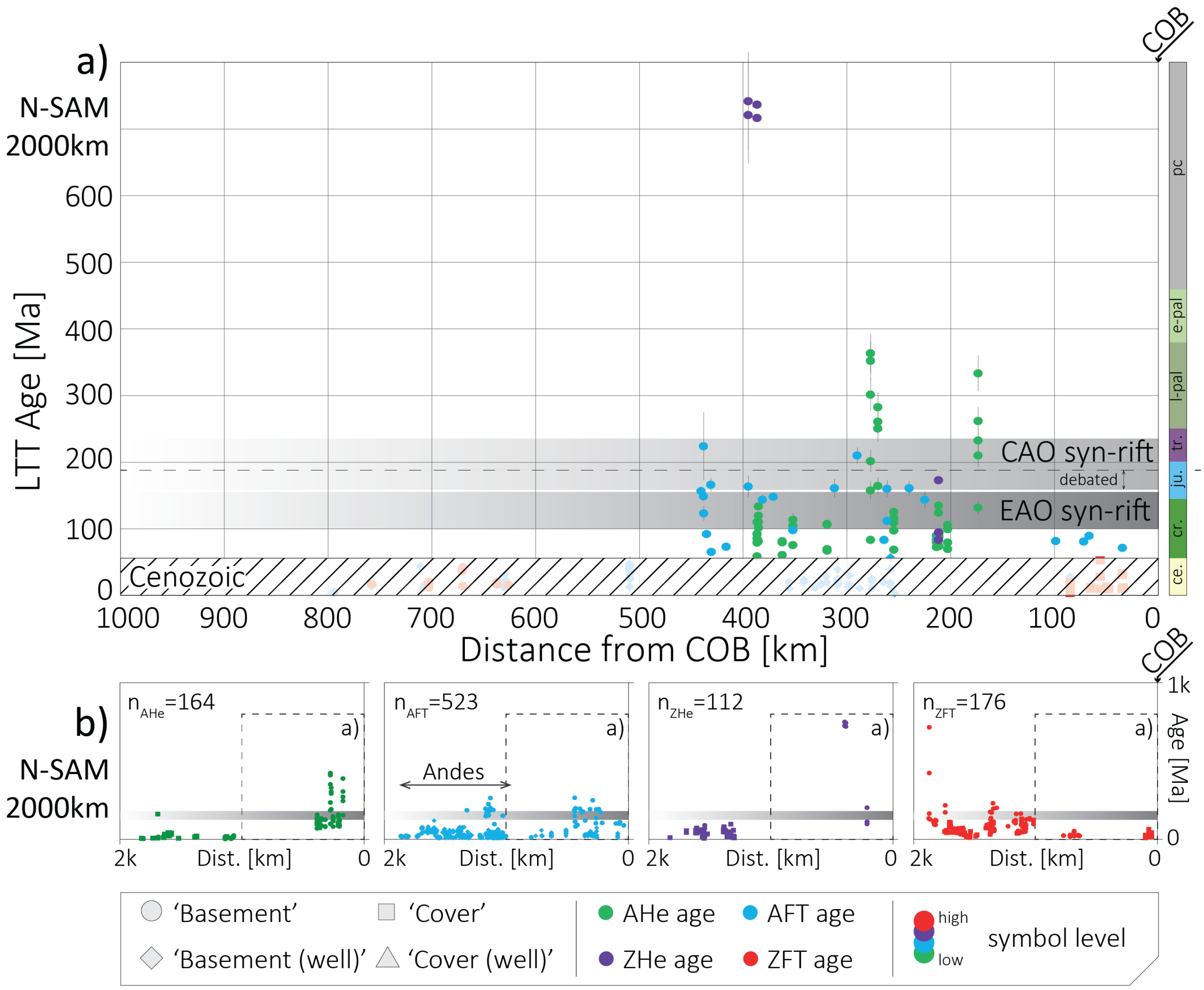

Figure 17 | LTT ages vs Distance to Continent-Ocean Boundary (*COB* on the right; data from Muller et al., 2016) for **N. South America** (N-SAM). See details in the caption of ***figure 16***. EA = Equatorial Atlantic rifting. LTT references are listed in ***table 3***. * Includes AFT from NE Brazil (see references b1-b2-b3 from ***figure 6***).

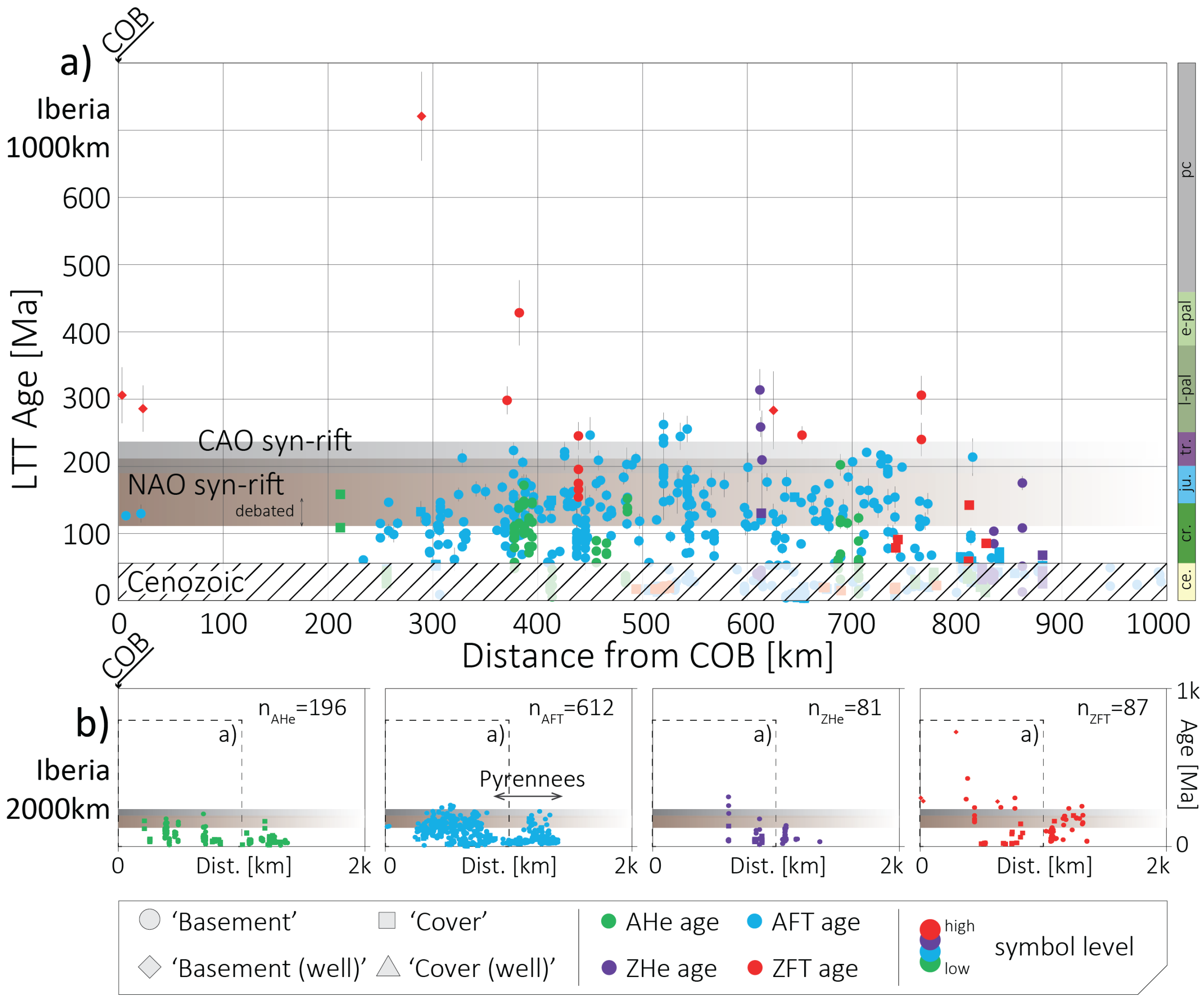

Figure 18 | LTT ages vs Distance to Continent-Ocean Boundary (*COB* on the right; data from Muller et al., 2016) for **Iberia** (IB). See details in the caption of ***figure 16***. LTT references are listed in ***table 4***. NAO = North Atlantic Ocean souther segment rifting (~215-150Ma and break-up ebated between 150 and 110Ma; Barbarand et al., 2021).

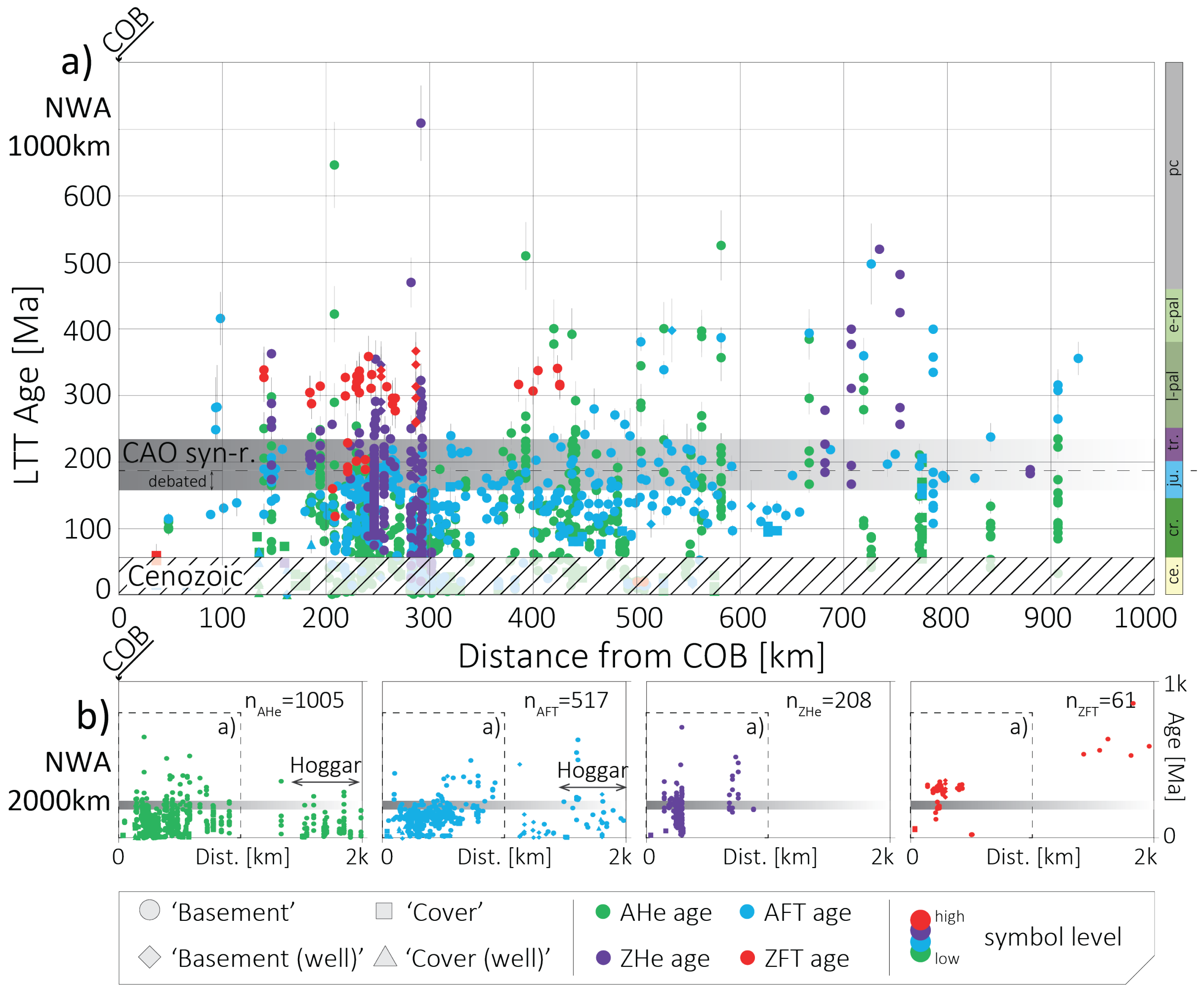

Figure 19 | LTT ages vs Distance to Continent-Ocean Boundary (*COB* on the right; data from Muller et al., 2016) for **Northwest Africa** (NWA). See details in the caption of ***figure 16***. LTT references are listed in ***tables 5***.

5. Phanerozoic cooling of the unstretched continental crust

5.1. Phanerozoic cooling events from Time-Temperature Modelling

Cooling events from available (i.e., published) Time-Temperature Models (TTM) have been digitized (see ***appendix***) to investigate modelled cooling events in the reviewed regions. We digitized the time and temperature values of the start and the end of cooling event from models spanning between the Cambrian and the Quaternary. Thus, cooling events modelled for times before 541 and after 2.6Ma are not included in the presented dataset. This time window is to illustrate the thermal evolution of the Present-day continental rims of the Central Atlantic Ocean in the Phanerozoic, accounting for the time of the Variscan orogeny and collapse, CAO rifting, the continental break-up, the CAO drifting, the adjacent oceanic branches rifting and drifting phases, and the Cenozoic orogens and volcanisms.

The 749 TTM that serve as the basis for this discussion have been organised (c.f., ***appendix***) and synthetized for several geological regions, as defined in ***figures 20*** and ***21***. As mentioned, most studies reviewed here have worked at a local scale, and thus merging these results in order to investigate that at the scale of the margins and their adjacent continental crusts has numerous limitations. For instance, the age mixing with spread of over 10s to 100s Myr for the same geological object, that may be explain locally by heterogeneous thermal structure, fault activities, or successive erosional exhumation events.

To compare both the LTT ages and the time-temperature curves, we have added on our synthesis of the TTM the timing of the KDE peaks (***Figs. 20*** and ***21***). Furthermore, we have added the timing geological events typically associated with thermal perturbation, and/or tectonic/erosional exhumation such as orogenies, rifting phases, and volcanism/magmatism, as reviewed in the Geological context (part 2) of this contribution.

Slow cooling rates (<1°C/Myr) appear ubiquitous in most geological regions, spanning the entire Phanerozoic (***Fig. 20a, b, c,*** and ***f***; ***Fig. 21a, f, i***, and ***j***). This is without a doubt the results of merging the results of different group of workers, studies, and spatial variations of the geological context. This observation does not hold for the Andes (***Fig. 20e***), the Iberian Ranges and the Pyrenees (***Figs. 21b*** and ***c***), and the Betics (***Fig. 21d***), whereby recent cooling event (Cretaceous to Cenozoic) overprinted Palaeo-Mesozoic ones or was simply the focus of the studies.

At the regional scale, we observe the following clear correlations:

- In the Labrador/Nova Scotia (Fig. 20b) between the CAMP, fast cooling rates, and ZFT KDE peak;
- In the Guyana Shield (***Fig. 20e***) between the Equatorial Atlantic Ocean (EAO) rifting, the PAAP, medium cooling rates, and all four KDE peaks;
- In the Iberian Massif and Ranges (***Figs. 21a*** and ***b***) between the PAAP and CAMP LIPs, fast cooling rates, and AFT/AHe and ZHe KDE peaks, respectively; and between the onset of Variscan Collapse and CAO rifting, medium cooling rates, and ZFT/ZHe KDE peaks;
- In the Meseta/Atlas system (***Figs. 21e*** and ***f***) between the Variscan Orogeny, medium/fast cooling rates, and ZFT KDE peak,
- In the Anti-Atlas (***Fig. 21f***) between the CAMP, fast cooling rates, and ZHe KDE peak;
- In the Reguibat Shield and Mauritanides (***Fig. 21g*** and ***h***) where the CAO break-up coincides with the onset of medium cooling rates;
- In the Leo Shield (***Fig. 21i***) between the EAO rifting and PAAP, more opaque medium cooling rates, and AFT/AHe KDE peaks;
- In the Hoggar Massif (***Fig. 21j***) between the Western Central Africa Rift System, fast cooling, and AHe KDE peak; and there too, between the Variscan orogeny and medium cooling rates.

Overall, we observe an excellent match between the KDE peaks and medium cooling rates (1 to 10°C/Myr) for 4/5 of the incidences, whereas fast cooling rates are nearly always coeval to a tectonic event. While this means that LTT alone cannot replace thorough TTM studies, it shows that large LTT datasets bear thermal and potentially geological meaning.

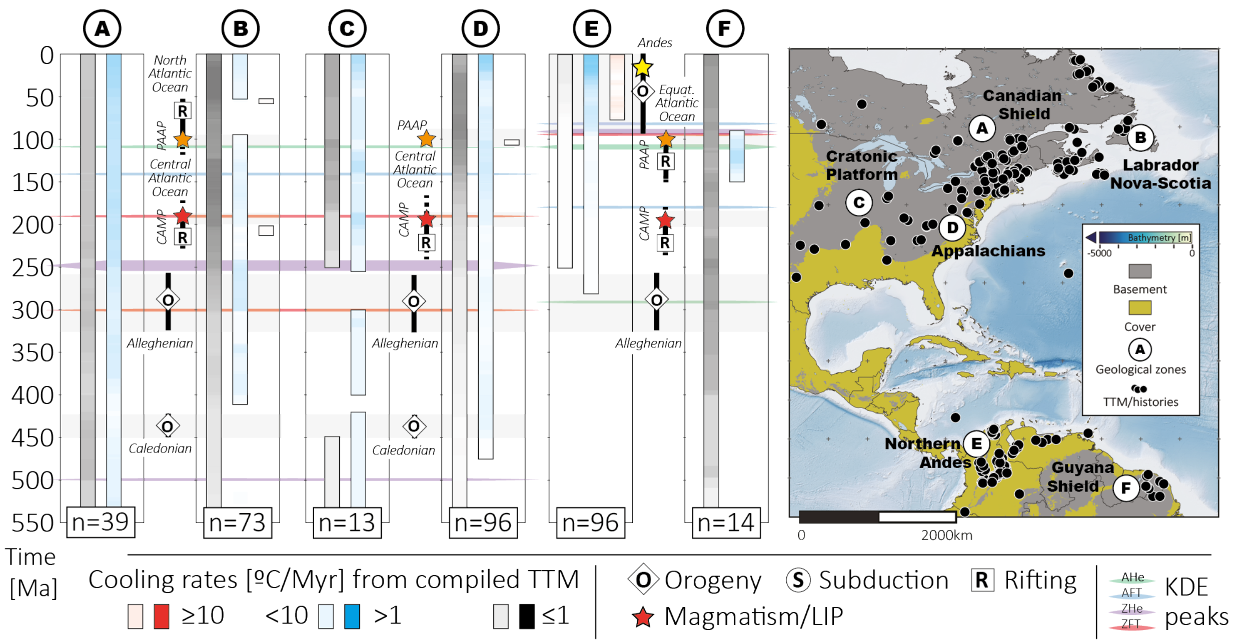

Figure 20 | Time-Temperature Modelling (TTM) “cooling events” charts for Eastern North America (A, B, C, and D), Northern South America (E and F). All TTM for each area (Appendix B) are stacked with transparency percentage normalised to the number of models for the area (transparency [%] = 100÷n). In other words, if all models were to overlap at the same time with similar cooling rate, the related part would be opaque (see legend for opaque colour for reference). The KDE peaks are after *figure 11*. Tectonic events displayed alongside the charts are based on the references listed in the geological setting.

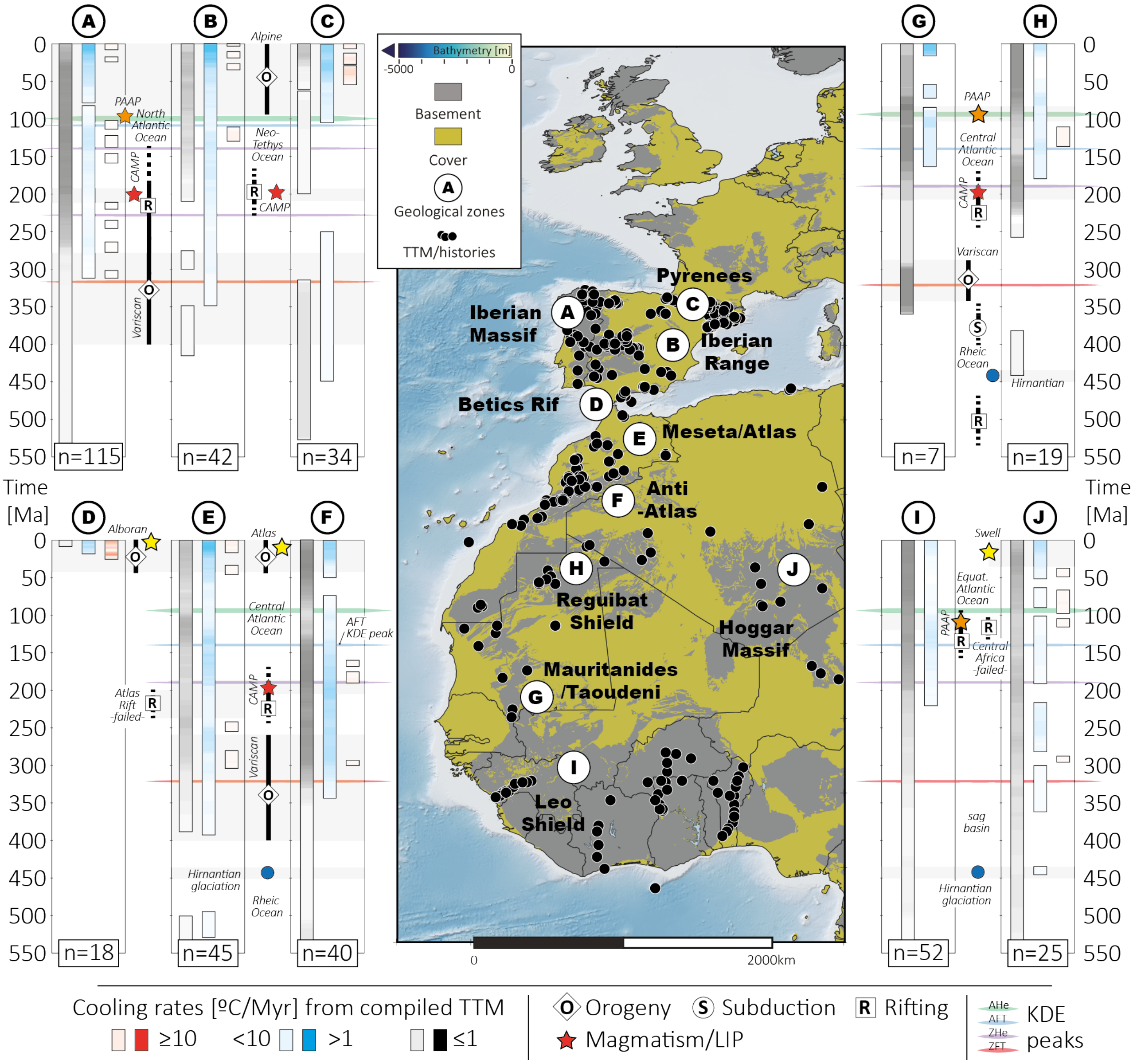

1008

1009 ***Figure 21*** | Time-Temperature Modelling (TTM) "cooling events" charts for Iberia (A, B, C, and D) and

1010 Northwest Africa (D, E, F, G, H, I, and J). See caption of ***figure 20*** for details.

5.2. The CAO evolution and predicted LTT distribution

The different compilations and comparisons of data hitherto gathered show that low-temperature thermochronology ages related to rifting, if ever present, have been largely overprinted by post-rift events. Several types of rifts and passive margins exists (e.g., Allen and Allen, 2013). These types may be categorised in several fashions, based on their geodynamic context, volcanic activity, width, or other aspects. We will focus on the tectonics expectedly involved in the case of the Central Atlantic rifting and drifting.

The rifting of the Central Atlantic is considered as passive (e.g., Tankard and Welsink, 1989; Frizon de Lamotte et al., 2015) and depending on the investigated segment, overall symmetric (Biari et al., 2021) and locally asymmetric (e.g., Piqué and Laville, 1996; Gouiza, 2011). The early Mesozoic rifting was characterised by a wide rifted zone (Leleu et al., 2016), important terrigenous inputs, salt sedimentation, and by the CAMP (e.g., Michard et al., 2008).

Passive rifting develops in an extensional geodynamic context, with extension driven by horizontal plate movements (e.g., Michon and Merle, 2003). It has been established that passive rifting is characterised by lithospheric stretching, asthenosphere upwelling, high surface heat-flow, seismic activity, negative Bouguer anomalies, normal faults reaching deep within the continental crust, and thermal anomalies at depth (e.g., Huismans and Beaumont, 2011; Allen and Allen, 2013). As reviewed in Frizon de Lamotte et al. (2015), characteristic events for passive rifting are as follow: 1) rifting with the formation of wide rift system, 2) possible uplift, 3) post-rift unconformity, and 4) possible post-rift magmatic flows. Asymmetric rifts, which may lead to mantle exhumation along a detachment fault, are characterised by simple shear and high extension rates (Michon and Merle, 2003). It was also evidenced that asymmetric rifts (or segment of rift in this case) can result from the migration of the rift zone after its initiation (for details, see Brune et al., 2014). The adjacent unstretched continental lithosphere (rift flanks) may be affected by small scale convection, volcanism, and uplift (e.g., Olsen, 1995; Allen and Allen, 2013). Predicted syn-rift vertical movements are substantial and rapid subsidence in the rift zone (McKenzie, 1978) and uplift or no motions in the rift flanks (Olsen, 1995; Huismans and Beaumont, 2011).

Rifted magma-poor continental margins are characterised by seaward dipping normal faults and a break-up unconformity (e.g., Paton et al., 2017). The predicted post-rift vertical movement in rifted margins is a slow and continuous subsidence (McKenzie, 1978), linked to thermal cooling of the lithosphere (e.g., Bertotti, 2001; Watts, 2012). The adjacent unstretched continental lithosphere is assumed as tectonically quiescent in most models of passive margins evolution (reviewed in Watts, 2012). However, at least two studies have shown that post-rift uplift and exhumation can be predicted in the unstretched lithosphere adjacent to rifted margins (Leroy et al., 2008; Yamato et al., 2013). The modelled vertical movements were explained as resulting from asthenosphere upwelling or thermal induced flexural response of the lithosphere.

The LTT ages produced in the rims of the CAO are perhaps related to cooling or heating events related to the rifting or drifting processes. Assuming that such signals were not superimposed by other processes, a clear pattern was expected to emerge in this review from spatial and temporal distributions of the LTT ages linking to the syn-rift period. If LTT age patterns were linked to post-breakup uplift in the unstretched lithosphere (e.g., Leroy et al., 2008), one would expect Middle/Late Jurassic to Early Cretaceous ages along the rifted continental margin of the Central Atlantic. Away from the margin, given the assumed tectonic inactivity in the models, no particular trend or pattern is expected. Thus, the rift-related age pattern should prevail.

From 6890 LTT ages compiled for this review, 50.5% belongs to the post-Alleghanian-Variscan orogeny (limit arbitrarily placed at 260Ma) and pre-Cenozoic events, characterised by the pre-, syn-, and post-rift stages of both the Central Atlantic and Atlas rifts. For the remaining data, 35.1% belongs to the Cenozoic (e.g., period of Atlas deformations; ca. 40-0Ma), 5.9% to the Alleghanian-Variscan orogeny (ca. 260-350 Ma) and 8.5% is older than the Late Palaeozoic orogeny. These cooling ages clearly show that widespread cooling events took place after the before, during, and after the rifting stages.

Based on numerical modelling and several passive margin case studies (outside of this contribution study area), Gallagher et al. (1994), Brown et al. (1994), and Gallagher and Brown (1997) established that the age distribution of compiled AFT datasets are the results of erosional exhumation, at least for their case studies. Indeed, the modelling shows that in the case of symmetrical break-up, the thermal perturbation linked to the rifting processes are present but not prevailing in the upper crust. Furthermore, the timing of erosional exhumation deduced from AFT data is not synchronous with that of rifting or break-up, either in the above-mentioned studies and this review. This, and the absence of spatial homogeneity within and across passive margins for large AFT datasets, was explained in terms of surface processes, tectonic reactivation of rift and pre-rift structures, and spatial distribution of drainage system, amongst others (Gallagher and Brown, 1997).

More recently, review of LTT studies and stratigraphic landscape analyses done in passive margins around the world (Green et al., 2018) shows that a series of positive and negative vertical km-scale crustal movements are controlled by plate-scale processes. There, they make the distinction between currently 'elevated' and 'low-lying' continental passive margins, where for both these vertical movements (e.g., Frizon de Lamotte et al., 2009; i.e., unpredicted km-scale exhumation and burial) occurred in the syn-, pre-, and post-rift periods, correlating with events/changes at plate tectonic boundaries.

5.3 Responsible processes: a review

Our observations show that the distribution of LTT ages, with basement rocks mostly characterised by ages younger than syn-rift ages, is at odds with most models of passive margin evolution (e.g., Allen and Allen, 2013). Unexpected vertical movements are labelled as such because our record of the geological history is not sufficiently detailed to provide concomitant and adequate geological processes supporting their occurrence. The proposed mechanisms must account for several observations about the km-scale burial and exhumation events, as they 1) affected a fairly large scale 2) occurred in multiple episodes, 3) are characterised by varying wavelengths landwards and along the coast, 4) affected the onshore domains of either side of the conjugate margins, and 5) were not restricted to the hinterlands directly adjacent to the rifted margins.

Studies have argued that these episodic exhumation and subsidence events can be explained in terms tectonic plate motions and driving forces (e.g., Green et al., 2013; 2018) or lithospheric folding of the continental margin (e.g., Japsen et al., 2012). Mantle-driven dynamic topography has also been proposed as a candidate for the initiation and preservation of these vertical movements (e.g., Hoggard et al., 2016; see Müller et al., 2018, for a review).

Numerical modelling studies show that post-rift changes in mantle convection (e.g., Yamato et al., 2013) or thermally induced flexural response of the lithosphere (Leroy et al., 2008) eventually lead to uplift in the rifted margin hinterlands. However, these modelled mechanisms only account for the post-rift tectonics along a rifted continental margin, and thus cannot be used to test the observed pre- and syn- rift movements observed in the unstretched continental margin.

Authors have tentatively associated the upward movements evidenced via time-Temperature Modelling (TTM) to the Alleghenian-Variscan chain erosion for the pre-rift exhumation (e.g., Ruiz et al., 2011), to the uplifted rift shoulders for the syn-rift exhumation (e.g., Oukassou et al., 2013), and to intra-plate horizontal crustal stresses related to the South Atlantic opening and drifting for the late post-rift exhumation (e.g., Gouiza et al., 2017a).

Gouiza (2011) however showed with lithospheric modelling that the rifting kinematics were not sufficient to explain km-scale vertical movements in the rift flanks during and after the rifting. Moreover, Ruiz et al. (2011; see references therein) demonstrated that the uppermost isotherms within the lithosphere of the Anti-Atlas (Morocco) are not much affected by thermal perturbations occurring close to the lithosphere-asthenosphere boundary or deeper. Domènech (2015) argues that the post-rift thermal relaxation of the lithosphere could not entirely explain the observed cooling in TTM results, and hence that exhumation must have occurred.

Based on a careful analysis of the terraces in the Anti-Atlas coastal area, Westaway et al. (2009) concluded that the observed Neogene uplift was climate driven. In the interior of the Anti-Atlas and High Atlas, other authors tentatively associated the uplift to a large mantle anomaly (Teixell et al., 2003; Oukassou et al., 2013), resulting from the Moroccan Hot Line (Arboleya *et al*, 2004; Teixell et al., 2005; Missenard, 2006; Babault et al., 2008; Frizon De Lamotte et al., 2009; Missenard and Cadoux, 2011).

Downward movements, also obtained with TTM, were solely explained in terms of sedimentation, of which deposits are now eroded from the sampled basement areas (e.g., Ghorbal et al., 2008; Leprêtre et al., 2013). To evidence that modelled heating events can be described in terms of sedimentary loading, Sehrt (2014) calculated subsidence rates from t-T models converted to depth. He then made a comparison to rates obtained from seismic interpretations in the north Tarfaya Basin (in Morocco) and observed that they were comparable.

Proposed mechanisms in NW Africa for the positive and negative vertical movements, as reviewed here, are large-scale processes (see Teixell et al., 2009). These processes may act at wavelengths from one to several hundreds of kilometres (e.g., Babault et al., 2008; Frizon de Lamotte et al., 2009). The proposed processes for the exhumation episodes with matching half wavelengths are rift flank uplifts (however discarded in the previous section), mantle driven doming, lithospheric flexure, crustal-scale folding, and erosional unloading. For the subsidence episodes, while sedimentary loading was the only process proposed, tectonic subsidence regimes have likely enhanced the downward movements. These may be explained in terms of crustal thinning (rift zone), thermal cooling ('old rift'), lithospheric flexure, and crustal-scale folding (see Teixell et al., 2009). However, not all of these proposed mechanisms account for the large-scale observations. On the other hand, recent studies have submitted that mantle-driven dynamic topography should be considered as a general underlying cause for both upward and downward movements observed in many places of the world. However, this process does not take into account the local and regional observations. We argue that a combination of large-scale crustal folding, mantle-driven dynamic topography, and thermal subsidence, was instrumental to the exhumation and subsidence episodes illustrated in this review. Moreover, these large-scale episodes were superimposed by changes in climates, sea level, and erodibility of the exposed rocks (Flowers and Ehlers, 2018), overall contributing to the vertical movement timings, patterns, and amplitudes observed in the rims of the Central Atlantic Ocean.

6. Conclusions: Uplift in the the rims of the Central Atlantic Ocean

As illustrated in this contribution by the compilation of TTM from the rims of the Central Atlantic Ocean (summarized in ***figures** 22* and *23*), each of the four studied regions behaved differently at times. The LTT datasets records different thermal signals depending on the investigated area and on the tool used. This review illustrates that the Alleghenien-Variscan orogeny, the several rifting, and Late-Cretaceous Cenozoic magmatic and orogenic events are well recorded by the LTT. We also document at the ocean scale, the presence of a (or a combinaison of) geological event(s) in the early post-rift time (Jurassic to earliest Cretaceous) that affected the rims of the ocean up to several 100s of km inland. Our interpretation of this important component of the LTT datasets as well as the TTM, is that of erosional exhumation, and not thermal relaxation following a potential rifting thermal perburbation.

The exhumation recorded on the rims of the CAO are commonly recognised by previous works during the post-rift phase, as reviewed here. This seemingly widespread exhumation event interrupted the classical subsidence post-rift phase. Substantial erosion on the coastal plain is classically explained by primary controls such as the geometry of the rifting and the flexural. Here, the asymmetrical mechanism of rifting and the different crust–lithosphere geometries of the conjugate margins do not favor both margins behaving in such a similar way.

We propose a hypothesis that involves mantle-related dynamic processes to account for the symmetrical uplifts on both sides of the northern Central Atlantic. The geographical extent of the eroded area points to a large-scale process, which could be attributed to ascending hot mantle material below the northern Central Atlantic Ocean.

Furthermore, periods of erosional exhumation can be linked to sediment production, which, depending on the source has far reaching implications for the siliciclastics reservoirs (e.g., Wildman et al., 2019). Erosional exhumation impacted the past topography, paleo-drainage systems, and ultimately drove the lithology distribution in the basins (e.g., Gallagher et al., 1998).

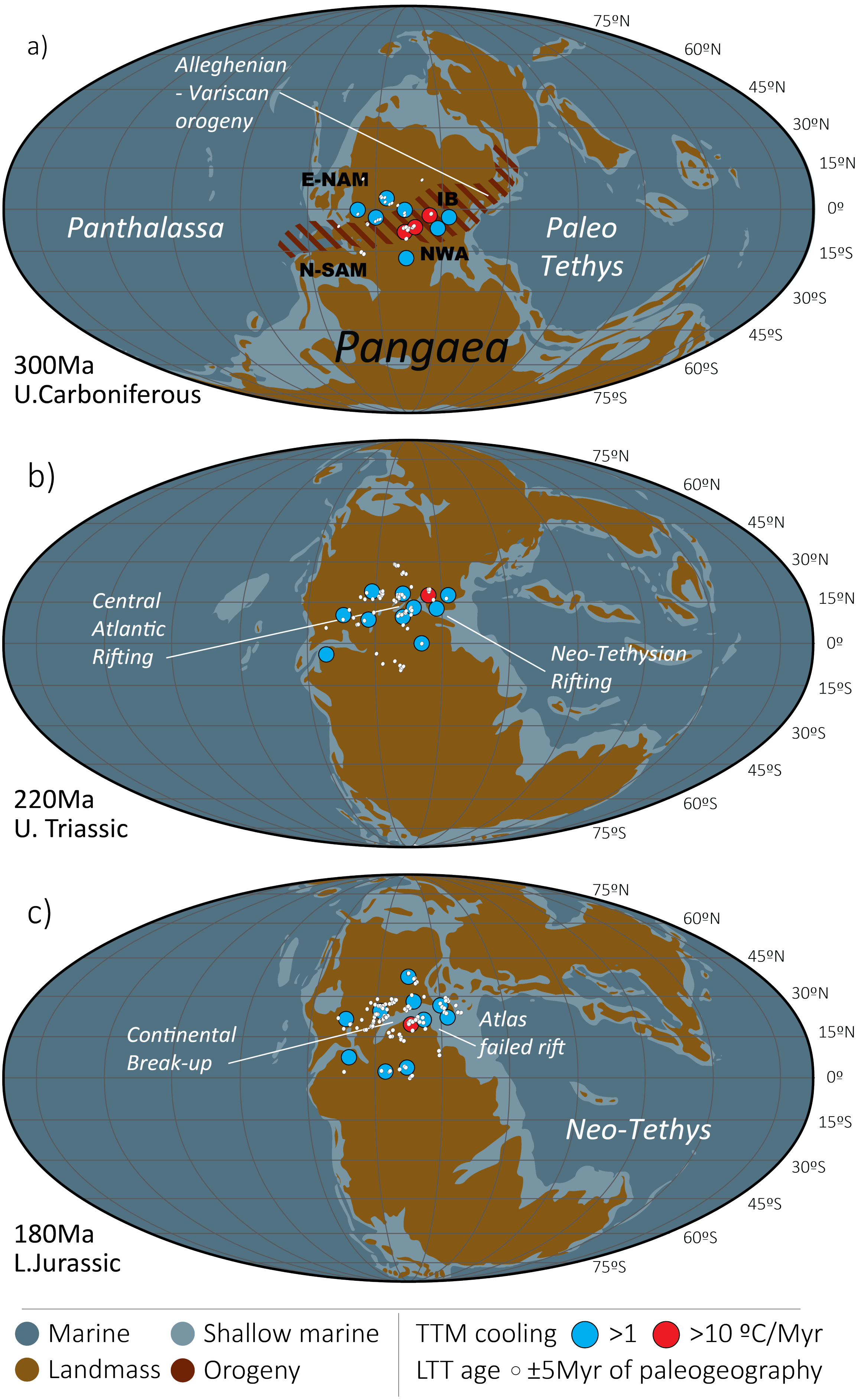
a)
Alleghenian
- Variscan
orogeny
E-NAM
IB
Panthalassa
Paleo
Tethys
NWA
N-SAM
Pangaea
300Ma
U.Carboniferous
75ºN
60ºN
45ºN
30ºN
15ºN
0º
15ºS
30ºS
45ºS
60ºS
75ºS
b)
Central
Atlantic
Rifting
Neo-Tethysian
Rifting
220Ma
U. Triassic
75ºN
60ºN
45ºN
30ºN
15ºN
0º
15ºS
30ºS
45ºS
60ºS
75ºS
c)
Continental
Break-up
Atlas
failed rift
Neo-Tethys
180Ma
L.Jurassic
75ºN
60ºN
45ºN
30ºN
15ºN
0º
15ºS
30ºS
45ºS
60ºS
75ºS
Marine
Shallow marine
Landmass
Orogeny
TTM cooling >1 >10 ºC/Myr
LTT age ±5Myr of paleogeography

1166

Figure 22 (previous page) | Landmass reconstructions focused around the Central Atlantic Ocean rims with TTM cooling events as reviewed in this work at a) 300Ma (ca. end Alleghenian-Variscan orogeny), b) 220Ma (ca. Central Atlantic syn-rift), d) 180Ma (ca. Central Atlantic break-up). LTT data shown on each map corresponds to LTT with age similar to that of the reconstruction (±5Myr). The plate tectonic reconstruction model of Muller et al. (2016) was use for the orientation of the four study regions for b) to f) and the Earthbtyte Phanerozoic model (available on GPlates) was used for the position of the coastline at 300Ma (a). The paleoreconstructions were modified from that of the Deep time map project (Blakey, 2016; Mollweide geographical projection).

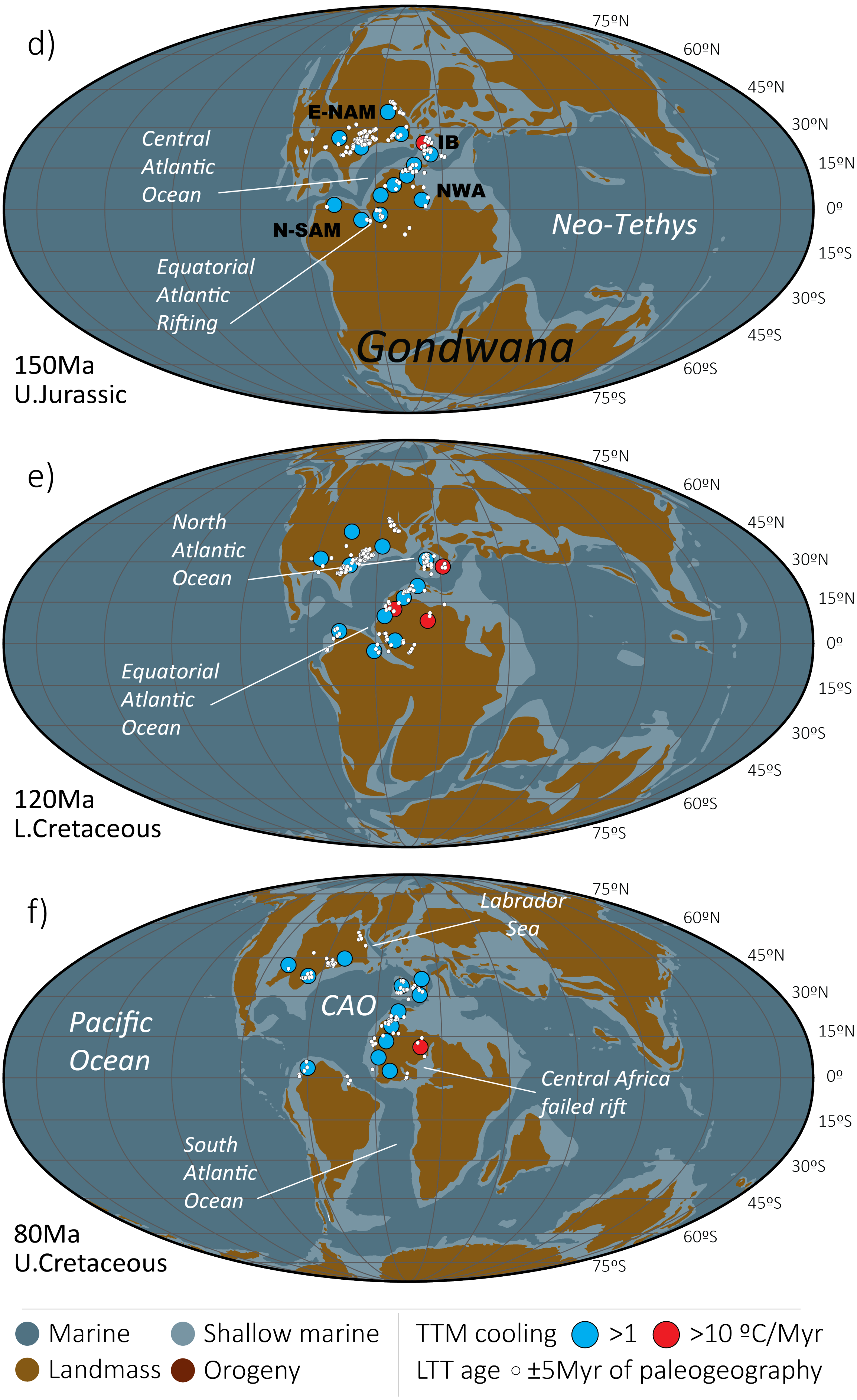
d)
75ºN
60ºN
45ºN
30ºN
15ºN
0º
15ºS
30ºS
45ºS
60ºS
75ºS
E-NAM
IB
NWA
N-SAM
Central Atlantic Ocean
Equatorial Atlantic Rifting
Neo-Tethys
Gondwana
150Ma
U.Jurassic
e)
North Atlantic Ocean
Equatorial Atlantic Ocean
120Ma
L.Cretaceous
f)
Labrador Sea
CAO
Pacific Ocean
Central Africa failed rift
South Atlantic Ocean
80Ma
U.Cretaceous
Marine
Shallow marine
Landmass
Orogeny
TTM cooling >1 >10 ºC/Myr
LTT age ◦ ±5Myr of paleogeography

1175

Figure 23 | Plate reconstruction of the Central Atlantic with cooling event as reviewed in this work at d) 150Ma (major clastic event), e) 120Ma (~PAAP South Atlantic rifting), and f) 80Ma (~onset of the Africa/Europe convergence).

References

Abioui, M., Ferry, S., Grosheny, D., Içame, N., Robert, E., Benssaou, M., **2019**. The Cretaceous marine onlap on Palaeozoic deposits (Smara–Lâayoune Basin, South Morocco). Comparison with neighbouring regions: Comptes Rendus Geoscience, in press, 10p.. https://doi.org/10.1016/j.crte.2019.09.003.

Accotto, C., Poyatos, D.M., Azor, A., Talavera, C., Evans, N.J., Jabaloy-Sánchez, A., El Hadi, H. and Tahiri, A., **2022**. Detrital zircon sources in the Ordovician metasedimentary rocks of the Moroccan Meseta: Inferences for northern Gondwanan passive-margin paleogeography. New developments in the Appalachian–Caledonian–Variscan orogen, GSA books, Special Publication. https://doi.org/10.1130/2021.2554(17)

Akkouche, M., **2007**. Application de la datation par traces de fission à l'analyse de la thermicité de bassins à potentialités pétrolières: exemple de la cuvette de Sbaâ et du bassin de l'Ahnet-Nord (plate-forme saharienne occidentale, Algérie) : Bordeaux 1, Ph.D. Thesis, 297 p.

Algar, S., Heady, E.C. and Pindell, J.L., **1998**. Fission-track dating in Trinidad: Implications for provenance, depositional timing and tectonic uplift. In: Paleogeographic Evolution and Non-Glacial Eustasy, Northern South America, SEPM Special Publication (58). https://doi.org/10.2110/pec.98.58.0111

Algar, S.T., **1993**. Structural, stratigraphic, and thermo-chronological evolution of Trinidad: Dartmouth College, Ph.D. Thesis, 297 p.

Allen, P.A. and **Allen**, J.R., **2013**. Basin analysis: Principles and application to petroleum play assessment. 3rd edition, Wiley-Blackwell, 632pp.

Amidon, W.H., Roden-Tice, M., Anderson, A.J., McKeon, R.E. and Shuster, D.L., **2016**. Late Cretaceous unroofing of the White Mountains, New Hampshire, USA: An episode of passive margin rejuvenation?: Geology, 44, p. 415–418. https://doi.org/10.1130/G37429.1

Andriessen, P.A.M. and **Zeck**, H.P., **1996**. Fission-track constraints on timing of Alpine nappe emplacement and rates of cooling and exhumation, Torrox area, Betic Cordilleras, S. Spain. Chemical Geology, 131(1-4), p.199-206. https://doi.org/10.1016/0009-2541(95)00148-4

Angrand, P., & **Mouthereau**, F., **2021**. Evolution of the Alpine orogenic belts in the Western Mediterranean region as resolved by the kinematics of the Europe-Africa diffuse plate boundary. BSGF-Earth Sciences Bulletin, 192(1), pp. 42. https://doi.org/10.1051/bsgf/2021031

Arboleya, M.L., Teixell, A., Charroud, M. and Julivert, M., **2004**. A structural transect through the High and Middle Atlas of Morocco. Journal of African Earth Sciences, 39(3-5), pp.319-327. https://doi.org/10.1016/j.jafrearsci.2004.07.036

Arne, D.C., **1992**. Evidence from apatite fission-track analysis for regional Cretaceous cooling in the Ouachita Mountain fold belt and Arkoma Basin of Arkansas. AAPG bulletin, 76(3), p. 392-402. https://doi.org/10.1306/BDFF8812-1718-11D7-8645000102C1865D

Arne, D.C., Duddy, I.R. and Sangster, D.F., **1990b**. Thermochronologic constraints on ore formation at the Gays River Pb–Zn deposit, Nova Scotia, Canada, from apatite fission track analysis. Canadian Journal of Earth Sciences, 27(8), p. 1013-1022. https://doi.org/10.1139/e90-105

Arne, D.C., Green, P.F. and Duddy, I.R., **1990a**. Thermochronologic constraints on the timing of Mississippi Valley-type ore formation from apatite fission track analysis. International Journal of Radiation Applications and Instrumentation. Part D. Nuclear Tracks and Radiation Measurements, 17(3), p. 319-323. https://doi.org/10.1016/1359-0189(90)90053-Z

Azdimousa, A., Bourgois, J., Poupeau, G. and Montigny, R., **1998**. Histoire thermique du massif de Ketama (Maroc) : sa place en Afrique du Nord et dans les Cordillères bétiques. Comptes Rendus de l'Académie des Sciences-Series IIA-Earth and Planetary Science, 326(12), p. 847-853. https://doi.org/10.1016/S1251-8050(98)80023-2

Azdimousa, A., Bourgois, J., Poupeau, G., Vazquez, M., Asebriy, L. and Labrin, E., **2013**. Fission track thermochronology of the Beni Bousera peridotite massif (Internal Rif, Morocco) and the exhumation of ultramafic rocks in the Gibraltar Arc. Arabian Journal of Geosciences, 7(5), p. 1993-2005.B https://doi.org/10.1007/s12517-013-0924-3

Babault, J., Teixell, A., Arboleya, M.L. and Charroud, M., **2008**. A Late Cenozoic age for long-wavelength surface uplift of the Atlas Mountains of Morocco. Terra nova, 20(2), pp.102-107. https://doi.org/10.1111/j.1365-3121.2008.00794.x

Baldwin, S.L., Harrison, T.M. and Burke, K., **1986**. Fission track evidence for the source of accreted sandstones, Barbados. Tectonics, 5(3), p. 457-468. https://doi.org/10.1029/TC005i003p00457

Balestrieri, M.L., Moratti, G., Bigazzi, G. and Algouti, A., **2009**. Neogene exhumation of the Marrakech High Atlas (Morocco) recorded by apatite fission-track analysis: Terra Nova, 21, p. 75–82. https://doi.org/10.1111/j.1365-3121.2008.00857.x

Barbarand, J., Lucazeau, F., Pagel, M. and Séranne, M., **2001**. Burial and exhumation history of the south-eastern Massif Central (France) constrained by apatite fission-track thermochronology. Tectonophysics, 335(3-4), p. 275-290. https://doi.org/10.1016/S0040-1951(01)00069-5

Barbarand, J., Marques, F.O., Hildenbrand, A., Pinna-Jamme, R. and Nogueira, C.R., **2021**. Thermal evolution of onshore West Iberia: A better understanding of the ages of breakup and rift-to-drift in the Iberia-Newfoundland Rift. Tectonophysics, 813, p.228926. https://doi.org/10.1016/j.tecto.2021.228926

Barbero, L., Jabaloy, A., Gómez-Ortiz, D., Pérez-Peña, J.V., Rodríguez-Peces, M.J., Tejero, R., Estupiñán, J., Azdimousa, A., Vázquez, M. and Asebriy, L., **2011**. Evidence for surface uplift of the Atlas Mountains and the surrounding peripheral plateaux: Combining apatite fission-track results and geomorphic indicators in the Western Moroccan Meseta (coastal Variscan Paleozoic basement): Tectonophysics, 502, p. 90–104. https://doi.org/10.1016/j.tecto.2010.01.005

Barbero, L., Glasmacher, U.A., Villaseca, C., López García, J.A. and Martín-Romera, C., **2005**. Long-term thermo-tectonic evolution of the Montes de Toledo area (Central Hercynian Belt, Spain): constraints from apatite fission-track analysis. International Journal of Earth Sciences, 94(2), p. 193-203. https://doi.org/10.1007/s00531-004-0455-y

Barbero, L. and **López-Garrido**, A.C., **2006**. Mesozoic thermal history of the Prebetic continental margin (southern Spain): Constraints from apatite fission-track analysis. Tectonophysics, 422(1-4), p. 115-128. https://doi.org/10.1016/j.tecto.2006.05.011

Barbero, L., Teixell, A., Arboleya, M.-L., Río, P.D., Reiners, P.W. and Bougadir, B., **2007**. Jurassic-to-present thermal history of the central High Atlas (Morocco) assessed by low-temperature thermochronology: Terra Nova, 19, p. 58–64. https://doi.org/10.1111/j.1365-3121.2006.00715.x

Basile, C., Girault, I., Paquette, J.L., Agranier, A., Loncke, L., Heuret, A. and Poetisi, E., **2020**. The Jurassic magmatism of the Demerara Plateau (offshore French Guiana) as a remnant of the Sierra Leone hotspot during the Atlantic rifting. Scientific Reports, 10(1), p.1-12. https://doi.org/10.1038/s41598-020-64333-5

Bea, F., Bortnikov, N., Montero, P., Zinger, T., Sharkov, E., Silantyev, S., Skolotnev, S., Trukhalev, A. and Molina-Palma, J.F., **2020**. Zircon xenocryst evidence for crustal recycling at the Mid-Atlantic Ridge. Lithos, 354, p. 105361. https://doi.org/10.1016/j.lithos.2019.105361

Bermudez, M.A., **2009.** Cenozoic exhumation patterns across the Venezuelan Andes: insights from fission-track thermochronology. Université Joseph Fourier-Grenoble I, Ph.D. Thesis, 314 p. (a, b, c, and d, are chapters).

Bermúdez, M.A., Kohn, B.P., van der Beek, P.A., Bernet, M., O'Sullivan, P.B. and Shagam, R., **2010**. Spatial and temporal patterns of exhumation across the Venezuelan Andes: Implications for Cenozoic Caribbean geodynamics. Tectonics, 29(5). https://doi.org/10.1029/2009TC002635

Bermúdez, M.A., van der Beek, P. and Bernet, M., **2011**. Asynchronous Miocene–Pliocene exhumation of the central Venezuelan Andes. Geology, 39(2), p. 139-142. https://doi.org/10.1130/G31582.1

Bernet, M., **2009**). A field-based estimate of the zircon fission-track closure temperature. Chemical Geology, 259(3-4), p. 181-189. https://doi.org/10.1016/j.chemgeo.2008.10.043

Bertotti, G., **2001**. Subsidence, deformation, thermal and mechanical evolution of the Mesozoic South Alpine rifted margin: an analogue for Atlantic-type margins. Geological Society, London, Special Publications, 187(1), pp.125-141. https://doi.org/10.1144/GSL.SP.2001.187.01.07

Bertotti, G. and **Gouiza**, M., **2012**. Post-rift vertical movements and horizontal deformations in the eastern margin of the Central Atlantic: Middle Jurassic to Early Cretaceous evolution of Morocco: International Journal of Earth Sciences, 101, p. 2151–2165. https://doi.org/10.1007/s00531-012-0773-4

Bessiere, E., Augier, R., Jolivet, L., Précigout, J. and Romagny, A., **2021**. Exhumation of the Ronda peridotite during hyper-extension: New structural and thermal constraints from the Nieves Unit (western Betic Cordillera, Spain). Tectonics, 40(10), p.e2020TC006271. https://doi.org/10.1029/2020TC006271

Blackmer, G.C., Omar, G.I. and Gold, D.P., **1994**. Post-Alleghanian unroofing history of the Appalachian Basin, Pennsylvania, from apatite fission track analysis and thermal models. Tectonics, 13(5), p. 1259-1276. https://doi.org/10.1029/94TC01507

Blackmer, G.C., **1992**. Post-Alleghanian thermal and unroofing history of the Appalachian Basin, Pennsylvania: The Pennsylvania State University, Ph.D. Thesis, 172 p.

Biari, Y., Klingelhoefer, F., Sahabi, M., Aslanian, D., Schnurle, P., Berglar, K., Moulin, M., Mehdi, K., Graindorge, D., Evain, M. and Benabdellouahed, M., **2015**. Deep crustal structure of the North-West

African margin from combined wide-angle and reflection seismic data (MIRROR seismic survey). Tectonophysics, 656, p.154-174. https://doi.org/10.1016/j.tecto.2015.06.019

Biari, Y., Klingelhoefer, F., Sahabi, M., Funck, T., Benabdellouahed, M., Schnabel, M., Reichert, C., Gutscher, M.A., Bronner, A. and Austin, J.A., **2017**. Opening of the central Atlantic Ocean: implications for geometric rifting and asymmetric initial seafloor spreading after continental breakup. Tectonics, 36(6), p.1129-1150. https://doi.org/10.1002/2017TC004596

Biari, Y., Klingelhoefer, F., Franke, D., Funck, T., Loncke, L., Sibuet, J.C., Basile, C., Austin, J.A., Rigoti, C.A., Sahabi, M. and Benabdellouahed, M., **2021**. Structure and evolution of the Atlantic passive margins: A review of existing rifting models from wide-angle seismic data and kinematic reconstruction. Marine and Petroleum Geology, 126, p. 104898. https://doi.org/10.1016/j.marpetgeo.2021.104898

Bird, D.E., Hall, S.A., Burke, K., Casey, J.F. and Sawyer, D.S., **2007**. Early central Atlantic Ocean seafloor spreading history. Geosphere, 3(5), p.282-298. https://doi.org/10.1130/GES00047.1

Boettcher, S.S. and **Milliken**, K.L., **1994**. Mesozoic-Cenozoic unroofing of the southern Appalachian Basin: Apatite fission track evidence from Middle Pennsylvanian sandstones. The Journal of Geology, 102(6), p. 655-668. https://doi.org/10.1086/629710

Bonilla, A., Franco, J.A., Cramer, T., Poujol, M., Cogné, N., Nachtergaele, S. and De Grave, J., **2019**. Apatite LA-ICP-MS U–Pb and fission-track geochronology of the Caño Viejita gabbro in E-Colombia: Evidence for Grenvillian intraplate rifting and Jurassic exhumation in the NW Amazonian Craton. Journal of South American Earth Sciences, 98, p.102438. https://doi.org/10.1016/j.jsames.2019.102438

Boscaini, A., Marzoli, A., Bertrand, H., Chiaradia, M., Jourdan, F., Faccenda, M., Meyzen, C.M., Callegaro, S. and Durán, L.S., **2022**. Cratonic keels controlled the emplacement of the Central Atlantic Magmatic Province (CAMP). Earth and Planetary Science Letters, 584, p. 117480. https://doi.org/10.1016/j.epsl.2022.117480

Botor, D. and **Anczkiewicz**, A.A., **2015**. Thermal history of the Sabero Coalfield (Southern Cantabrian Zone, NW Spain) as revealed by apatite fission track analyses from tonstein horizons: implications for timing of coalification. International Journal of Earth Sciences, 104(7), p. 1779-1793. https://doi.org/10.1007/s00531-015-1169-z

Bouillin, J.P., Poupeau, G., Labrin, E., Basile, C., Sabil, N., Mascle, J., Mascle, G., Gillot, F. and Riou, L., **1997**. Fission track study: heating and denudation of marginal ridge of the Ivory Coast–Ghana transform margin. Geo-Marine Letters, 17(1), p. 55-61. https://doi.org/10.1007/PL00007208

Bradley, D.C., O'Sullivan, P., Cosca, M.A., Motts, H.A., Horton, J.D., Taylor, C.D., Beaudoin, G., Lee, G.K., Ramezani, J., Bradley, D.B., Jones, J.V., and Bowring, S., **2015**. Second Projet de Renforcement Institutionnel du Secteur Minier de la République Islamique de Mauritanie (PRISM-II) Phase V. USGS, Open-File Report 2013-1280. https://doi.org/10.3133/ofr20131280

Brandon, M.T., Roden-Tice, M.K. and Garver, J.I., **1998**. Late Cenozoic exhumation of the Cascadia accretionary wedge in the Olympic Mountains, northwest Washington State. Geological Society of America Bulletin, 110(8), p. 985-1009. https://doi.org/10.1130/0016-7606(1998)110<0985:LCEOTC>2.3.CO;2

Brown, R., Gallagher, K. and Duane, M., **1994**. A quantitative assessment of the effects of magmatism on the thermal history of the Karoo sedimentary sequence. Journal of African Earth Sciences, 18(3), pp.227-243. https://doi.org/10.1016/0899-5362(94)90007-8

Brownfield, M.E. and **Charpentier**, R.R., **2003**. Assessment of the undiscovered oil and gas of the Senegal Province, Mauritania, Senegal, the Gambia, and Guinea-Bissau, Northwest Africa (Vol. 25). Denver: US Department of the Interior, US Geological Survey Bulletin 2207-A, p. 1–29.

Brune, S., Heine, C., Pérez-Gussinyé, M. and Sobolev, S.V., **2014**. Rift migration explains continental margin asymmetry and crustal hyper-extension. Nature communications, 5(1), pp.1-9. https://doi.org/10.1038/ncomms5014

Burke, K. and **Gunnell**, Y., **2008**. The African erosion surface: a continental-scale synthesis of geomorphology, tectonics, and environmental change over the past 180 million years (Vol. 201). Geological Society of America, Memoir 201.

Caballero, V., Mora, A., Quintero, I., Blanco, V., Parra, M., Rojas, L.E., Lopez, C., Sánchez, N., Horton, B.K., Stockli, D. and Duddy, I., **2013**. Tectonic controls on sedimentation in an intermontane hinterland basin adjacent to inversion structures: The Nuevo Mundo syncline, Middle Magdalena Valley, Colombia. Geological Society, London, Special Publications, 377(1), p. 315-342. https://doi.org/10.1144/SP377.12

Caby, R. and **Kienast**, J.R., **2009**. Neoproterozoic and Hercynian metamorphic events in the Central Mauritanides: implications for the geodynamic evolution of West Africa. Journal of African Earth Sciences, 53(3), p. 122-136. https://doi.org/10.1016/j.jafrearsci.2008.09.004

Callegaro, S., Rapaille, C., Marzoli, A., Bertrand, H., Chiaradia, M., Reisberg, L., Bellieni, G., Martins, L., Madeira, J., Mata, J. and Youbi, N., **2014**. Enriched mantle source for the Central Atlantic magmatic province: new supporting evidence from southwestern Europe. Lithos, 188, p. 15-32. https://doi.org/10.1016/j.lithos.2013.10.021

Campanile, D.J., **2007**. The post-breakup evolution of the western Indian high-elevation passive margin: University of Glasgow, Ph.D. Thesis, 223 p.

Carpéna, J., Kienast, J.R., Ouzegane, K. and Jehanno, C., **1988**. Evidence of the contrasted fission-track clock behavior of the apatites from In Ouzzal carbonatites (northwest Hoggar): The low-temperature thermal history of an Archean basement. Geological Society of America Bulletin, 100(8), p. 1237-1243.

Carpena, J., **1982**. Late thermal history of the Hoggar shield (western Africa). In Abstracts workshop on Fission-Track Dating, 5th Int. Conf. Geochronology, Cosmochronology and Isotope Geology, Nikko National Park (Japan) (p. 6).

Carrière, K.L., **2006**. Neoproterozoic to Holocene tectonothermal evolution of the southern Cantabrian Mountains NW Iberia, revealed by apatite fission-track thermochronology. Heidelberg University, Ph.D. Thesis, 289 p.

Casson, M., Jeremiah, J., Calvès, G., de Goyet, F.D.V., Reuber, K., Bidgood, M., Reháková, D., Bulot, L. and Redfern, J., **2021**. Evaluating the segmented post-rift stratigraphic architecture of the Guyanas continental margin. Petroleum Geoscience, 27(3), p. petgeo2020-099. https://doi.org/10.1144/petgeo2020-099

Casson, M., Calvès, G., Huuse, M., Sayers, B. and Redfern, J., **2021**. Cretaceous continental margin evolution revealed using quantitative seismic geomorphology, offshore northwest Africa. Basin Research, 33(1), p. 66-90. https://doi.org/10.1111/bre.12455

Cavellec, S., **2006**. Evolution diagénétique du bassin de Tim Mersoï et conséquences pour la genèse des minéralisations uranifères dans les formations carbonifères du Guezouman et du Tarat (district Arlit-Akokan, Niger). Paris 11, Ph.D. Thesis, 449 p.

Centeno, J.P., **2005**. Exhumation and incision history of the Torngat Mountains, northern Labrador and Quebec, Canada, using apatite (U-Th)/He thermochronology. University of Kansas, M.Sc. Thesis, 99 p.

Chang, C., **2017**. Low Temperature Thermal History of Mainland Nova Scotia Using Apatite and Zircon (U-Th)/He Thermochronology. Halifax University, B.Sc. Thesis, 63 p.

Charrière, A. and **Haddoumi**, H., **2016**. Les «Couches rouges» continentales jurassico-crétacées des Atlas marocains (Moyen Atlas, Haut Atlas central et oriental): Bilan stratigraphique, paléogéographies successives et cadre géodynamique: Boletín geológico y minero, 127, p. 407–430.

Charton, R., Bertotti, G., Arantegui, A. and Bulot, L., **2018**. The Sidi Ifni transect across the rifted margin of Morocco (Central Atlantic): Vertical movements constrained by low-temperature thermochronology: Journal of African Earth Sciences, 141, p. 22-32. https://doi.org/10.1016/j.jafrearsci.2018.01.006

Charton, R., Bertotti, G., Duval-Arnould, A., Storms, J.E.A. and Redfern, J., **2021**. Low-temperature thermochronology as a control on vertical movements for semi-quantitative source-to-sink analysis: A case study for the Permian to Neogene of Morocco and surroundings. Basin Research, 33(2), p. 1337-1383. https://doi.org/10.1111/bre.12517

Chopin, F., Corsini, M., Schulmann, K., Houicha, El, M., Ghienne, J.-F. and Edel, J.-B., **2014**. Tectonic evolution of the Rehamna metamorphic dome (Morocco) in the context of the Alleghanian-Variscan orogeny: Tectonics, 33, p. 1154–1177. https://doi.org/10.1002/2014TC003539

Chopin, F., et al., in review. In U–Pb geochronology of granitoids from the Meseta (Northwest Africa): a two-step tale for the evolution of the Variscan domain (minor revisions)

Clark, S.J.P. and Dempster, T.J., **2009**. The record of tectonic denudation and erosion in an emerging orogen: an apatite fission-track study of the Sierra Nevada, southern Spain. Journal of the Geological Society, 166(1), p. 87-100. https://doi.org/10.1144/0016-76492008-041

Clift, P., Carter, A., & Hurford, A., **1998**. Apatite fission track analysis of sites 959 and 960 on the transform continental margin of Ghana, West Africa. Proceedings of the Ocean Drilling Program: Scientific Results, 159, 35-41. https://doi.org/10.2973/odp.proc.sr.159.004.1998

Clift, P.D., Dewey, J.F., Draut, A.E., Chew, D.M., Mange, M. and Ryan, P.D., **2004**). Rapid tectonic exhumation, detachment faulting and orogenic collapse in the Caledonides of western Ireland: Tectonophysics, 384, p. 91–113. https://doi.org/10.1016/j.tecto.2004.03.009

Cogné, N., Gallagher, K. and Cobbold, P.R., **2011**). Post-rift reactivation of the onshore margin of southeast Brazil: Evidence from apatite (U–Th)/He and fission-track data. Earth and Planetary Science Letters, 309(1-2), p. 118-130. https://doi.org/10.1016/j.epsl.2011.06.025

Corrigan, J., Cervany, P.F., Donelick, R. and Bergman, S.C., **1998**. Postorogenic denudation along the late Paleozoic Ouachita trend, south central United States of America: Magnitude and timing constraints from apatite fission track data. Tectonics, 17(4), pp.587-603. https://doi.org/10.1029/98TC01316

Crowley, K.D. and Kuhlman, S.L., **1988.** Apatite thermochronometry of western Canadian Shield: implications for origin of the Williston Basin. Geophysical Research Letters, 15(3), pp.221-224. https://doi.org/10.1029/GL015i003p00221

Crowley, K.D., Naeser, C.W. and Babel, C.A., **1986**. Tectonic significance of Precambrian apatite fission-track ages from the midcontinent United States. Earth and Planetary Science Letters, 79(3-4), pp.329-336. https://doi.org/10.1016/0012-821X(86)90189-5

Crowley, K.D., **1991**. Thermal history of Michigan Basin and Southern Canadian Shield from apatite fission track analysis. Journal of Geophysical Research: Solid Earth, 96(B1), pp.697-711. https://doi.org/10.1029/90JB02174

Cruz, L., Fayon, A., Teyssier, C., Weber, J. and Till, A.B., **2007**. Exhumation and deformation processes in transpressional orogens: The Venezuelan Paria Peninsula, SE Caribbean-South American plate boundary. SPECIAL PAPERS-GEOLOGICAL SOCIETY OF AMERICA, 434, p.149. in : Exhumation Associated with Continental Strike-Slip Fault Systems, Sarah M. Roeske, Alison B. Till, David A. Foster, James C. Sample. https://doi.org/10.1130/2007.2434(08)

Currie, K.L., Eby, G.N. and Gittins, J., **1986**. The petrology of the Mont Saint Hilaire complex, southern Quebec: An alkaline gabbro-peralkaline syenite association. Lithos, 19(1), pp.65-81. https://doi.org/10.1016/0024-4937(86)90016-2

Davison, I., **2005**). Central Atlantic margin basins of North West Africa: Geology and hydrocarbon potential (Morocco to Guinea): Journal of African Earth Sciences, 43, p. 254–274. https://doi.org/10.1016/j.jafrearsci.2005.07.018

De Bruijne, C.H. and **Andriessen**, P.A.M., **2000**. Interplay of intraplate tectonics and surface processes in the Sierra de Guadarrama (central Spain) assessed by apatite fission track analysis. Physics and

Chemistry of the Earth, Part A: Solid Earth and Geodesy, 25(6-7), pp.555-563. https://doi.org/10.1016/S1464-1895(00)00085-5

de Pina, A.C.M., Moura, C.A. and Vignol-Lelarge, M.L., **2014**. Termocronologia por traços de fissão em apatita em rochas ígneas do embasamento e sedimentar da Bacia do Amazonas, na região de Itaituba, PA, Brasil. Pesquisas em Geociências, 41(1), pp.39-50. https://doi.org/10.22456/1807-9806.78033

DeFelipe, I., Pedreira, D., Pulgar, J.A., Van der Beek, P.A., Bernet, M. and Pik, R., **2019**. Unraveling the Mesozoic and Cenozoic tectonothermal evolution of the eastern Basque-Cantabrian zone–western Pyrenees by low-temperature thermochronology. Tectonics, 38(9), pp.3436-3461. https://doi.org/10.1029/2019TC005532

Del Rio, P., Barbero, L. and Stuart, F.M., **2009**. Exhumation of the Sierra de Cameros (Iberian Range, Spain): constraints from low-temperature thermochronology. Geological Society, London, Special Publications, 324(1), pp.153-166. https://doi.org/10.1144/SP324.12

Delchini, S., Lahfid, A., Lacroix, B., Baudin, T., Hoepffner, C., Guerrot, C., Lach, P., Saddiqi, O. and Ramboz, C., **2018**). The geological evolution of the Variscan Jebilet Massif, Morocco, inferred from new structural and geochronological analyses. Tectonics, 37(12), p. 4470-4493. https://doi.org/10.1029/2018TC005002

Delfaud, **1974**. La sédimentation deltaïque ancienne : exemples nord sahariens. Bull. Centre Rech. Pau, SNPA, 8(1), pp.241-263.

DeLucia, M.S., Guenthner, W.R., Marshak, S., Thomson, S.N. and Ault, A.K., **2018**. Thermochronology links denudation of the Great Unconformity surface to the supercontinent cycle and snowball Earth. Geology, 46(2), pp.167-170. https://doi.org/10.1130/G39525.1

Derycke, A., Gautheron, C., Bourbon, P., Pinna-Jamme, R., Aertgeerts, G., Simon-Labric, T., **2018.** French Guyana margin evolution: insight by low-temperature thermochronological data. Thermo2018. https://doi.org/10.13140/RG.2.2.27509.01769/1

Derycke, A., Gautheron, C., Barbarand, J., Bourbon, P., Aertgeerts, G., Simon-Labric, T., Sarda, P., Pinna-Jamme, R., Boukari, C. and Haurine, F., **2021**. French Guiana margin evolution: From Gondwana break-up to Atlantic opening. Terra Nova, 33(4), pp.415-422. https://doi.org/10.1111/ter.12526

Doherty, J.T. and **Lyons**, J.B., **1980**. Mesozoic erosion rates in northern New England. Geological Society of America Bulletin, 91(1), pp.16-20. https://doi.org/10.1130/0016-7606(1980)91%3C16:MERINN%3E2.0.CO;2

Domènech, M., **2015**. Rift opening and inversion in the Marrakech High Atlas: integrated structural and thermochronologic study. Universitat Autònoma de Barcelona, Ph.D. Thesis, 157 p.

Domènech, M., Teixell, A. and Stöckli, D.F., **2016**. Magnitude of rift-related burial and orogenic contraction in the Marrakech High Atlas revealed by zircon (U-Th)/He thermochronology and thermal modeling: Tectonics, 35, p. 2609–2635. https://doi.org/10.1002/2016TC004283

Eby, G.N., Roden-Tice, M., Krueger, H.L., Ewing, W., Faxon, E.H. and Woolley, A.R., **1995**. Geochronology and cooling history of the northern part of the Chilwa Alkaline Province, Malawi. Journal of African Earth Sciences, 20(3-4), pp.275-288. https://doi.org/10.1016/0899-5362(95)00054-W

Emberley, J., **2016**. Tracking low temperature tectonism of the St. Lawrence Platform and Humber Zone, southern Quebec Appalachians through apatite and zircon (U-Th)/He thermochronology. University of Ottawa, M.Sc. Thesis, 94 p.

Emberley, J.M. and **Schneider**, D.A., **2017**. Tracking low-temperature tectonism of the St. Lawrence Platform and Humber Zone, southern Quebec Appalachians, through apatite and zircon (U–Th)/He thermochronology. Canadian Journal of Earth Sciences, 54(8), pp.827-849. https://doi.org/10.1139/cjes-2016-0199

Escosa, F.O., Leprêtre, R., Spina, V., Gimeno-Vives, O., Kergaravat, C., Mohn, G. and de Lamotte, D.F., **2021**. Polyphased mesozoic rifting from the Atlas to the north-west Africa paleomargin. Earth-Science Reviews, 220, p.103732. https://doi.org/10.1016/j.earscirev.2021.103732

Esteban, J.J., Tubía, J.M., Cuevas, J., Seward, D., Larionov, A., Sergeev, S. and Navarro-Vilá, F., **2013**. Insights into extensional events in the Betic Cordilleras, southern Spain: New fission-track and U–Pb SHRIMP analyses. Tectonophysics, 603, pp.179-188. https://doi.org/10.1016/j.tecto.2013.05.027

El Hadi, H., Simancas, J.F., Tahiri, A., González-Lodeiro, F., Azor, A. and Martínez-Poyatos, D., **2006**. Comparative review of the Variscan granitoids of Morocco and Iberia: proposal of a broad zonation. Geodinamica Acta, 19(2), p. 103-116. https://doi.org/10.3166/ga.19.103-116

El Haimer, F.Z., **2014**. Mouvements verticaux post-Varisques des domaines Mesetien et Atlasique: Thermochronology basse température sur apatite et zircon: Université Hassan II, Ph.D. Thesis, 124 p.

England, P. and **Molnar**, P., **1990**. Surface uplift, uplift of rocks, and exhumation of rocks. Geology, 18(12), pp.1173-1177. https://doi.org/10.1130/0091-7613(1990)018%3C1173:SUUORA%3E2.3.CO;2

English, K.L., Redfern, J., Bertotti, G., English, J.M. and Cherif, R.Y., 2017. Intraplate uplift: new constraints on the Hoggar dome from the Illizi basin (Algeria). Basin Research, 29(3), pp.377-393. https://doi.org/10.1111/bre.12182

Etheve, N., Mohn, G., Frizon de Lamotte, D., Roca, E., Tugend, J. and Gómez-Romeu, J., **2018**. Extreme Mesozoic crustal thinning in the eastern Iberia margin: The example of the Columbrets Basin (Valencia Trough). Tectonics, 37(2), pp.636-662. https://doi.org/10.1002/2017TC004613

Fabre, J., **2005**. Géologie du Sahara occidental et central. Musée Royal de l'Afrique Central, Tervuren, African Geoscience Collection, 108.

Fame, M.L., Spotila, J.A., Owen, L.A. and Shuster, D.L., **2019**. Consistent slow exhumation in a late Cenozoic glaciated landscape: The Presidential and Carter Ranges of the White Mountains in New Hampshire, USA. Geomorphology, 345, p.106842. https://doi.org/10.1016/j.geomorph.2019.106842

Feinstein, S., Kohn, B., Osadetz, K., Everitt, R. and O'Sullivan, P., **2009**. Variable Phanerozoic thermal history in the Southern Canadian Shield: Evidence from an apatite fission track profile at the Underground Research Laboratory (URL), Manitoba. Tectonophysics, 475(1), pp.190-199. https://doi.org/10.1016/j.tecto.2009.01.016

Fernandez, O., **2019**. The Jurassic evolution of the Africa-Iberia conjugate margin and its implications on the evolution of the Atlantic-Tethys triple junction. Tectonophysics, 750, pp.379-393. https://doi.org/10.1016/j.tecto.2018.12.006

Fernie, N., Glorie, S., Jessell, M.W. and Collins, A.S., **2018**. Thermochronological insights into reactivation of a continental shear zone in response to Equatorial Atlantic rifting (northern Ghana). Scientific reports, 8(1), pp.1-14. https://doi.org/10.1038/s41598-018-34769-x

Filleaudeau, P.Y., Mouthereau, F. and Pik, R., **2012**. Thermo-tectonic evolution of the south-central Pyrenees from rifting to orogeny: Insights from detrital zircon U/Pb and (U-Th)/He thermochronometry. Basin Research, 24(4), pp.401-417. https://doi.org/10.1111/j.1365-2117.2011.00535.x

Fillon, C. and **van der Beek**, P., **2012**. Post-orogenic evolution of the southern Pyrenees: Constraints from inverse thermo-kinematic modelling of low-temperature thermochronology data. Basin Research, 24(4), pp.418-436. https://doi.org/10.1111/j.1365-2117.2011.00533.x

Fillon, C., Gautheron, C. and van der Beek, P., **2013**. Oligocene–Miocene burial and exhumation of the Southern Pyrenean foreland quantified by low-temperature thermochronology. Journal of the Geological Society, 170(1), pp.67-77. https://doi.org/10.1144/jgs2012-051

Fillon, C., Pedreira, D., Van der Beek, P.A., Huismans, R.S., Barbero, L. and Pulgar, J.A., **2016**. Alpine exhumation of the central Cantabrian mountains, northwest Spain. Tectonics, 35(2), pp.339-356. https://doi.org/10.1002/2015TC004050

Fitzgerald, P.G., Muñoz, J.A., Coney, P.J. and Baldwin, S.L., **1999**. Asymmetric exhumation across the Pyrenean orogen: implications for the tectonic evolution of a collisional orogen. Earth and Planetary Science Letters, 173(3), pp.157-170. https://doi.org/10.1016/S0012-821X(99)00225-3

Flowers, R.M. and **Ehlers**, T.A., **2018**. Rock erodibility and the interpretation of low-temperature thermochronologic data: Earth and Planetary Science Letters, 482, p. 312–323. https://doi.org/10.1016/j.epsl.2017.11.018

Flowers, R.M. & **Kelley**, S.A., **2011**. Interpreting data dispersion and 'inverted' dates in apatite (U–Th)/He and fission-track datasets: An example from the US Midcontinent. Geochimica et Cosmochimica Acta, 75, p. 5169–5186. https://doi.org/10.1016/j.gca.2011.06.016

Ford, D. and **Golonka**, J., **2003**. Phanerozoic paleogeography, paleoenvironment and lithofacies maps of the circum-Atlantic margins. Marine and petroleum geology, 20(3-4), pp.249-285. https://doi.org/10.1016/S0264-8172(03)00041-2

Frizon de Lamotte, D., Zizi, M. et al. **2008**. The Atlas system. In: Michard, A., Chalouan, A. & Saddiqi, O. (eds) Continental Evolution: The Geology of Morocco. Structure, Stratigraphy, and Tectonics of the Africa–Atlantic–Mediterranean Triple Junction. Lecture Notes in Earth Sciences, 116. Springer, Berlin, 133–202, https://doi.org/10.1007/978-3-540-77076-3_4

Frizon de Lamotte, D., Fourdan, B., Leleu, S., Leparmentier, F. and de Clarens, P., **2015**. Style of rifting and the stages of Pangea breakup: Tectonics, 34, p. 1009–1029. https://doi.org/10.1002/2014TC003760

Frizon de Lamotte, D., Leturmy, P., Missenard, Y., Khomsi, S., Ruiz, G., Saddiqi, O., Guillocheau, F. and Michard, A., **2009**. Mesozoic and Cenozoic vertical movements in the Atlas system (Algeria, Morocco, Tunisia): An overview: Tectonophysics, 475, p. 9–28. https://doi.org/10.1016/j.tecto.2008.10.024

Fügenschuh, B., Froitzheim, N., Capdevila, R. and Boillot, G., **2003**. Offshore granulites from the Bay of Biscay margins: fission tracks constrain a Proterozoic to Tertiary thermal history. Terra Nova, 15(5), pp.337-342. https://doi.org/10.1046/j.1365-3121.2003.00502.x

Funck, T., Jackson, H.R., Louden, K.E., Dehler, S.A. and Wu, Y., **2004**. Crustal structure of the northern Nova Scotia rifted continental margin (eastern Canada). Journal of Geophysical Research: Solid Earth, 109(B9). https://doi.org/10.1029/2004JB003008

Gallagher, K., **2012**. Transdimensional inverse thermal history modeling for quantitative thermochronology: Solid Earth, 117, p. 2156–2202. https://doi.org/10.1029/2011JB008825

Gallagher, K., Brown, R. and Johnson, C., **1998**. Fission track analysis and its applications to geological problems: Annual Review of Earth and Planetary Sciences, 26, p. 519–572. https://doi.org/10.1146/annurev.earth.26.1.519

Gallagher, K., Hawkesworth, C.J. and Mantovani, M.S.M., **1994**. The denudation history of the onshore continental margin of SE Brazil inferred from apatite fission track data. Journal of Geophysical Research: Solid Earth, 99(B9), pp.18117-18145. https://doi.org/10.1029/94JB00661

Gallagher, K. and **Brown**, R., **1997**. The onshore record of passive margin evolution. Journal of the Geological Society, 154(3), pp.451-457. https://doi.org/10.1144/gsjgs.154.3.0451

Gallagher, K. and **Brown**, R., **1999**. Denudation and uplift at passive margins: the record on the Atlantic Margin of southern Africa. Philosophical Transactions of the Royal Society of London. Series A: Mathematical, Physical and Engineering Sciences, 357(1753), pp.835-859. https://doi.org/10.1098/rsta.1999.0354

Gallen, S.F., Wegmann, K.W. and Bohnenstiehl, D.R., **2013**. Miocene rejuvenation of topographic relief in the southern Appalachians. GSA Today, 23(2), pp.4-10. https://doi.org/10.1130/GSATG163A.1.

Gasquet, D., Stussi, J.M. and Nachit, H., **1996**. Les granitoïdes hercyniens du Maroc dans le cadre de l'évolution géodynamique régionale. Bulletin de la Société Géologique de France, 167(4), pp.517-528.

Geoffroy, L., **2005**. Volcanic passive margins. Comptes Rendus Geoscience, 337(16), pp.1395-1408. https://doi.org/10.1016/j.crte.2005.10.006

Gemignani, L., Sun, X., Braun, J., van Gerve, T.D. and Wijbrans, J.R., **2017**. A new detrital mica 40Ar/39Ar dating approach for provenance and exhumation of the Eastern Alps. Tectonics, 36(8), pp.1521-1537. https://doi.org/10.1002/2017TC004483

Gibson, M., Sinclair, H.D., Lynn, G.J. and Stuart, F.M., **2007**. Late-to post-orogenic exhumation of the Central Pyrenees revealed through combined thermochronological data and modelling. Basin Research, 19(3), pp.323-334. https://doi.org/10.1111/j.1365-2117.2007.00333.x

Ghorbal, B., **2009**. Mesozoic to Quaternary thermo-tectonic evolution of Morocco (NW Africa): Vrije Universiteit Amsterdam, Ph.D. Thesis, 226 p.

Ghorbal, B., Bertotti, G., Foeken, J. and Andriessen, P., **2008**. Unexpected Jurassic to Neogene vertical movements in ‘stable’ parts of NW Africa revealed by low temperature geochronology: Terra Nova, 20, p. 355–363. https://doi.org/10.1111/j.1365-3121.2008.00828.x

Gimeno-Vives, O., Frizon de Lamotte, D., Leprêtre, R., Haissen, F., Atouabat, A. and Mohn, G., **2020**. The structure of the Central-Eastern External Rif (Morocco); Poly-phased deformation and role of the under-thrusting of the North-West African paleo-margin. Earth-science reviews, 205, p.103198. https://doi.org/10.1016/j.earscirev.2020.103198

Gimeno-Vives, O., Mohn, G., Bosse, V., Haissen, F., Zaghloul, M. N., Atouabat, A., and Frizon de Lamotte, D., **2019**. The Mesozoic margin of the Maghrebian Tethys in the Rif belt (Morocco): Evidence for polyphase rifting and related magmatic activity: Tectonics, 38, 2894–2918. https://doi.org/10.1029/2019TC005508

Girard, J.P., Eichenseer, H., Kabbej, A. and Idris, K.M., **2015**. Regional Synthesis of Thermal-Burial Regimes in the Paleozoic-Proterozoic Series of the Taoudenni Basin, Adrar, Mauritania: Fluid Inclusion and Thermochronology Data. In International Petroleum Technology Conference. OnePetro. https://doi.org/10.2523/IPTC-18423-MS

Glover, R.T., **1999**. Aspects of intraplate deformation in Saharan cratonic basins. University of Wales, Aberystwyth, Ph.D. Thesis, 479 p.

Gouiza, M., **2011**. Mesozoic source-to-sink systems in NW Africa: Geology of vertical movements during the birth and growth of the Moroccan rifted margin: Vrije Universiteit Amsterdam, Ph.D. Thesis, 170 p.

Gouiza, M., Charton, R., Bertotti, G., Andriessen, P. and Storms, J.E.A., **2017a**. Post-Variscan evolution of the Anti-Atlas belt of Morocco constrained from low-temperature geochronology: International Journal of Earth Sciences, 106, p. 593–616. https://doi.org/10.1007/s00531-016-1325-0

Gouiza, M., Bertotti, G., and Andriessen, P. A., **2017b**. Mesozoic and Cenozoic thermal history of the Western Reguibat Shield (West African Craton). Terra Nova, 30, p. 135-145. https://doi.org/10.1111/ter.12318

Gouiza, M., Bertotti, G., Charton, R., Haimoudane, K., Dunkl, I., and Anczkiewicz, A. A., **2019**. New Evidence of 'Anomalous' Vertical Movements along the Hinterland of the Atlantic NW African Margin. Journal of Geophysical Research: Solid Earth, 24, p. 13 333-13 353. https://doi.org/10.1029/2019JB017914.

Gradstein, F.M., Agterberg, F. P., Ogg, J. G., Hardenbol, J., Van Veen, P., Thierry, J. & Huang, Z., 1994. A Mesozoic time scale. Journal of Geophysical Research, 99(B12), pp.24051-24074.

Gradstein, F.M., Ogg, J.G., Smith, A.G., Bleeker, W., Lourens, L.J., **2004**. A new Geologic Time Scale, with special reference to Precambrian and Neogene. Episodes, 27, pp.83-100.

Gray, G.G., Villagomez, D., Pindell, J., Molina-Garza, R., O'Sullivan, P., Stockli, D., Farrell, W., Blank, D. and Schuba, J., **2021**. Late Mesozoic and Cenozoic thermotectonic history of eastern, central and southern Mexico as determined through integrated thermochronology, with implications for sediment delivery to the Gulf of Mexico. Geological Society, London, Special Publications, 504(1), pp.255-283. https://doi.org/10.1144/SP504-2019-243

Green, P.F., Duddy, I.R., Laslett, G.M., Hegarty, K.A., Gleadow, A.W. and Lovering, J.F., **1989**. Thermal annealing of fission tracks in apatite 4. Quantitative modelling techniques and extension to geological timescales. Chemical Geology: Isotope Geoscience Section, 79(2), pp.155-182. https://doi.org/10.1016/0168-9622(89)90018-3

Green, P.F., Japsen, P., Chalmers, J.A., Bonow, J.M. and Duddy, I.R., **2018**. Post-breakup burial and exhumation of passive continental margins: Seven propositions to inform geodynamic models: Gondwana Research, 53, p. 58–81. https://doi.org/10.1016/j.gr.2017.03.007

Green, P.F. and **Machado**, V., **2017**. Pre-rift and syn-rift exhumation, post-rift subsidence and exhumation of the onshore Namibe Margin of Angola revealed from apatite fission track analysis. Geological Society, London, Special Publications, 438(1), pp.99-118. https://doi.org/10.1144/SP438.2

Grist, A.M. and **Zentilli**, M., **2003**. Post-Paleocene cooling in the southern Canadian Atlantic region: evidence from apatite fission track models. Canadian Journal of Earth Sciences, 40(9), pp.1279-1297. https://doi.org/10.1139/e03-045

Grist, A.M., Ryan, R.J. and Zentilli, M., **1995**. The thermal evolution and timing of hydrocarbon generation in the Maritimes Basin of eastern Canada: evidence from apatite fission track data. Bulletin of Canadian Petroleum Geology, 43(2), pp.145-155. https://doi.org/10.35767/gscpgbull.43.2.145

Grobe, R.W., Alvarez-Marrón, J., Glasmacher, U.A. and Menéndez-Duarte, R., **2010**. Low-temperature exhumation history of Variscan-age rocks in the western Cantabrian Mountains (NW Spain) recorded by apatite fission-track data. Tectonophysics, 489(1-4), pp.76-90. https://doi.org/10.1016/j.tecto.2010.04.006

Grobe, R.W., Alvarez-Marrón, J., Glasmacher, U.A. and Stuart, F.M., **2014**. Mesozoic exhumation history and palaeolandscape of the Iberian Massif in eastern Galicia from apatite fission-track and (U-Th)/He data. International Journal of Earth Sciences, 103(2), pp.539-561. https://doi.org/10.1007/s00531-013-0976-3

Guenthner, W.R., Reiners, P.W., Ketcham, R.A., Nasdala, L. and Giester, G., **2013**. Helium diffusion in natural zircon: Radiation damage, anisotropy, and the interpretation of zircon (U-Th)/He thermochronology. American Journal of Science, 313(3), pp.145-198. https://doi.org/10.2475/03.2013.01

Guerit, L., Barrier, L., Jolivet, M., Fu, B. and Métivier, F., **2016**. Denudation intensity and control in the Chinese Tian Shan: new constraints from mass balance on catchment-alluvial fan systems. Earth Surface Processes and Landforms, 41(8), pp.1088-1106. https://doi.org/10.1002/esp.3890

Guiraud, R. and **Maurin**, J.C., **1992**. Early Cretaceous rifts of Western and Central Africa: an overview. Tectonophysics, 213(1-2), pp.153-168. https://doi.org/10.1016/0040-1951(92)90256-6

Gunnell, Y., **2003**. Radiometric ages of laterites and constraints on long-term denudation rates in West Africa. Geology, 31(2), pp.131-134. https://doi.org/10.1130/0091-7613(2003)031%3C0131:RAOLAC%3E2.0.CO;2

Gutiérrez-Alonso, G., Fernández-Suárez, J., Jeffries, T.E., Johnston, S.T., Pastor-Galán, D., Murphy, J.B., Franco, M.P. and Gonzalo, J.C., **2011**. Diachronous post-orogenic magmatism within a developing orocline in Iberia, European Variscides. Tectonics, 30(5). https://doi.org/10.1029/2010TC002845

Hafid, M., **2000**. Triassic–early Liassic extensional systems and their Tertiary inversion, Essaouira Basin (Morocco). Marine and Petroleum Geology, 17(3), pp.409-429. https://doi.org/10.1016/S0264-8172(98)00081-6

Hafid, M., Zizi, M., Bally, A.W. and Ait Salem, A., **2006**. Structural styles of the western onshore and offshore termination of the High Atlas, Morocco: Comptes Rendus Geoscience, 338, p. 50–64. https://doi.org/10.1016/j.crte.2005.10.007

Hafid, M., Tari, G., Bouhadioui, D., Moussaid, I.E., Echarfaoui, H., Salem, A.A., Nahim, M. and Dakki, M., **2008**. Atlantic basins. In Continental evolution: The geology of Morocco (pp. 303-329). Springer, Berlin, Heidelberg. https://doi.org/10.1007/978-3-540-77076-3_6

Hardie, R.A., **2016**. (U-Th)/He thermochronology of the Ottawa Embayment, Eastern Canada: The temperature-time history of an ancient, intracratonic rift basin. University of Ottawa, M.Sc. Thesis, 109 p.

Hatcher, R.D., **1989**. Tectonic synthesis of the US Appalachians. https://doi.org/10.1130/DNAG-GNA-F2.511

Hatcher, R.D., Tollo, R.P., Bartholomew, M.J., Hibbard, J.P. and Karabinos, P.M., **2010**. The Appalachian orogen: A brief summary. From Rodinia to Pangea: The Lithotectonic Record of the Appalachian Region: Geological Society of America Memoir, 206, pp.1-19.

Harman, R., Gallagher, K., Brown, R., Raza, A. and Bizzi, L., **1998**. Accelerated denudation and tectonic/geomorphic reactivation of the cratons of northeastern Brazil during the Late Cretaceous. Journal of Geophysical Research: Solid Earth, 103(B11), pp.27091-27105. https://doi.org/10.1029/98JB02524

Hayford, E.K., Lisker, F. and Apaalse, L., **2008**. Cretaceous rifting of the Ghana transform margin-Evidence from on shore apatite fission track data and optimum thermal history models. Ghana Journal of Science, 48. https://doi.org/10.4314/gjs.v48i1.56251

Hendriks, M., Jamieson, R.A., Willett, S.D. and Zentilli, M., **1993**. Burial and exhumation of the Long Range Inlier and its surroundings, western Newfoundland: results of an apatite fission-track study. Canadian Journal of Earth Sciences, 30(8), pp.1594-1606. https://doi.org/10.1139/e93-137

Hendriks, B., Andriessen, P., Huigen, Y., Leighton, C., Redfield, T., Murrell, G., Gallagher, K. and Nielsen, S.B., **2007**. A fission track data compilation for Fennoscandia. Norwegian Journal of Geology/Norsk Geologisk Forening, 87.

Herman, F., Seward, D., Valla, P.G., Carter, A., Kohn, B., Willett, S.D. and Ehlers, T.A., **2013**. Worldwide acceleration of mountain erosion under a cooling climate. Nature, 504(7480), pp.423-426. https://doi.org/10.1038/nature12877

Heyman, MAW., **1989**. Tectonic and depositional history of the Moroccan continental margin. In: Tankard, A., Balkwill, H., (Eds). Extensional Tectonics and Stratigraphy of the North Atlantic Margin. AAPG Memoir 46, pp. 323-340.

Hibbard, J.P., van Staal, C.R., Rankin, D.W., Tollo, R.P. and Bartholomew, M.J., **2010**. Comparative analysis of the geological evolution of the northern and southern Appalachian orogen: Late Ordovician-Permian. From Rodinia to Pangea: The Lithotectonic Record of the Appalachian Region: Geological Society of America Memoir, 206, pp.51-69. https://doi.org/10.1130/2010.1206(03)

Hoggard, M.J., White, N. and Al-Attar, D., **2016**. Global dynamic topography observations reveal limited influence of large-scale mantle flow. Nature Geoscience, 9(6), pp.456-463. https://doi.org/10.1038/ngeo2709

Horton, B.K., Parra, M., Saylor, J.E., Nie, J., Mora, A., Torres, V., Stockli, D.F. and Strecker, M.R., **2010**. Resolving uplift of the northern Andes using detrital zircon age signatures. GSA today, 20(7), pp.4-10. https://doi.org/10.1130/GSATG76A.1

Huismans, R. and **Beaumont**, C., **2011**. Depth-dependent extension, two-stage breakup and cratonic underplating at rifted margins. Nature, 473(7345), pp.74-78. https://doi.org/10.1038/nature09988

Huismans, R.S. and **Beaumont**, C., **2014**. Rifted continental margins: The case for depth-dependent extension. Earth and Planetary Science Letters, 407, pp.148-162. https://doi.org/10.1016/j.epsl.2014.09.032

Hurford, A.J., Platt, J.P. and Carter, A., **1999**. Fission-track analysis of samples from the Alboran Sea basement. Scientific Results, 161, pp.295-300. http://dx.doi.org/10.2973/odp.proc.sr.161.213.1999

Hulver, M.L., **1997**. Post-orogenic evolution of the Appalachian Mountain System and its foreland. The University of Chicago, PhD Thesis, 1055 p.

Janowski, M., Loget, N., Gautheron, C., Barbarand, J., Bellahsen, N., Van Den Driessche, J., Babault, J. and Meyer, B., **2016**. Neogene exhumation and relief evolution in the eastern Betics (SE Spain): insights from the Sierra de Gador. Terra Nova, 29(2), pp.91-97.

Jansa, L.F., **1981**. Mesozoic carbonate platforms and banks of the eastern North American margin. Marine Geology, 44(1-2), pp.97-117. https://doi.org/10.1016/0025-3227(81)90114-6

Jansa, L.F. and Wiedmann, J., **1982**. Mesozoic-Cenozoic development of the Eastern North American and Northwest African continental margins: a comparison. In Geology of the northwest African continental margin (pp. 215-269). Springer, Berlin, Heidelberg. https://doi.org/10.1007/978-3-642-68409-8_11

Japsen, P., Bonow, J.M., Green, P.F., Chalmers, J.A. and Lidmar-Bergström, K., **2009**. Formation, uplift and dissection of planation surfaces at passive continental margins - a new approach: Earth Surface Processes and Landforms, 34, p. 683–699. https://doi.org/10.1002/esp.1766

Japsen, P., Chalmers, J.A., Green, P.F. and Bonow, J.M., **2012**. Elevated, passive continental margins: Not rift shoulders, but expressions of episodic, post-rift burial and exhumation: Global and Planetary Change, 90-91, p. 73–86. https://doi.org/10.1016/j.gloplacha.2011.05.004

Johnson, C., **1995**. Neogene tectonics in South Eastern Spain: constraints from fission track analysis. University of London, Ph.D. Thesis, 395 p.

Johnson, C., Harbury, N. and Hurford, A.J., **1997**. The role of extension in the Miocene denudation of the Nevado-Filábride Complex, Betic Cordillera (SE Spain). Tectonics, 16(2), pp.189-204.

Juez-Larre, J. and **Andriessen**, P., **2006**. Tectonothermal evolution of the northeastern margin of Iberia since the break-up of Pangea to present, revealed by low-temperature fission-track and (U–Th)/He thermochronology. A case history of the Catalan Coastal Ranges: Earth and Planetary Science Letters, 243, p. 159–180. https://doi.org/10.1016/j.epsl.2005.12.026

Ketcham, R.A., **2005**. Forward and Inverse Modeling of Low-Temperature Thermochronometry Data: Reviews in Mineralogy and Geochemistry, 58, p. 275–314. https://doi.org/10.2138/rmg.2005.58.11

Ketcham, R.A., Donelick, R.A. and Donelick, M.B., **2000**. AFTSolve: A program for multi-kinetic modeling of apatite fission-track data: Geological Materials Research, 2, p. 1–32.

Ketcham, R.A., van der Beek, P., Barbarand, J., Bernet, M. and Gautheron, C., **2018**. Reproducibility of thermal history reconstruction from apatite fission-track and (U-Th)/He data. Geochemistry, Geophysics, Geosystems, 19(8), pp.2411-2436. https://doi.org/10.1029/2018GC007555

Klitgord, K.D., Hutchinson, D.R. and Schouten, H., **1988**. US Atlantic continental margin; structural and tectonic framework. https://doi.org/10.1130/DNAG-GNA-I2.19

Klitgord, K.D. and **Schouten**, H., **1986**. Plate kinematics of the central Atlantic. https://doi.org/10.1130/DNAG-GNA-M.351

Klingelhoefer, F., Labails, C., Cosquer, E., Rouzo, S., Geli, L., Aslanian, D., Olivet, J.L., Sahabi, M., Nouze, H. and Unternehr, P., **2009**. Crustal structure of the SW-Moroccan margin from wide-angle and reflection seismic data (the DAKHLA experiment) Part A: Wide-angle seismic models. Tectonophysics, 468(1-4), pp.63-82. https://doi.org/10.1016/j.tecto.2008.07.022

Kohn, B.P., Gleadow, A.J., Brown, R.W., Gallagher, K., Lorencak, M. and Noble, W.P., **2005**. Visualizing thermotectonic and denudation histories using apatite fission track thermochronology. Reviews in mineralogy and geochemistry, 58(1), pp.527-565. https://doi.org/10.2138/rmg.2005.58.20

Kohn, B.P., Shagam, R., Banks, P.O. and Burkley, L.A., **1984b**. Mesozoic-Pleistocene fission-track ages on rocks of the Venezuelan Andes and their tectonic implications. The Caribbean-South American Plate Boundary and Regional Tectonics, William E. Bonini, Robert B. Hargraves, Reginald Shagam. Geological Society of America, Memoire 162. https://doi.org/10.1130/MEM162-p365

Kohn, B.P., Shagam, R. and Subieta, T., **1984a**. Results and preliminary implications of sixteen fission-track ages from rocks of the western Caribbean Mountains, Venezuela. The Caribbean-South American Plate Boundary and Regional Tectonics, William E. Bonini, Robert B. Hargraves, Reginald Shagam. Geological Society of America, Memoire 162. https://doi.org/10.1130/MEM162-p415

Kohn, B.P., Wagner, M.E., Lutz, T.M. and Organist, G., **1993**. Anomalous Mesozoic thermal regime, central Appalachian Piedmont: evidence from sphene and zircon fission-track dating. The Journal of Geology, 101(6), pp.779-794. https://doi.org/10.1086/648274

Kuiper, Y.D., Thompson, M.D., Barr, S.M., White, C.E., Hepburn, J.C. and Crowley, J.L., **2017**. Detrital zircon evidence for Paleoproterozoic West African crust along the eastern North American continental margin, Georges Bank, offshore Massachusetts, USA. Geology, 45(9), pp.811-814. https://doi.org/10.1130/G39203.1

Kuiper, Y.D., Murphy, J.B., Nance, R.D., Strachan, R.A. and Thompson, M.D. eds., **2022**. New Developments in the Appalachian-Caledonian-Variscan Orogen (Vol. 554). Geological Society of America. https://doi.org/10.1130/SPE554

Kunk, M.J., Wintsch, R.P., Naeser, C.W., Naeser, N.D., Southworth, C.S., Drake Jr, A.A. and Becker, J.L., **2005**. Contrasting tectonothermal domains and faulting in the Potomac terrane, Virginia–Maryland—discrimination by 40Ar/39Ar and fission-track thermochronology. Geological Society of America Bulletin, 117(9-10), pp.1347-1366. https://doi.org/10.1130/B25599.1

Kusznir, N.J., Roberts, A.M. and Alvey, A.D., **2020**. Crustal structure of the conjugate Equatorial Atlantic Margins, derived by gravity anomaly inversion. Geological Society, London, Special Publications, 476(1), pp.83-107. https://doi.org/10.1144/SP476.5

Labails, C., Olivet, J.-L., Aslanian, D. and Roest, W.R., **2010**. An alternative early opening scenario for the Central Atlantic Ocean: Earth and Planetary Science Letters, 297, p. 355–368. https://doi.org/10.1016/j.epsl.2010.06.024

Lafforgue, L., **2016**. Place de la minéralisation de manganèse de Bouarfa dans l'évolution méso-cénozoïque de l'oriental marocain, Doctoral dissertation, Paris Saclay, 360p.

Lanari, R., Fellin, M. G., Faccenna, C., Balestrieri, M. L., Pazzaglia, F., and Youbi, N., **2020**. Exhumation and surface evolution of the Western High-Atlas and surrounding regions as constrained by low-temperature thermochronology. Tectonics, e2019TC005562. https://doi.org/10.1029/2019TC005562

LASE Study Group, **1986**. Deep structure of the US East Coast passive margin from large aperture seismic experiments (LASE). Marine and Petroleum Geology, 3(3), pp.234-242. https://doi.org/10.1016/0264-8172(86)90047-4

Le Roy, P. and **Piqué**, A., **2001**. Triassic–Liassic Western Moroccan synrift basins in relation to the Central Atlantic opening. Marine Geology, 172(3-4), pp.359-381. https://doi.org/10.1016/S0025-3227(00)00130-4

Leeder, M.R., **2006**. Sedimentology and sedimentary basins: From turbulence to tectonics: John Wiley and Sons, 608 p.

Leleu, S., Hartley, A.J., van Oosterhout, C., Kennan, L., Ruckwied, K. and Gerdes, K., **2016**. Structural, stratigraphic and sedimentological characterisation of a wide rift system: The Triassic rift system of the Central Atlantic Domain: Earth Science Reviews, 158, p. 89–124. https://doi.org/10.1016/j.earscirev.2016.03.008

Leprêtre, R., **2015**. Evolution Phanerozoïque du Craton Ouest Africain et de ses bordures Nord et Ouest: Université Paris 11, Ph.D. Thesis, 423 p.

Leprêtre, R., Barbarand, J., Missenard, Y., Gautheron, C., Pinna-Jamme, R. and Saddiqi, O., **2017**. Mesozoic evolution of NW Africa: implications for the Central Atlantic Ocean dynamics: Journal of the Geological Society, 174, p. 817–835. https://doi.org/10.1144/jgs2016-100

Leprêtre, R., Barbarand, J., Missenard, Y., Leparmentier, F. and Frizon de Lamotte, D., **2013**. Vertical movements along the northern border of the West African Craton: The Reguibat Shield and adjacent basins: Geological Magazine, 151, p. 1–14. https://doi.org/10.1017/S0016756813000939

Leprêtre, R., Frizon de Lamotte, D., Combier, V., Gimeno-Vives, O., Mohn, G., and Eschard, R., **2018**. The Tell-Riforogenic system (Morocco, Algeria, Tunisia) and the structural heritage of the southern Tethys margin: BSGF. BSGF-Earth Sciences Bulletin, 189, 10. https://doi.org/10.1051/bsgf/2018009

Leprêtre, R., Missenard, Y., Barbarand, J., Gautheron, C., Saddiqi, O. and Pinna-Jamme, R., **2015**. Post-rift history of the eastern Central Atlantic passive margin: insights from the Saharan region of South Morocco: Solid Earth, 120, p. 4645–4666. https://doi.org/10.1002/2014JB011549

Leprêtre, R., Chopin, F., El Houicha, M., Tabaud, A.S., Schulmann, K., Barbarand, J., Míková, J. and Chebli, R., **2022**. U-Pb geochronology of granitoids from northern Morocco: a two-step tale for the evolution of the Variscan domain in NW Africa (No. EGU22-12505). Copernicus Meetings. https://doi.org/10.5194/egusphere-egu22-12505

Leroy, M., Gueydan, F. and Dauteuil, O., **2008**. Uplift and strength evolution of passive margins inferred from 2-D conductive modelling: Geophysical Journal International, 172, p. 464–476. https://doi.org/10.1111/j.1365-246X.2007.03566.x

Li, G., Ravenhurst, C.E. and Zentilli, M., **1995**. Implications of apatite fission track analysis for the thermal history of the Scotian Basin, offshore Nova Scotia, Canada. Bulletin of Canadian Petroleum Geology, 43(2), pp.127-144. https://doi.org/10.35767/gscpgbull.43.2.127

Littlefield, K.V., **2010**. (Uranium-Thorium)/Helium analysis of denudation rates and exhumation histories in southern West Virginia. West Virginia University, M.Sc. thesis, 86 p.

Locke, B.D., **2001**. Thermal evolution of the eastern Serranía del Interior foreland fold and thrust belt, northeastern Venezuela, based on apatite fission track analyses. Rice University, M.Sc. Thesis, 178 p.

Locke, B.D. and **Garver**, J.I., **2005**. Thermal evolution of the eastern Serranía del Interior foreland fold and thrust belt, northeastern Venezuela, based on apatite fission-track analyses. Caribbean-South American plate interactions, Venezuela, 394, p.315. https://doi.org/10.1130/0-8137-2394-9.315

Logan, P., and **Duddy**, I., **1998**. An investigation of the thermal history of the Ahnet and Reggane Basins, Central Algeria, and the consequences for hydrocarbon generation and accumulation. Geological Society, London, Special Publications, 132, p. 131-155. https://doi.org/10.1144/GSL.SP.1998.132.01.07

Lonergan, L. and **Johnson**, C., **1998**. Reconstructing orogenic exhumation histories using synorogenic detrital zircons and apatites: an example from the Betic Cordillera, SE Spain. Basin Research, 10(3), pp.353-364. https://doi.org/10.1046/j.1365-2117.1998.00071.x

Lorencak, M., Kohn, B.P., Osadetz, K.G. and Gleadow, A.J.W., **2004**. Combined apatite fission track and (U–Th)/He thermochronometry in a slowly cooled terrane: results from a 3440-m-deep drill hole in the southern Canadian Shield. Earth and Planetary Science Letters, 227(1-2), pp.87-104. https://doi.org/10.1016/j.epsl.2004.08.015

Lorencak, M., **2003**. Low temperature thermochronology of the Canadian and Fennoscandian Shields: Integration of apatite fission track and (U-Th)/He methods. University of Melbourne, Ph.D. Thesis, 300 p.

Louden, K. and **Liu**, H., **2010**. Refraction Crustal Models and Plate Reconstruction of the Nova Scotia and Morocco Margins. Unpublished research report to OETR, Halifax, Nova Scotia.

Louden, K., Wu, Y. and Tari, G., **2013**. Systematic variations in basement morphology and rifting geometry along the Nova Scotia and Morocco conjugate margins. Geological Society, London, Special Publications, 369(1), pp.267-287.

Maillard, A., Malod, J., Thiébot, E., Klingelhoefer, F. and Réhault, J.P., **2006**. Imaging a lithospheric detachment at the continent–ocean crustal transition off Morocco. Earth and Planetary Science Letters, 241(3-4), pp.686-698. https://doi.org/10.1016/j.epsl.2005.11.013

Malusà, M.G., Polino, R., Feroni, A.C., Ellero, A., Ottria, G., Baidder, L. and Musumeci, G., **2007**. Post-Variscan tectonics in eastern Anti-Atlas (Morocco): Terra Nova, 19, p. 481–489. https://doi.org/10.1111/j.1365-3121.2007.00775.x

Malusà, M.G., Danisik, M., Kuhlemann, J., **2016**. Tracking the Adriatic-slab travel beneath the Tethyan margin of Corsica-Sardinia by low-temperature thermochronology: Gondwana Research, 31, p. 135-149. https://doi.org/10.1016/j.gr.2014.12.011

Malusà, M.G., Fitzgerald, P.G., **2019a**. Fission-Track Thermochronology and its Application to Geology: Springer Textbooks in Earth Sciences, Geography and Environment. Springer, Cham, 393 p.. https://doi.org/10.1007/978-3-319-89421-8

Malusà, M.G., **Fitzgerald**, P.G., **2019b**. From Cooling to Exhumation: Setting the Reference Frame for the Interpretation of Thermochronologic Data. In: Malusà M., Fitzgerald P. (eds). Fission-Track Thermochronology and its Application to Geology: Springer Textbooks in Earth Sciences, Geography and Environment. Springer, Cham , p. 147-164.

Mansour, E.M., **1991**). Thermochronologie par la méthode des traces de fission dans l'apatite. Application aux massifs de l'Argentera-Mercantour (Alpes occidentales) et des Jebilet (Meseta marocaine): Université Joseph-Fourier - Grenoble I, PhD Thesis, 197 p.

Martín-González, F., Barbero, L., Capote, R., Heredia, N. and Gallastegui, G., **2012**. Interaction of two successive Alpine deformation fronts: constraints from low-temperature thermochronology and structural mapping (NW Iberian Peninsula). International Journal of Earth Sciences, 101(5), pp.1331-1342. https://doi.org/10.1007/s00531-011-0712-9

Martín-Monge, A., Baudino, R., Gairifo-Ferreira, L.M., Tocco, R., Badalì, M., Ochoa, M., Haryono, S., Soriano, S., El Hafiz, N., Hernán-Gómez, J. and Chacón, B., **2017**. An unusual Proterozoic petroleum play in Western Africa: the Atar Group carbonates (Taoudeni Basin, Mauritania). Geological Society, London, Special Publications, 438(1), pp.119-157. https://doi.org/10.1144/SP438.5

Martínez Catalán, J.R., Díaz García, F., Arenas Martín, R., Abati Gómez, J., Castiñeiras García, P., González Cuadra, P., Gómez Barreiro, J. and Rubio Pascual, F.J., **2002**. Thrust and detachment systems in the Ordenes Complex (northwestern Spain): Implications for the Variscan-Appalachian geodynamics. https://doi.org/10.1130/SPE364

Martínez Catalán, J.R., Schulmann, K. and Ghienne, J.F., 2021. The Mid-Variscan Allochthon: Keys from correlation, partial retrodeformation and plate-tectonic reconstruction to unlock the geometry of a non-cylindrical belt. Earth-Science Reviews, 220, p.103700. https://doi.org/10.1016/j.earscirev.2021.103700

Marzen, R.E., Shillington, D.J., Lizarralde, D., Knapp, J.H., Heffner, D.M., Davis, J.K. and Harder, S.H., **2020**. Limited and localized magmatism in the Central Atlantic Magmatic Province. Nature communications, 11(1), pp.1-8. https://doi.org/10.1038/s41467-020-17193-6

Marzoli, A., Renne, P.R., Piccirillo, E.M., Ernesto, M., Bellieni, G. and Min, A.D., **1999**. Extensive 200-million-year-old continental flood basalts of the Central Atlantic Magmatic Province. Science, 284(5414), pp.616-618. https://doi.org/10.1126/science.284.5414.616

Marzoli, A., Davies, J.H.F.L., Youbi, N., Merle, R., Corso, J.D., Dunkley, D.J., Fioretti, A.M., Bellieni, G., Medina, F., Wotzlaw, J.-F., McHone, G., Font, E. and Bensalah, M.K., **2017**. Proterozoic to Mesozoic evolution of North-West Africa and Peri-Gondwana microplates: Detrital zircon ages from Morocco and Canada: Lithos, 278, p. 1–44. https://doi.org/10.1016/j.lithos.2017.01.016

Matton, G. and **Jébrak**, M., **2009**. The Cretaceous Peri-Atlantic Alkaline Pulse (PAAP): Deep mantle plume origin or shallow lithospheric break-up?: Tectonophysics, 469, p. 1–12. https://doi.org/10.1016/j.tecto.2009.01.001

Maurel, O., Monie, P., Pik, R., Arnaud, N., Brunel, M. and Jolivet, M., **2008**. The Meso-Cenozoic thermo-tectonic evolution of the Eastern Pyrenees: an 40Ar/39Ar fission track and (U–Th)/He thermochronological study of the Canigou and Mont-Louis massifs. International Journal of Earth Sciences, 97(3), pp.565-584. https://doi.org/10.1007/s00531-007-0179-x

McDannell, K.T., Schneider, D.A., Zeitler, P.K., O'Sullivan, P.B. and Issler, D.R., **2019**. Reconstructing deep-time histories from integrated thermochronology: An example from southern Baffin Island, Canada. Terra Nova, 31(3), pp.189-204. https://doi.org/10.1111/ter.12386

McDannell, K.T., Zeitler, P.K. and Schneider, D.A., **2018**. Instability of the southern Canadian Shield during the late Proterozoic. Earth and Planetary Science Letters, 490, pp.100-109. https://doi.org/10.1016/j.epsl.2018.03.012

McKenzie, D., **1978**. Some remarks on the development of sedimentary basins. Earth and Planetary science letters, 40(1), pp.25-32. https://doi.org/10.1016/0012-821X(78)90071-7

McKeon, R.E., Zeitler, P.K., Pazzaglia, F.J., Idleman, B.D. and Enkelmann, E., **2013**. Decay of an old orogen: Inferences about Appalachian landscape evolution from low-temperature thermochronology. GSA Bulletin, 126(1-2), pp.31-46. https://doi.org/10.1130/B30808.1

McKillop, K., **1990**. Apatite fission track analysis of the Digby NSDME Dl drill hole. Dalhousie University, Unpublished M.Sc. Thesis.

Merle, R.E., Jourdan, F., Chiaradia, M., Olierook, H.K. and Manatschal, G., **2019**. Origin of widespread Cretaceous alkaline magmatism in the Central Atlantic: A single melting anomaly?. Lithos, 342, pp.480-498. https://doi.org/10.1016/j.lithos.2019.06.002

Merle, R., Marzoli, A., Bertrand, H., Reisberg, L., Verati, C., Zimmermann, C., Chiaradia, M., Bellieni, G. and Ernesto, M., **2011**. 40Ar/39Ar ages and Sr–Nd–Pb–Os geochemistry of CAMP tholeiites from Western Maranhão basin (NE Brazil). Lithos, 122(3-4), pp.137-151. https://doi.org/10.1016/j.lithos.2010.12.010

Metcalf, J.R., Fitzgerald, P.G., Baldwin, S.L. and Muñoz, J.A., **2009**. Thermochronology of a convergent orogen: Constraints on the timing of thrust faulting and subsequent exhumation of the Maladeta

Pluton in the Central Pyrenean Axial Zone. Earth and Planetary Science Letters, 287(3-4), pp.488-503. https://doi.org/10.1016/j.epsl.2009.08.036

Miall, A.D., Balkwill, H.R. and McCracken, J., **2008**. The Atlantic Margin Basins of North America. Sedimentary Basins of the World, 5, pp.473-504. https://doi.org/10.1016/S1874-5997(08)00014-2

Michard, A., Soulaimani, A., Hoepffner, C., Ouanaimi, H., Baidder, L., Rjimati, E.C. and Saddiqi, O., **2010**. The South-Western Branch of the Variscan Belt: Evidence from Morocco: Tectonophysics, 492, p. 1–24. https://doi.org/10.1016/j.tecto.2010.05.021

Michard, A., Saddiqi, O., Chalouan, A. and de Lamotte, D.F. eds., **2008**. Continental evolution: The geology of Morocco: Structure, stratigraphy, and tectonics of the Africa-Atlantic-Mediterranean triple junction (Vol. 116). Berlin: Springer. 426 p. https://doi.org/10.1007/978-3-540-77076-3

Michon, L. and **Merle**, O., **2003**. Mode of lithospheric extension: Conceptual models from analogue modeling. Tectonics, 22(4). https://doi.org/10.1029/2002TC001435

Miller, D.S. and **Duddy**, I.R., **1989**. Early Cretaceous uplift and erosion of the northern Appalachian Basin, New York, based on apatite fission track analysis. Earth and Planetary Science Letters, 93(1), pp.35-49. https://doi.org/10.1016/0012-821X(89)90182-9

Miller, K.G., Kominz, M.A., Browning, J.V., Wright, J.D., Mountain, G.S., Katz, M.E., Sugarman, P.J., Cramer, B.S., Christie-Blick, N. and Pekar, S.F., **2005**. The Phanerozoic record of global sea-level change. Science, 310(5752), pp.1293-1298. https://doi.org/10.1126/science.1116412

Miller, K.G., Kopp, R.E., Horton, B.P., Browning, J.V. and Kemp, A.C., **2013**. A geological perspective on sea-level rise and its impacts along the US mid-Atlantic coast. Earth's Future, 1(1), pp.3-18. https://doi.org/10.1002/2013EF000135

Missenard, Y., **2006**. Le relief des Atlas Marocains: Contribution des processus asthénosphériques et du raccourcissement crustal, aspects chronologiques: Université de Cergy Pontoise, Ph.D. Thesis, 236 p.

Missenard, Y., Saddiqi, O., Barbarand, J., Leturmy, P., Ruiz, G., El Haimer, F.Z. and Frizon de Lamotte, D., **2008**. Cenozoic denudation in the Marrakech High Atlas, Morocco: insight from apatite fission-track thermochronology. Terra Nova, 20(3), pp.221-228. https://doi.org/10.1111/j.1365-3121.2008.00810.x

Missenard, Y. and **Cadoux**, A., **2011**. Can Moroccan Atlas lithospheric thinning and volcanism be induced by Edge-Driven Convection?: Terra Nova, 24, p. 27–33. https://doi.org/10.1111/j.1365-3121.2011.01033.x

Mrini, Z., Rafi, A., Duthou, J.L. and Vidal, P., **1992**. Chronologie Rb-Sr des granitoides hercyniens du Maroc; consequences. Bulletin de la Société géologique de France, 163(3), pp.281-291.

Moore, M.E., Gleadow, A.J. and Lovering, J.F., **1986**. Thermal evolution of rifted continental margins: new evidence from fission tracks in basement apatites from southeastern Australia. Earth and Planetary Science Letters, 78(2-3), pp.255-270. https://doi.org/10.1016/0012-821X(86)90066-X

Mora, A., Horton, B.K., Mesa, A., Rubiano, J., Ketcham, R.A., Parra, M., Blanco, V., Garcia, D. and Stockli, D.F., **2010a**. Migration of Cenozoic deformation in the Eastern Cordillera of Colombia interpreted from fission track results and structural relationships: Implications for petroleum systems. AAPG bulletin, 94(10), pp.1543-1580. https://doi.org/10.1306/01051009111

Mora, A., Parra, M., Strecker, M.R., Sobel, E.R., Zeilinger, G., Jaramillo, C., Da Silva, S.F. and Blanco, M., **2010b**. The eastern foothills of the Eastern Cordillera of Colombia: An example of multiple factors controlling structural styles and active tectonics. GSA Bulletin, 122(11-12), pp.1846-1864. https://doi.org/10.1130/B30033.1

Mora, A., Parra, M., Forero, G.R., Blanco, V., Moreno, N., Caballero, V., Stockli, D., Duddy, I. and Ghorbal, B., **2015**. What drives orogenic asymmetry in the Northern Andes?: A case study from the apex of the Northern Andean Orocline. In: Petroleum Geology and Potential of the Colombian Caribbean Margin, Claudio Bartolini, Paul Mann. https://doi.org/10.1306/13531949M1083652

Neto, J.M., Hegarty, K.A., Karner, G.D. and Alkmim, F.F.D., **2009**. Timing and mechanisms for the generation and modification of the anomalous topography of the Borborema Province, northeastern Brazil. Marine and Petroleum Geology, 26(7), pp.1070-1086. https://doi.org/10.1016/j.marpetgeo.2008.07.002

Morris, R.G., Sinclair, H.D. and Yelland, A.J., **1998**. Exhumation of the Pyrenean orogen: implications for sediment discharge. Basin Research, 10(1), pp.69-86. https://doi.org/10.1046/j.1365-2117.1998.00053.x

Moulin, M., Schnurle, P., Afilhado, A., Gallais, F., Dias, N., Evain, M., Soares, J., Fuck, R., Neto, O.D.C.P., Viana, A. and Aslanian, D., **2021**. Imaging Early Oceanic Crust spreading in the Equatorial Atlantic

Ocean: Insights from the MAGIC wide-angle experiment. Journal of South American Earth Sciences, 111, p.103493. https://doi.org/10.1016/j.jsames.2021.103493

Müller, R.D., Sdrolias, M., Gaina, C., Steinberger, B. and Heine, C., **2008**. Long-term sea-level fluctuations driven by ocean basin dynamics. Science, 319(5868), pp.1357-1362. https://doi.org/10.1126/science.1151540

Müller, R.D., Flament, N., Matthews, K.J., Williams, S.E. and Gurnis, M., **2016**. Formation of Australian continental margin highlands driven by plate–mantle interaction. Earth and Planetary Science Letters, 441, pp.60-70. https://doi.org/10.1016/j.epsl.2016.02.025

Murray, K.E., Braun, J. and Reiners, P.W., **2018**. Toward robust interpretation of low-temperature thermochronometers in magmatic terranes. Geochemistry, Geophysics, Geosystems, 19(10), pp.3739-3763. https://doi.org/10.1029/2018GC007595

Naeser, C.W., Naeser, N.D., Newell, W.L., Southworth, S., Edwards, L.E. and Weems, R.E., **2016**. Erosional and depositional history of the Atlantic passive margin as recorded in detrital zircon fission-track ages and lithic detritus in Atlantic Coastal Plain sediments. American Journal of Science, 316(2), pp.110-168. https://doi.org/10.2475/02.2016.02

Najih, A., Montero, P., Verati, C., Charaf Chabou, M., Fekkak, A., Baidder, L., Ezzouhairi, H., Bea F., Michard A., **2019**. Initial Pangean rifting north of the West African Craton: Insights from late Permian U-Pb and 40Ar/39Ar dating of alkaline magmatism from the Eastern Anti-Atlas (Morocco): Journal of Geodynamics, 132, https://doi.org/10.1016/j.jog.2019.101670.

Nirrengarten, M., Manatschal, G., Tugend, J., Kusznir, N. and Sauter, D., **2018**. Kinematic evolution of the southern North Atlantic: Implications for the formation of hyperextended rift systems. Tectonics, 37(1), pp.89-118. https://doi.org/10.1002/2017TC004495

Nomade, S., Knight, K.B., Beutel, E., Renne, P.R., Verati, C., Féraud, G., Marzoli, A., Youbi, N. and Bertrand, H., **2007**. Chronology of the Central Atlantic Magmatic Province: implications for the Central Atlantic rifting processes and the Triassic–Jurassic biotic crisis. Palaeogeography, Palaeoclimatology, Palaeoecology, 244(1-4), pp.326-344. https://doi.org/10.1016/j.palaeo.2006.06.034

Noriega-Londoño, S., Restrepo-Moreno, S.A., Vinasco, C., Bermúdez, M.A. and Min, K., **2019**. Thermochronologic and geomorphometric constraints on the Cenozoic landscape evolution of the

Northern Andes: Northwestern Central Cordillera, Colombia. Geomorphology, 351, p.106890. https://doi.org/10.1016/j.geomorph.2019.106890

Olsen, P.E., **1997**. Stratigraphic record of the early Mesozoic breakup of Pangea in the Laurasia-Gondwana rift system. Annual Review of Earth and Planetary Sciences, 25(1), pp.337-401. https://doi.org/10.1146/annurev.earth.25.1.337

Olsen, K.H. ed., **1995**. Continental rifts: evolution, structure, tectonics. 1st edition, Elsevier, 463 p.

Oukassou, M., Saddiqi, O., Barbarand, J., Sebti, S., Baidder, L. and Michard, A., **2013**. Post-Variscan exhumation of the Central Anti-Atlas (Morocco) constrained by zircon and apatite fission-track thermochronology: Terra Nova, 25, p. 151–159. https://doi.org/10.1111/ter.12019

Parra, M., Mora, A., Sobel, E.R., Strecker, M.R. and González, R., **2009**. Episodic orogenic front migration in the northern Andes: Constraints from low-temperature thermochronology in the Eastern Cordillera, Colombia. Tectonics, 28(4). https://doi.org/10.1029/2008TC002423

Parra, M., Mora, A., Lopez, C., Ernesto Rojas, L. and Horton, B.K., **2012**. Detecting earliest shortening and deformation advance in thrust belt hinterlands: Example from the Colombian Andes. Geology, 40(2), pp.175-178. https://doi.org/10.1130/G32519.1

Paton, D.A., Pindell, J., McDermott, K., Bellingham, P. and Horn, B., **2017**. Evolution of seaward-dipping reflectors at the onset of oceanic crust formation at volcanic passive margins: Insights from the South Atlantic. Geology, 45(5), pp.439-442. https://doi.org/10.1130/G38706.1

Pazzaglia, F.J. and **Brandon**, M.T., **1996**. Macrogeomorphic evolution of the post-Triassic Appalachian mountains determined by deconvolution of the offshore basin sedimentary record. Basin Research, 8(3), pp.255-278. https://doi.org/10.1046/j.1365-2117.1996.00274.x

Pereira, A.J.S.C., Carter, A., Hurford, A.J., Neves, L.J.P.F. and Godinho, M.M., **1998**. Evidence for the unroofing history of Hercynian Granitoids in central Portugal derived from late Palaeozoic and Mesozoic Sedimentary Zircons. In Advances in Fission-Track Geochronology (pp. 173-186). Springer, Dordrecht. http://dx.doi.org/10.1007/978-94-015-9133-1

Pérez de Armas, J., **2005**. "Tectonic and thermal history of the western Serranía del Interior foreland fold and thrust belt and Guárico basin, north-central Venezuela: Implications of new apatite fission-track analysis and seismic interpretation", GSA Special Paper 394,, Caribbean-South American plate interactions, Venezuela, Hans G. Avé Lallemant, Virginia B. Sisson. https://doi.org/10.1130/0-8137-2394-9.271

Perez-Arlucea, M., Mendez, G., Clemente, F., Nombela, M., Rubio, B. and Filgueira, M., **2005**. Hydrology, sediment yield, erosion and sedimentation rates in the estuarine environment of the Ria de Vigo, Galicia, Spain. Journal of Marine Systems, 54(1-4), pp.209-226. https://doi.org/10.1016/j.jmarsys.2004.07.013

Peucat, J.J., Capdevila, R., Drareni, A., Mahdjoub, Y. and Kahoui, M., **2005**. The Eglab massif in the West African Craton (Algeria), an original segment of the Eburnean orogenic belt: petrology, geochemistry and geochronology. Precambrian Research, 136(3-4), pp.309-352. https://doi.org/10.1016/j.precamres.2004.12.002

Pichel, L.M., Huuse, M., Redfern, J. and Finch, E., **2019**. The influence of base-salt relief, rift topography and regional events on salt tectonics offshore Morocco. Marine and Petroleum Geology, 103, pp.87-113. https://doi.org/10.1016/j.marpetgeo.2019.02.007

Piqué, A. and **Laville**, E., **1996**. The central Atlantic rifting: Reactivation of Palaeozoic structures?. Journal of Geodynamics, 21(3), pp.235-255. https://doi.org/10.1016/0264-3707(95)00022-4

Pinet, N., **2018**. The ups and downs of the Canadian Shield: 2-preliminary results of apatite fission-track analysis from a 3.6 km vertical profile, LaRonde mine, Quebec. Quebec: Geological Survey of Canada.

Pinet, N., Sack, P., Mercier-Langevin, P., Colpron, M., Lavoie, D., Dubé, B. and Brake, V.I., **2020**. Neoproterozoic-hosted Carlin-type mineralization in central Yukon, part 1: Regional-to prospect-scale geological controls. Geological Survey of Canada, 8712, pp.281-297. https://doi.org/10.4095/326045

Piraquive, A., **2017a, b**. Cadre structurel, déformations et exhumation des Schistes du Santa Marta: accumulation et histoire de déformation d'un terrain caraïbe au nord de la Sierra Nevada de Santa Marta. Université Grenoble Alpes, Ph.D. Thesis, 394 p.

Platt, J.P., Whitehouse, M.J., Kelley, S.P., Carter, A. and Hollick, L., **2003a**. Simultaneous extensional exhumation across the Alboran Basin: implications for the causes of late orogenic extension. Geology, 31(3), pp.251-254. https://doi.org/10.1130/0091-7613(2003)031%3C0251:SEEATA%3E2.0.CO;2

Platt, J.P., Argles, T.W., Carter, A., Kelley, S.P., Whitehouse, M.J. and Lonergan, L., **2003b**. Exhumation of the Ronda peridotite and its crustal envelope: constraints from thermal modelling of a P–T–time array. Journal of the Geological Society, 160(5), pp.655-676. https://doi.org/10.1144/0016-764902-108

Platt, J.P., Kelley, S.P., Carter, A. and Orozco, M., **2005**. Timing of tectonic events in the Alpujárride Complex, Betic Cordillera, southern Spain. Journal of the Geological Society, 162(3), pp.451-462. https://doi.org/10.1144/0016-764903-039

Poag, C.W., **1991**. Rise and demise of the Bahama-Grand Banks gigaplatform, northern margin of the Jurassic proto-Atlantic seaway. Marine Geology, 102(1-4), pp.63-130. https://doi.org/10.1016/0025-3227(91)90006-P

Poag, C.W. and **Sevon**, W.D., **1989**. A record of Appalachian denudation in postrift Mesozoic and Cenozoic sedimentary deposits of the US middle Atlantic continental margin. Geomorphology, 2(1-3), pp.119-157. https://doi.org/10.1016/0169-555X(89)90009-3

Poag, C.W. and **Valentine**, P.C., **1988**. Mesozoic and Cenozoic stratigraphy of the United States Atlantic continental shelf and slope. In : The Atlantic Continental Margin, Robert E. Sheridan, John A. Grow, Geological Society of America, volume 1-2. https://doi.org/10.1130/DNAG-GNA-I2.67

Poupeau, G., Fabre, J., Labrin, E., Azdimoussa, A., Netto, A.M. and Monod, T., **1996**. Nouvelles datations par traces de fission de la structure circulaire des Richat (Mauritanie). Mémoires du Service Géologique de l'Algérie, 8, pp.231-236.

Powell, J.W., Schneider, D.A. and Issler, D.R., **2018**. Application of multi-kinetic apatite fission track and (U-Th)/He thermochronology to source rock thermal history: a case study from the Mackenzie Plain, NWT, Canada. Basin Research, 30, pp.497-512. https://doi.org/10.1111/bre.12233

Rat, J., Mouthereau, F., Brichau, S., Crémades, A., Bernet, M., Balvay, M., Ganne, J., Lahfid, A. and Gautheron, C., **2019**. Tectonothermal evolution of the Cameros Basin: Implications for tectonics of North Iberia. Tectonics, 38(2), pp.440-469. https://doi.org/10.1029/2018TC005294

Ravenhurst, C.E., Reynolds, P.H., Zentilli, M., Krueger, H.W. and Blenkinsop, J., **1989**. Formation of Carboniferous Pb-Zn and barite mineralization from basin-derived fluids, Nova Scotia, Canada. Economic Geology, 84(6), pp.1471-1488. https://doi.org/10.1016/1359-0189(90)90060-B

Ravenhurst, C., Donelick, R., Zentilli, M., Reynolds, P. and Beaumont, C., **1990**. A fission track pilot study of the thermal effects of rifting on the onshore Nova Scotian margin, Canada. International Journal of Radiation Applications and Instrumentation. Part D. Nuclear Tracks and Radiation Measurements, 17(3), pp.373-378. https://doi.org/10.1016/1359-0189(90)90060-B

Recanati, A., Missenard, Y., Leprêtre, R., Gautheron, C., Barbarand, J., Abbassene, F., Abdallah, N., Ouabadi, A., Derder, M.E.M., Boukari, C. and Pinna-Jamme, R., **2019**. A Tortonian onset for the

Algerian margin inversion: Evidence from low-temperature thermochronology. Terra Nova, 31(1), pp.39-48. https://doi.org/10.1111/ter.12367

Reed, J.C., Wheeler, J.O., Tucholke, B.E., **2004**. Geological map of North America: Decade of North American Geology Continental Scale Map 001, Boulder, Geol. Soc. America, scale 1:5,000,000.

Reed, J.S., Spotila, J.A., Eriksson, K.A. and Bodnar, R.J., **2005**. Burial and exhumation history of Pennsylvanian strata, central Appalachian basin: An integrated study. Basin Research, 17(2), pp.259-268. https://doi.org/10.1111/j.1365-2117.2005.00265.x

Reiners, P.W., **2005**. Zircon (U-Th)/He thermochronometry. Reviews in Mineralogy and Geochemistry, 58(1), pp.151-179.

Reiners, P.W., Ehlers, T.A. and Zeitler, P.K., **2005**. Past, present, and future of thermochronology. Reviews in Mineralogy and Geochemistry, 58(1), pp.1-18. https://doi.org/10.2138/rmg.2005.58.1

Reiners, P.W., Spell, T.L., Nicolescu, S. and Zanetti, K.A., **2004**. Zircon (U-Th)/He thermochronometry: He diffusion and comparisons with 40Ar/39Ar dating. Geochimica et cosmochimica acta, 68(8), pp.1857-1887. https://doi.org/10.1016/j.gca.2003.10.021

Reinhardt, L.J., Dempster, T.J., Shroder Jr, J.F. and Persano, C., **2007**. Tectonic denudation and topographic development in the Spanish Sierra Nevada. Tectonics, 26(3). https://doi.org/10.1029/2006TC001954

Reuber, K.R., Pindell, J. and Horn, B.W., **2016**. Demerara Rise, offshore Suriname: Magma-rich segment of the Central Atlantic Ocean, and conjugate to the Bahamas hot spot. Interpretation, 4(2), pp.T141-T155. https://doi.org/10.1190/INT-2014-0246.1

Reynolds, P.H., Elias, P., Muecke, G.K. and Grist, A.M., **1987**. Thermal history of the southwestern Meguma zone, Nova Scotia, from an 40Ar/39Ar and fission track dating study of intrusive rocks. Canadian Journal of Earth Sciences, 24(10), pp.1952-1965. https://doi.org/10.1139/e87-186

Ring, U., Brandon, M.T., Willett, S.D. and Lister, G.S., **1999**. Exhumation processes. Geological Society, London, Special Publications, 154(1), pp.1-27. https://doi.org/10.1144/GSL.SP.1999.154.01.01

Roden, M.K., **1991**. Apatite fission-track thermochronology of the southern Appalachian basin: Maryland, West Virginia, and Virginia. The Journal of Geology, 99(1), pp.41-53. https://doi.org/10.1086/629472

Roden, M.K., Elliott, W.C., Aronson, J.L. and Miller, D.S., **1993**. A comparison of fission-track ages of apatite and zircon to the K/Ar ages of illite-smectite (I/S) from Ordovician K-bentonites, southern Appalachian Basin. The Journal of Geology, 101(5), pp.633-641. https://doi.org/10.1086/648254

Roden-Tice, M.K. and **Tice**, S.J., **2005**. Regional-scale Mid-Jurassic to Late Cretaceous unroofing from the Adirondack Mountains through central New England based on apatite fission-track and (U-Th)/He thermochronology. The Journal of Geology, 113(5), pp.535-552. https://doi.org/10.1086/431908

Roden-Tice, M.K. and **Wintsch**, R.P., **2002**. Early Cretaceous normal faulting in southern New England: evidence from apatite and zircon fission-track ages. The Journal of geology, 110(2), pp.159-178. https://doi.org/10.1086/338281

Roden-Tice, M.K., West Jr, D.P., Potter, J.K., Raymond, S.M. and Winch, J.L., **2009**. Presence of a long-term lithospheric thermal anomaly: Evidence from apatite fission-track analysis in northern New England. The Journal of Geology, 117(6), pp.627-641. https://doi.org/10.1086/605995

Roden-Tice, M.K., Eusden Jr, J.D. and Wintsch, R.P., **2012**. Apatite fission-track evidence for the Cretaceous development of kilometer-scale relief and steady-state Tertiary topography in New England. Geomorphology, 141, pp.114-120. https://doi.org/10.1016/j.geomorph.2011.12.029

Roden-Tice, M.K., Tice, S.J. and Schofield, I.S., **2000**. Evidence for differential unroofing in the Adirondack Mountains, New York State, determined by apatite fission-track thermochronology. The Journal of Geology, 108(2), pp.155-169. https://doi.org/10.1086/314395

Rodrigues, B., **2014**. An integrated thermochronology, organic maturation and provenance study in the South Portuguese Zone and Algarve Basin (South Portugal). University of Algarve, Ph.D. Thesis, 199 p.

Rodríguez Fernández, L.R., López Olmedo, F., Oliveira, J.T., Medialdea, T., Matas, J., Martín-Serrano, A., Martín Parra, L.M., Rubio, F., Montes, M., Nozal, F., Marín, C., and Terrinha, P., **2015**. The Geological Map of Spain and Portugal 1:1M scale. IGME ; Spanish Geological Survey.

Rohrman, M., van der Beek, P. and Andriessen, P., **1994**. Syn-rift thermal structure and post-rift evolution of the Oslo Rift (southeast Norway): New constraints from fission track thermochronology. Earth and Planetary Science Letters, 127(1-4), pp.39-54. https://doi.org/10.1016/0012-821X(94)90196-1

Romagny, A., Münch, P., Cornée, J.J., Corsini, M., Azdimousa, A., Melinte-Dobrinescu, M.C., Drinia, H., Bonno, M., Arnaud, N., Monié, P., Quillévéré, F. and Ben Moussa, A., **2014**. Late Miocene to present-day exhumation and uplift of the Internal Zone of the Rif chain: Insights from low-temperature thermochronometry and basin analysis: Journal of Geodynamics, 77, p. 39–55. https://doi.org/10.1016/j.jog.2014.01.006

Rougier, S., **2012**. Interactions lithosphère–asthénosphère et mouvements verticaux: le cas du massif du Hoggar. Université Paris Sud-Paris XI, Ph.D. Thesis, 277 p.

Ruiz, G.M.H., Sebti, S., Negro, F., Saddiqi, O., Frizon de Lamotte, D., Stockli, D., Foeken, J., Stuart, F., Barbarand, J. and Schaer, J.P., **2011**. From central Atlantic continental rift to Neogene uplift - western Anti-Atlas (Morocco): Terra Nova, 23, p. 35–41. https://doi.org/10.1111/j.1365-3121.2010.00980.x

Rushlow, C.R., Barnes, J.B., Ehlers, T.A. and Vergés, J., **2013**. Exhumation of the southern Pyrenean fold-thrust belt (Spain) from orogenic growth to decay. Tectonics, 32(4), pp.843-860. https://doi.org/10.1002/tect.20030

Ryan, R.J., **1993**. Metallogenetic and thermal evolution of the upper Paleozoic Maritimes Basin: Evidence from the Cumberland Basin of Nova Scotia. Dalhousie University, Ph.D. Thesis, 361 p.

Sabil, N., **1995**. La datation par traces de fission: Aspects méthodologiques et applications thermochronologiques en contexte alpin et de marge continentale: Université de Grenoble, Ph.D. Thesis, 245 p.

Saddiqi, O., Haimer, El, F.Z., Michard, A., Barbarand, J., Ruiz, G.M.H., Mansour, E.M., Leturmy, P. and de Lamotte, D.F., **2009**. Apatite fission-track analyses on basement granites from south-western Meseta, Morocco: Paleogeographic implications and interpretation of AFT age discrepancies: Tectonophysics, 475, p. 29–37. https://doi.org/10.1016/j.tecto.2009.01.007

Saenz, E., **2003**. Fission track thermochronology and denudational response to tectonics in the north of The Colombian Central Cordillera. Shimane University, M.Sc. Thesis, 131 pp.

Sahabi, M., Aslanian, D. and Olivet, J.L., **2004**. A new starting point for the history of the central Atlantic. Comptes Rendus Geoscience, 336(12), pp.1041-1052. https://doi.org/10.1016/j.crte.2004.03.017

Schettino, A. and **Turco**, E., **2009**. Breakup of Pangaea and plate kinematics of the central Atlantic and Atlas regions. Geophysical Journal International, 178(2), pp.1078-1097. https://doi.org/10.1111/j.1365-246X.2009.04186.x

Schlische, R.W., **1993**. Anatomy and evolution of the Triassic-Jurassic continental rift system, eastern North America. Tectonics, 12(4), pp.1026-1042. https://doi.org/10.1029/93TC01062

Sebti, S., Saddiqi, O., El Haimer, F.Z., Michard, A., Ruiz, G., Bousquet, R., Baidder, L. and de Lamotte, D.F., **2009**. Vertical movements at the fringe of the West African Craton: First zircon fission track datings from the Anti-Atlas Precambrian basement, Morocco. Comptes Rendus Geoscience, 341(1), pp.71-77. https://doi.org/10.1016/j.crte.2008.11.006

Sebti, S., **2011**. Mouvements verticaux de l'Anti-Atlas occidental marocain (Kerdous and Ifni): Thermochronologie par traces de fission: Université Hassan II, Ph.D. Thesis, 172 p.

Sehrt, M., **2014**. Variscan to Neogene long-term landscape evolution at the Moroccan passive continental margin (Tarfaya Basin and western Anti-Atlas): University of Heidelberg, Ph.D. Thesis, 174 p.

Sehrt, M., Glasmacher, U.A., Stockli, D.F., Jabour, H. and Kluth, O., **2018**. Meso-/Cenozoic long-term landscape evolution at the southern Moroccan passive continental margin, Tarfaya Basin, recorded by low-temperature thermochronology: Tectonophysics, 717, p. 499–518. https://doi.org/10.1016/j.tecto.2017.08.028

Sehrt, M., Glasmacher, U.A., Stockli, D.F., Jabour, H. and Kluth, O., **2017**. The southern Moroccan passive continental margin: An example of differentiated long-term landscape evolution in Gondwana: Gondwana Research, 53, p. 129–144. https://doi.org/10.1016/j.gr.2017.03.013

Şengör, 2003

Shagam, R., Kohn, B.P., Banks, P. O., Dasch, L.E., Vargas, R., Rodríguez, G.I., Pimentel, N., **1984**. Tectonic implications of Cretaceous-Pliocene fission-track ages from rocks of the circum-Maracaiho Basin region of western Venezuela and eastern Colombia. In: The Caribbean-South American Plate Boundary and Regional Tectonics, William E. Bonini, Robert B. Hargraves, Reginald Shagam https://doi.org/10.1130/MEM162-p385

Sheridan, R.E., **1974**. Atlantic continental margin of North America. In The geology of continental margins (pp. 391-407). Springer, Berlin, Heidelberg. https://doi.org/10.1007/978-3-662-01141-6_29

Sheridan, R.E., **1983**. Phenomena of pulsation tectonics related to the breakup of the eastern North American continental margin. In Developments in Geotectonics (Vol. 19, pp. 169-185). Elsevier. https://doi.org/10.1016/B978-0-444-42198-2.50017-1

Sheridan, R.E., **Grow** J.A., **1988**. The Atlantic Continental Margin. The Geological Society of America https://doi.org/10.1130/DNAG-GNA-I2

Sheridan, R.E., Musser, D.L., Glover III, L., Talwani, M., Ewing, J.I., Holbrook, W.S., Purdy, G.M., Hawman, R. and Smithson, S., **1993**. Deep seismic reflection data of EDGE US mid-Atlantic continental-margin experiment: Implications for Appalachian sutures and Mesozoic rifting and magmatic underplating. Geology, 21(6), pp.563-567. https://doi.org/10.1130/0091-7613(1993)021%3C0563:DSRDOE%3E2.3.CO;2

Shuster, D.L., Flowers, R.M. and Farley, K.A., **2006**. The influence of natural radiation damage on helium diffusion kinetics in apatite. Earth and Planetary Science Letters, 249(3-4), pp.148-161. https://doi.org/10.1016/j.epsl.2006.07.028

Shorten, C.M. and **Fitzgerald**, P.G., **2019**. Post-orogenic thermal history and exhumation of the northern Appalachian Basin: Low-temperature thermochronologic constraints. Basin Research, 31(6), pp.1017-1039. https://doi.org/10.1111/bre.12354

Sibuet, J.-C., Rouzo, S., Srivastava, S., Dehler, S., Deptuck, M. and Karim, A., **2012**. Plate tectonic reconstructions and paleogeographic maps of the Central and North Atlantic oceans: Canadian Journal of Earth Sciences, 49, p. 1395–1415. https://doi.org/10.1139/e2012-071

Silva, A., Mora, A., Caballero, V., Rodriguez, G., Ruiz, C., Moreno, N., Parra, M., Ramirez-Arias, J.C., Ibañez, M. and Quintero, I., **2013**. Basin compartmentalization and drainage evolution during rift inversion: evidence from the Eastern Cordillera of Colombia. Geological Society, London, Special Publications, 377(1), pp.369-409. https://doi.org/10.1144/SP377.15

Simancas, J.F., Tahiri, A., Azor, A., Lodeiro, F.G., Poyatos, D.J.M. and El Hadi, H., **2005**. The tectonic frame of the Variscan–Alleghanian orogen in Southern Europe and Northern Africa. Tectonophysics, 398(3-4), pp.181-198. https://doi.org/10.1016/j.tecto.2005.02.006

Sinclair, H.D., Gibson, M., Naylor, M. and Morris, R.G., **2005**. Asymmetric growth of the Pyrenees revealed through measurement and modeling of orogenic fluxes. American Journal of Science, 305(5), pp.369-406. https://doi.org/10.2475/ajs.305.5.369

Sinha, A.K. and **Zietz**, I., **1982**. Geophysical and geochemical evidence for a Hercynian magmatic arc, Maryland to Georgia. Geology, 10(11), pp.593-596. https://doi.org/10.1130/0091-7613(1982)10%3C593:GAGEFA%3E2.0.CO;2

Sisson, V.B., Lallemant, H.A., Ostos, M., Blythe, A.E., Snee, L.W., Copeland, P., Wright, J.E., Donelick, R.A. and Guth, L.R., **2005**. Overview of radiometric ages in three allochthonous belts of northern

Venezuela: Old ones, new ones, and their impact on regional geology. Special Papers-Geological Society of America, 394, p.91. https://doi.org/10.1130/0-8137-2394-9.91

Siravo, G., Fellin, M.G., Faccenna, C., Bayona, G., Lucci, F., Molin, P. and Maden, C., **2018**. Constraints on the Cenozoic deformation of the northern Eastern Cordillera, Colombia. Tectonics, 37(11), pp.4311-4337. https://doi.org/10.1029/2018TC005162

Snedden, J.W., Galloway, W.E., Milliken, K.T., Xu, J., Whiteaker, T. and Blum, M.D., **2018**. Validation of empirical source-to-sink scaling relationships in a continental-scale system: The Gulf of Mexico basin Cenozoic record. Geosphere, 14(2), pp.768-784. https://doi.org/10.1130/GES01452.1

Snedden, J.W., Hull, H.L., Whiteaker, T.L., Virdell, J.W. and Ross, C.H., **2022**. Late Mesozoic sandstone volumes recorded in Gulf of Mexico subsurface depocentres: Deciphering long-term sediment supply trends and contributions by paleo river systems. Basin Research, 34(4), pp.1269-1291. https://doi.org/10.1111/bre.12659

Sosson, M., Morrillon, A.C., Bourgois, J., Féraud, G., Poupeau, G. and Saint-Marc, P., **1998**. Late exhumation stages of the Alpujarride Complex (western Betic Cordilleras, Spain): new thermochronological and structural data on Los Reales and Ojen nappes. Tectonophysics, 285(3-4), pp.253-273. https://doi.org/10.1016/S0040-1951(97)00274-6

Stapel, G., **1999**. The nature of isostasy in western Iberia. Vrije Universiteit Amsterdam, Ph.D. Thesis, 148 p.

Spiegel, C., Kohn, B., Raza, A., Rainer, T. and Gleadow, A., **2007**. The effect of long-term low-temperature exposure on apatite fission track stability: A natural annealing experiment in the deep ocean. Geochimica et Cosmochimica Acta, 71(18), pp.4512-4537. https://doi.org/10.1016/j.gca.2007.06.060

Spikings, R.A. and **Crowhurst**, P.V., **2004**. (U–Th)/He thermochronometric constraints on the late Miocene–Pliocene tectonic development of the northern Cordillera Real and the Interandean Depression, Ecuador. Journal of South American Earth Sciences, 17(4), pp.239-251. https://doi.org/10.1016/j.jsames.2004.07.001

Spikings, R.A., Winkler, W., Hughes, R.A. and Handler, R., **2005**. Thermochronology of allochthonous terranes in Ecuador: Unravelling the accretionary and post-accretionary history of the Northern Andes. Tectonophysics, 399(1-4), pp.195-220. https://doi.org/10.1016/j.tecto.2004.12.023

Spotila, J.A., Bank, G.C., Reiners, P.W., Naeser, C.W., Naeser, N.D. and Henika, B.S., **2004**. Origin of the Blue Ridge escarpment along the passive margin of Eastern North America. Basin Research, 16(1), pp.41-63. https://doi.org/10.1111/j.1365-2117.2003.00219.x

Steckler, M.S., Omar, G.I., Karner, G.D. and Kohn, B.P., **1993**. Pattern of hydrothermal circulation within the Newark basin from fission-track analysis. Geology, 21(8), pp.735-738. https://doi.org/10.1130/0091-7613(1993)021%3C0735:POHCWT%3E2.3.CO;2

Sueoka, S. and **Tagami**, T., **2019**. Low-temperature thermochronological database of bedrock in the Japanese Islands. Island Arc, 28(4), p.e12305. https://doi.org/10.1111/iar.12305

Tankard, A.J. and **Welsink**, H.J., **1989**. Mesozoic Extension and Styles of Basin Formation in Atlantic Canada: Chapter 12: North American Margins. https://doi.org/10.1306/M46497C12

Tari, G. and **Jabour**, H., **2013**. Salt tectonics along the Atlantic margin of Morocco: Geological Society, London, Special Publications, 369, p. 337–353. https://doi.org/10.1144/SP369.23

Taylor, J.P. and **Fitzgerald**, P.G., **2011**. Low-temperature thermal history and landscape development of the eastern Adirondack Mountains, New York: Constraints from apatite fission-track thermochronology and apatite (U-Th)/He dating. GSA Bulletin, 123(3-4), pp.412-426. https://doi.org/10.1130/B30138.1

Teixell, A., Ayarza, P., Zeyen, H., Fernandez, M. and Arboleya, M.L., **2005**. Effects of mantle upwelling in a compressional setting: the Atlas Mountains of Morocco. Terra Nova, 17(5), pp.456-461. https://doi.org/10.1111/j.1365-3121.2005.00633.x

Teixell, A., Bertotti, G., de Lamotte, D.F. and Charroud, M., **2009**. The geology of vertical movements of the lithosphere: An overview: Tectonophysics, 475, p. 1–8. https://doi.org/10.1016/j.tecto.2009.08.018

Tremblay, A., Roden-Tice, M.K., Brandt, J.A. and Megan, T.W., **2013**. Mesozoic fault reactivation along the St. Lawrence rift system, eastern Canada: Thermochronologic evidence from apatite fission-track dating. GSA Bulletin, 125(5-6), pp.794-810. https://doi.org/10.1130/B30703.1

Turner, J.P., Green, P.F., Holford, S.P. and Lawrence, S.R., **2008**. Thermal history of the Rio Muni (West Africa)–NE Brazil margins during continental breakup. Earth and Planetary Science Letters, 270(3-4), pp.354-367. https://doi.org/10.1016/j.epsl.2008.04.002

Underdown, R., Redfern, J. and Lisker, F., **2007**. Constraining the burial history of the Ghadames Basin, North Africa: an integrated analysis using sonic velocities, vitrinite reflectance data and apatite fission track ages. Basin Research, 19(4), pp.557-578. https://doi.org/10.1111/j.1365-2117.2007.00335.x

Uranga, R.M., Ferrer, O., Zamora, G., Muñoz, J.A. and Rowan, M.G., **2022**. Salt tectonics of the offshore Tarfaya Basin, Moroccan Atlantic margin. Marine and Petroleum Geology, 138, p.105521. https://doi.org/10.1016/j.marpetgeo.2021.105521

van der Lelij, R., Spikings, R. and Mora, A., **2016**. Thermochronology and tectonics of the Mérida Andes and the Santander massif, NW South America. Lithos, 248, pp.220-239. https://doi.org/10.1016/j.lithos.2016.01.006

van der Wiel, A.M. and **Andriessen**, P.A.M., **1991**. Precambrian to Recent thermotectonic history of the Garzon massif (Eastern Cordillera of the Colombian Andes) as revealed by fission-track analysis. In: Uplift and volcanism of the SE Colombian Andes in relation to Neogene sedimentation of the upper Magdalena Valley. Marian van der Wiel. Amsterdam Vrij University, Ph. D. Thesis, 212 p.

van Staal, C.R., Whalen, J.B., Valverde-Vaquero, P., Zagorevski, A. and Rogers, N., **2009**. Pre-Carboniferous, episodic accretion-related, orogenesis along the Laurentian margin of the northern Appalachians. Geological Society, London, Special Publications, 327(1), pp.271-316. https://doi.org/10.1144/SP327.13

van Staal, C.R., Barr, S.M., Waldron, J.W., Schofield, D.I., Zagorevski, A. and White, C.E., **2021**. Provenance and Paleozoic tectonic evolution of Ganderia and its relationships with Avalonia and Megumia in the Appalachian-Caledonide orogen. Gondwana Research, 98, pp.212-243. https://doi.org/10.1016/j.gr.2021.05.025

Vanderhaeghe, O., Laurent, O., Gardien, V., Moyen, J.F., Gébelin, A., Chelle-Michou, C., Couzinié, S., Villaros, A. and Bellanger, M., **2020**. Flow of partially molten crust controlling construction, growth and collapse of the Variscan orogenic belt: the geologic record of the French Massif Central. Bulletin de la Société géologique de France, 191(1). https://doi.org/10.1051/bsgf/2020013

Vázquez-Vílchez, M., Jabaloy-Sánchez, A., Azor, A., Stuart, F., Persano, C., Alonso-Chaves, F.M., Martín-Parra, L.M., Matas, J. and García-Navarro, E., **2015**. Mesozoic and Cenozoic exhumation history of the SW Iberian Variscides inferred from low-temperature thermochronology. Tectonophysics, 663, pp.110-121. https://doi.org/10.1016/j.tecto.2015.06.034

Vermeesch, P., **2008**. Three new ways to calculate average (U–Th)/He ages. Chemical Geology, 249(3-4), pp.339-347. https://doi.org/10.1016/j.chemgeo.2008.01.027

Vermeesch, P., **2018**. IsoplotR: A free and open toolbox for geochronology. Geoscience Frontiers, 9(5), pp.1479-1493. https://doi.org/10.1016/j.gsf.2018.04.001

Vila, J.M., **1980**. La chaîne alpine d'Algérie orientale et des confins algéro-tunisiens. Université Pierre et Marie Curie, Ph.D. Thesis, 665 p.

Villagómez, D., Spikings, R., Mora, A., Guzmán, G., Ojeda, G., Cortés, E. and Van Der Lelij, R., **2011**. Vertical tectonics at a continental crust-oceanic plateau plate boundary zone: Fission track thermochronology of the Sierra Nevada de Santa Marta, Colombia. Tectonics, 30(4). https://doi.org/10.1029/2010TC002835

Villagómez, D. and **Spikings**, R., **2013**. Thermochronology and tectonics of the Central and Western Cordilleras of Colombia: Early Cretaceous–Tertiary evolution of the northern Andes. Lithos, 160, pp.228-249. https://doi.org/10.1016/j.lithos.2012.12.008

Villeneuve, M., **2008**. Review of the orogenic belts on the western side of the West African craton: the Bassarides, Rokelides and Mauritanides. Geological Society, London, Special Publications, 297(1), pp.169-201. https://doi.org/10.1144/SP297.8

Villeneuve, M., Gärtner, A., Youbi, N., El Archi, A., Vernhet, E., Rjimati, E.C., Linnemann, U., Bellon, H., Gerdes, A., Guillou, O. and Corsini, M., **2015**. The southern and central parts of the "Souttoufide" belt, Northwest Africa. Journal of African Earth Sciences, 112, pp.451-470. https://doi.org/10.1016/j.jafrearsci.2015.04.016

Vogler, K.A., **2021**. Thermal history of the Labrador rifted margin: Insights from apatite and zircon (U-Th)/He and apatite fission track thermochronology. Dalhousie University, M.Sc. Thesis, 318 p.

Wade, J.A. and **McLean**, B.C., **1990**. The stratigraphy of Georges Bank Basin and relationships to the Scotian Basin. Geology of the Continental Margin of Eastern Canada. Geological Survey of Canada, Geology of Canada Series, 2, pp.190-238.

Waldner, M., Bellahsen, N., Mouthereau, F., Bernet, M., Pik, R., Rosenberg, C.L. and Balvay, M., **2021**. Central Pyrenees mountain building: Constraints from new LT thermochronological data from the Axial Zone. Tectonics, 40(3), p.e2020TC006614. https://doi.org/10.1029/2020TC006614

Wang, H.F., Crowley, K.D. and Nadon, G.C., **1994**. Thermal history of the Michigan Basin from apatite fission-track analysis and vitrinite reflectance. https://archives.datapages.com/data/specpubs/memoir61/ch12/0167.htm

Watts, A.B., **2012**. Models for the evolution of passive margins. In: Regional geology and tectonics: Phanerozoic rift systems and sedimentary basins, Roberts, D.G. and Bally, A.W. eds, (Vol. 1). Elsevier. https://doi.org/10.1016/C2010-0-67671-1

Weber, J.C., Poulos, C., Donelick, R.A., Pope, M.C. and Heller, N., **2005**. The Kentland impact crater, Indiana (USA): an apatite fission-track age determination attempt. In Impact tectonics (pp. 447-466). Springer, Berlin, Heidelberg. https://doi.org/10.1007/3-540-27548-7_18

Welsink, H.J., Dwyer, J.D. and Knight, R.J., **1989**. Tectono-stratigraphy of the Passive Margin Off Nova Scotia: Chapter 14: North American Margins. https://doi.org/10.1306/M46497C14

Wernert, P., Schulmann, K., Chopin, F., Štípská, P., Bosch, D. and El Houicha, M., **2016**. Tectonometamorphic evolution of an intracontinental orogeny inferred from P–T–t–d paths of the metapelites from the Rehamna massif (Morocco). Journal of metamorphic Geology, 34(9), pp.917-940. https://doi.org/10.1111/jmg.12214

West, D.P., Roden-Tice, M.K., Potter, J.K. and Barnard, N.Q., **2008**. Assessing the role of orogen-parallel faulting in post-orogenic exhumation: low-temperature thermochronology across the Norumbega Fault System, Maine. Canadian Journal of Earth Sciences, 45(3), pp.287-301. https://doi.org/10.1139/E07-073

Westaway, R., Hssaine, A.A., Demir, T. and Beck, A., **2009**. Field reconnaissance of the Anti-Atlas coastline, Morocco: Fluvial and marine evidence for Late Cenozoic uplift. Global and Planetary Change, 68(4), pp.297-310. https://doi.org/10.1016/j.gloplacha.2009.03.016

Wiedmann, J., Butt, A. and Einsele, G., **1982**. Cretaceous stratigraphy, environment, and subsidence history at the Moroccan continental margin. In Geology of the northwest African continental margin (pp. 366-395). Springer, Berlin, Heidelberg.

Wildman, M., Cogné, N., Beucher, R., **2019**. Fission-Track Thermochronology Applied to the Evolution of Passive Continental Margins. In: Malusà M., Fitzgerald P. (eds) Fission-Track Thermochronology and its Application to Geology. Springer Textbooks in Earth Sciences, Geography and Environment. Springer, Cham, p. 351-371. https://doi.org/10.1007/978-3-319-89421-8

Willner, A.P., Barr, S.M., Glodny, J., Massonne, H.J., Sudo, M., Thomson, S.N., Van Staal, C.R. and White, C.E., **2015**. Effects of fluid flow, cooling and deformation as recorded by 40Ar/39Ar, Rb–Sr and zircon fission track ages in very low-to low-grade metamorphic rocks in Avalonian SE Cape Breton Island (Nova Scotia, Canada). Geological Magazine, 152(5), pp.767-787. https://doi.org/10.1017/S0016756814000508

Willner, A.P., Thomson, S.N., Glodny, J., Massonne, H.J., Romer, R.L., van Staal, C.R. and Zagorevski, A., **2019**. Zircon fission-track ages from Newfoundland—A proxy for high geothermal gradients and exhumation before opening of the Central Atlantic Ocean. Terra Nova, 31(1), pp.1-10. https://doi.org/10.1111/ter.12361

Winkler, J.E., Kelley, S.A. and Bergman, S.C., **1999**. Cenozoic denudation of the Wichita Mountains, Oklahoma, and southern mid-continent: apatite fission-track thermochronology constraints. Tectonophysics, 305(1-3), pp.339-353. https://doi.org/10.1016/S0040-1951(99)00025-6

Wipf, M., Glasmacher, U.A., Stockli, D.F., Emmerich, A., Bechstädt, T. and Baur, H., **2010**. Reconstruction of the differentiated long-term exhumation history of Fuerteventura, Canary Islands, Spain, through fission-track and (U-Th–Sm)/He data: International Journal of Earth Sciences, 99, p. 675–686. https://doi.org/10.1007/s00531-008-0415-z

Withjack, M.O., Schlische, R.W., Olsen, P.E. and Zhang, Q., **1998**. Diachronous rifting, drifting, and inversion on the passive margin of central eastern North America: an analog for other passive margins. AAPG bulletin, 82(5), pp.817-835. https://doi.org/10.1306/1D9BC60B-172D-11D7-8645000102C1865D

Withjack, M.O. and **Schlische**, R.W., **2005**. A Review of Tectonic Events on the Passive Margin of Eastern North America: Bob S. Perkins Research Conference, 25, Houston, p. 203–235. https://doi.org/10.5724/gcs.05.25.0203

Withjack, M., Malinconico, M., Durcanin, M. and Godin, L., **2020**. The “passive” margin of eastern North America: Rifting and the influence of prerift orogenic activity on postrift development. Lithosphere, 2020(1). https://doi.org/10.2113/2020/8876280

Yamato, P., Husson, L., Becker, T.W. and Pedoja, K., **2013**. Passive margins getting squeezed in the mantle convection vice: Tectonics, 32, p. 1559–1570. https://doi.org/10.1002/2013TC003375

Ye, J., **2016**. Evolution topographique, tectonique et sédimentaire syn- à post-rift de la marge transformante ouest africaine : GET Toulouse, Ph.D. Thesis, 273 p.

Ye, J., Chardon, D., Rouby, D., Guillocheau, F., Dall'asta, M., Ferry, J.-N. and Broucke, O., **2017**). Paleogeographic and structural evolution of northwestern Africa and its Atlantic margins since the early Mesozoic: Geosphere, 13, p. 1254-1284. https://doi.org/10.1130/GES01426

Appendix: time-Temperature curves

Reference [-]	Zone [-]	TTM [count]	Software [-]
Amidon et al., 2016	Appalachian	3	QtQT
Blackmer et al., 1994	Appalachian	2	Annealing model
Boettcher and Miliken, 1994	Appalachian	2	Annealing model
Emberley, 2016	Appalachian	6	HeFTy
Fame et al., 2019	Appalachian	1	QtQT
Kohn et al., 1993	Appalachian	1	No software
Kunk et al., 2005	Appalachian	3	No software
McKoen et al., 2013	Appalachian	2	HeFTy
Miller and Duddy, 1989	Appalachian	2	No software
Reed et al., 2005	Appalachian	2	No software
Roden et al., 1993	Appalachian	4	Annealing model
Roden-Tice and Tice, 2005	Appalachian	9	Annealing model
Roden-Tice and Wintsch, 2002	Appalachian	8	Annealing model
Roden-Tice et al., 2000	Appalachian	8	Annealing model
Roden-Tice et al., 2009	Appalachian	6	Annealing model
Roden-Tice et al., 2012	Appalachian	5	Annealing model
Shorten and Fitzgerald, 2019	Appalachian	6	HeFTy
Taylor and Fitzgerald, 2011	Appalachian	16	HeFTy
West et al., 2008	Appalachian	10	AFTINV
Spiegel et al., 2007	Atantic	2	AFTSolve
Crowley, 1991	Canadian Shield	2	No software
Feinstein et al., 2009	Canadian Shield	5	HeFTy
Hardi, 2016	Canadian Shield	11	HeFTy
Lorencak et al., 2004	Canadian Shield	2	Forward modelling
McDannell et al., 2018	Canadian Shield	2	Arvert
Pinet, 2018	Canadian Shield	7	HeFTy
Tremblay et al., 2013	Canadian Shield	10	HeFTy
Arne, 1992	Cratonic Platform	1	No software
Corrigan et al., 1998	Cratonic Platform	1	Annealing model
Corrigan et al., 1999	Cratonic Platform	2	Annealing model
DeLucia et al., 2018	Cratonic Platform	1	HeFTy
Flowers and Kelley, 2011	Cratonic Platform	1	HeFTy
Hardi, 2016	Cratonic Platform	4	HeFTy
Weber et al., 2005	Cratonic Platform	2	AFTSolve
Winkler et al., 1999	Cratonic Platform	1	Annealing model
Chang, 2017	NovaScotia/Labrador	5	No software
Grist and Zentilli, 2003	NovaScotia/Labrador	12	AFTINV
Grist et al., 1995	NovaScotia/Labrador	4	AFTINV
Hendriks et al., 1993	NovaScotia/Labrador	7	Annealing model
Li et al., 1995	NovaScotia/Labrador	6	Inverse modelling
Powell et al., 2018	NovaScotia/Labrador	4	HeFTy
Ravenhurst et al., 1990	NovaScotia/Labrador	2	No software
Ryan, 1993	NovaScotia/Labrador	11	Inverse modelling
Vogler, 2021	NovaScotia/Labrador	22	HeFTy

Table A1 | Time-Temperature Models from E-NAM

Reference [-]	Zone [-]	TTM [count]	Software [-]
Bermudez et al., 2009	Andes	10	HeFTy
Caballero et al., 2013	Andes	3	HeFTy
Mora et al., 2010b	Andes	12	HeFTy
Mora et al., 2015	Andes	1	HeFTy
Noriega-Londono et al., 2019	Andes	2	HeFTy
Parra et al., 2009	Andes	4	HeFTy
Parra et al., 2012	Andes	2	HeFTy
Piraquive, 2017	Andes	9	HeFTy
Silva et al., 2013	Andes	19	HeFTy
Spikings et al., 2004	Andes	1	Annealing model
van der Lelij et al., 2016	Andes	12	HeFTy
Villagomez et al., 2011	Andes	9	HeFTy
Villagomez et al., 2013	Andes	12	HeFTy
Bonilla et al., 2019	Guyana Shield	1	QtQT
Derycke et al., 2018	Guyana Shield	5	QtQT
Derycke et al., 2021	Guyana Shield	6	QtQT
Harman et al., 1998	N Brazil	2	Annealing model
Algar et al., 1998	SA-Caribbean	1	No software
Kohn et al., 1984a	SA-Caribbean	1	No software
Perez de Armas, 2005	SA-Caribbean	4	AFTSolve
Sisson et al., 2005	SA-Caribbean	2	Annealing model
Spiegel et al., 2007	SA-Caribbean	1	AFTSolve

Table A2 | Time-Temperature Models from N-SAM

Reference [-]	Zone [-]	TTM [count]	Software [-]
Clark and Dempster, 2009	Betics/Rif	7	AFTSolve
Janowski et al., 2016	Betics/Rif	1	QtQT
Lonergan and Johnson, 1998	Betics/Rif	1	Inverse modelling
Sosson et al., 1998	Betics/Rif	1	Monte Trax
Barbero et al., 2005	Iberian Massif	10	AFTSolve
Botor and Anczkiewicz, 2015	Iberian Massif	3	HeFTy
Carriere, 2006	Iberian Massif	20	AFTSolve
de Bruijn and Andriessen, 2001	Iberian Massif	31	Monte Trax
Grobe et al., 2010	Iberian Massif	12	HeFTy
Grobe et al., 2014	Iberian Massif	6	HeFTy
Martin-Gonzalez et al., 2012	Iberian Massif	10	HeFTy
Pereira et al., 1998	Iberian Massif	4	Annealing model
Stapel, 1999	Iberian Massif	13	Inverse modelling
Vasquez-Vilchez et al., 2015	Iberian Massif	6	HeFTy
Barbero and Lopez-Garrido, 2006	Iberian Range	2	AFTSolve
Del Rio et al., 2009	Iberian Range	4	AFTSolve
Juez-Larre and Andriessen, 2006	Iberian Range	32	AFTSolve
Rat et al., 2019	Iberian Range	4	QtQT
DeFelipe et al., 2019	Pyrenees	6	QtQT
Fillon et al., 2013	Pyrenees	3	QtQT
Gibson et al., 2007	Pyrenees	2	Annealing model
Maurel et al., 2008	Pyrenees	4	Monte Trax
Metcalf et al., 2009	Pyrenees	6	HeFTy
Rushlow et al., 2013	Pyrenees	8	HeFTy
Waldner et al., 2021	Pyrenees	5	QtQT

Table A3 | Time-Temperature Models from IB

Reference [-]	Zone [-]	TTM [count]	Software [-]
Charton et al., 2018	Anti-Atlas	1	HeFTy
Gouiza et al., 2017a	Anti-Atlas	6	HeFTy
Leprêtre, 2015	Anti-Atlas	2	QtQT
Malusa et al., 2007	Anti-Atlas	3	HeFTy
Oukassou et al., 2013	Anti-Atlas	2	HeFTy
Ruiz et al., 2011	Anti-Atlas	5	HeFTy
Sebti, 2011	Anti-Atlas	6	HeFTy
Sehrt et al., 2018 (in Sehrt, 2014)	Anti-Atlas	10	HeFTy
Sehrt, 2014	Anti-Atlas	4	HeFTy
Clift et al., 1998	Atlantic	4	Annealing model
Azdimousa et al., 2013	Betics/Rif	2	HeFTy
Romagny et al., 2014	Betics/Rif	1	QtQT
Balestrieri et al., 2009	High Atlas	2	HeFTy
Barbero et al., 2007	High Atlas	3	AFTSolve
Domenech , 2015	High Atlas	1	QtQT
Domenech et al., 2016	High Atlas	2	QtQT
El Haimer, 2014	High Atlas	1	HeFTy
Lanari et al., 2020	High Atlas	1	QtQT
Lepretre et al., 2018	High Atlas	11	QtQT
Recanati et al., 2018	High Atlas	4	QtQT
English et al., 2017	Hoggar	2	HeFTy
Glover, 1999	Hoggar	5	Monte Trax
Loggan and Duddy, 1998	Hoggar	2	No software
Rougier, 2012	Hoggar	14	HeFTy
Underdown et al., 2007	Hoggar	2	NoData
Fernie et al., 2018	Leo Shield	11	QtQT
Gunnell, 2003	Leo Shield	6	Annealing model
Wildman et al., 2019	Leo Shield	16	QtQT
Ye, 2016	Leo Shield	19	QtQT
Girard et al., 2015	Mauritanides	2	HeFTy
Gouiza et al., 2019	Mauritanides	5	QtQT
Hurford et al., 1999	Mediteranean Sea	1	Monte Trax
Barbero et al., 2011	Meseta	5	HeFTy
Ghorbal et al., 2008	Meseta	4	HeFTy
Lafforgue, 2016	Meseta	4	QtQT
Sabbil, 1995	Meseta	4	Inverse modelling
Saddiqi et al., 2009	Meseta	4	AFTSolve
Gouiza et al., 2017b	Reguibat	1	QtQT
Leprêtre et al., 2015 (in Leprêtre, 2015)	Reguibat	3	QtQT
Leprêtre et al., 2017 (in Leprêtre, 2015)	Reguibat	15	QtQT
Charton et al., 2018	Tarfaya	1	HeFTy
Sehrt et al., 2017 (in Sehrt, 2014)	Tarfaya	4	HeFTy

Table A4 | Time-Temperature Models from NWA

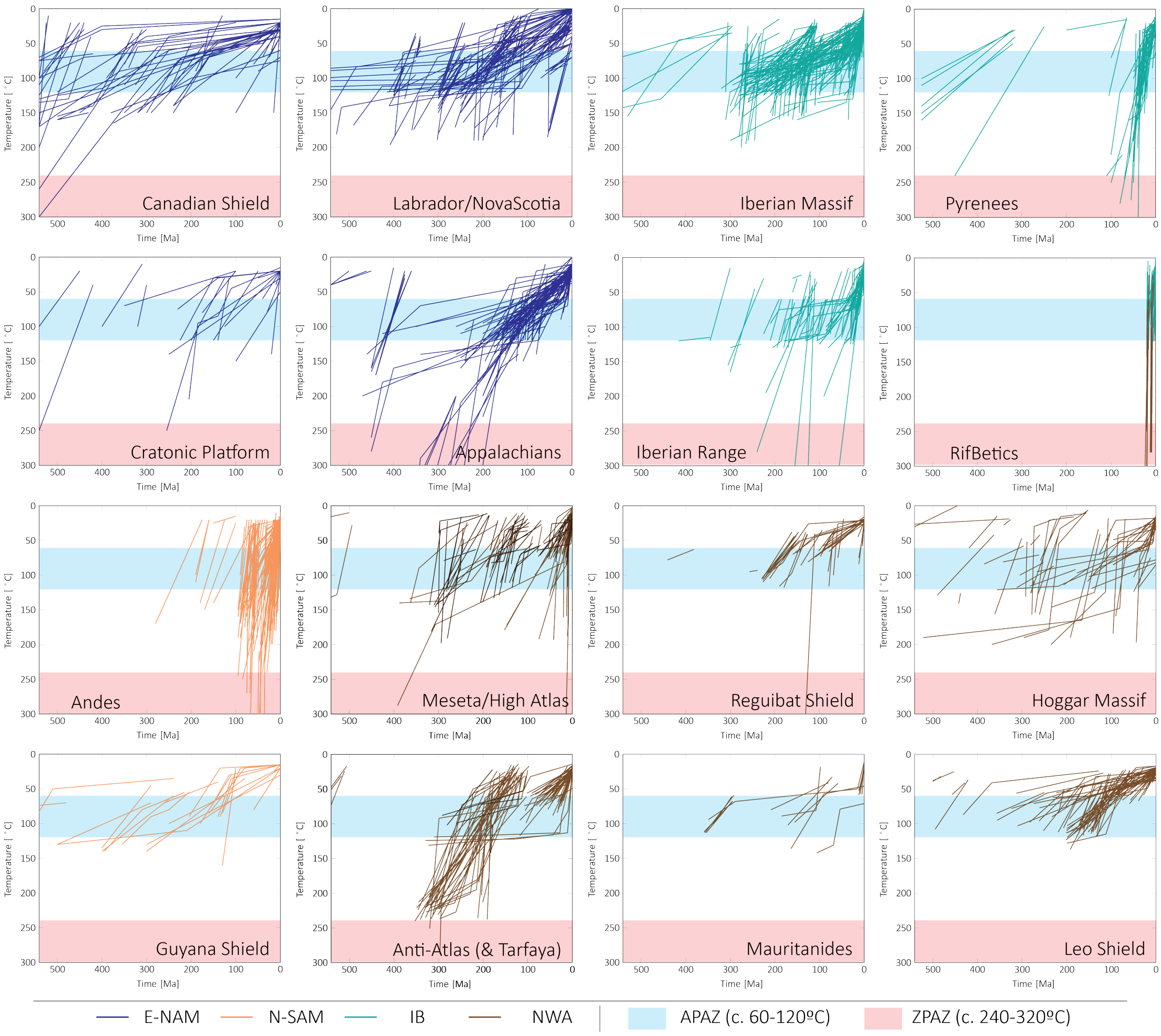

Figure A1 | Digitised cooling events from published time-temperature histories, forward models, and inverse models from the literature (see ***tables 2*** to ***5*** for references). *APAZ*, *ZPAZ* = Apatite and Zircon Partial Annealing Zones, respectively. Only up to five cooling events are been digitized here. If a model displayed 6 or more cooling events, then we digitized ones with smaller amplitude or shorter time span together with longer or more important one(s). Plots were digitized using the web tool 'Web Plot Digitizer' developed by Ankit Rohatgi and available at the following link: https://automeris.io/WebPlotDigitizer/.

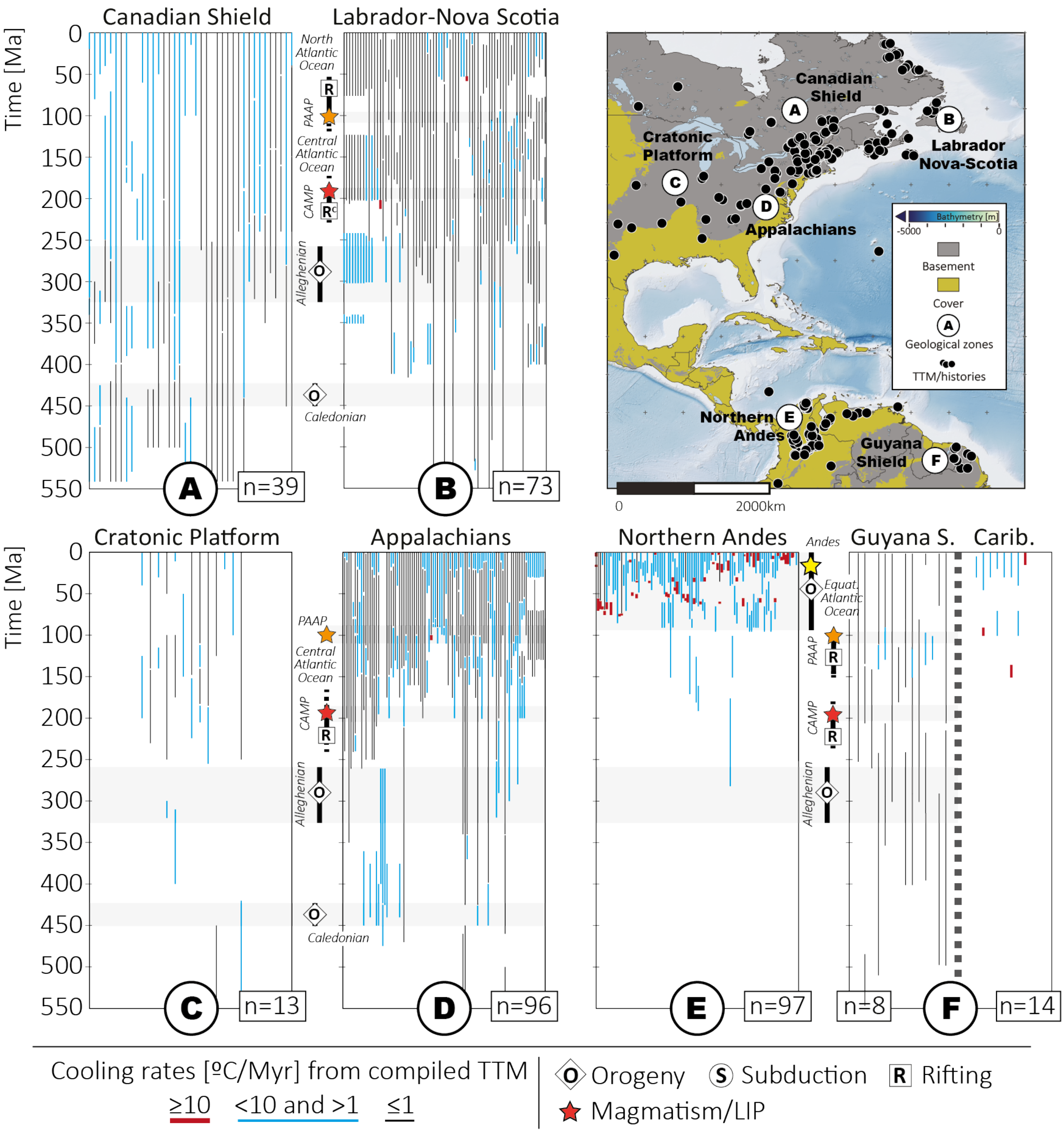

Figure A2 | Time-temperature “cooling events” charts for Eastern North America (A, B, C, and D), Northern South America (E and F). Rates are calculated based on the slope of each cooling event as presented in ***figure A1*** and are arbitrarily colour-coded using 1 and 10°C/Myr as limits. Each model is depicted on one line separated by the other model evenly, depending on the total number of models for each area. Models are organised by ‘Longitude’, from low (left) to high (right), i.e., from W to E. Tectonic events displayed alongside the charts are based on the references listed in the geological setting.

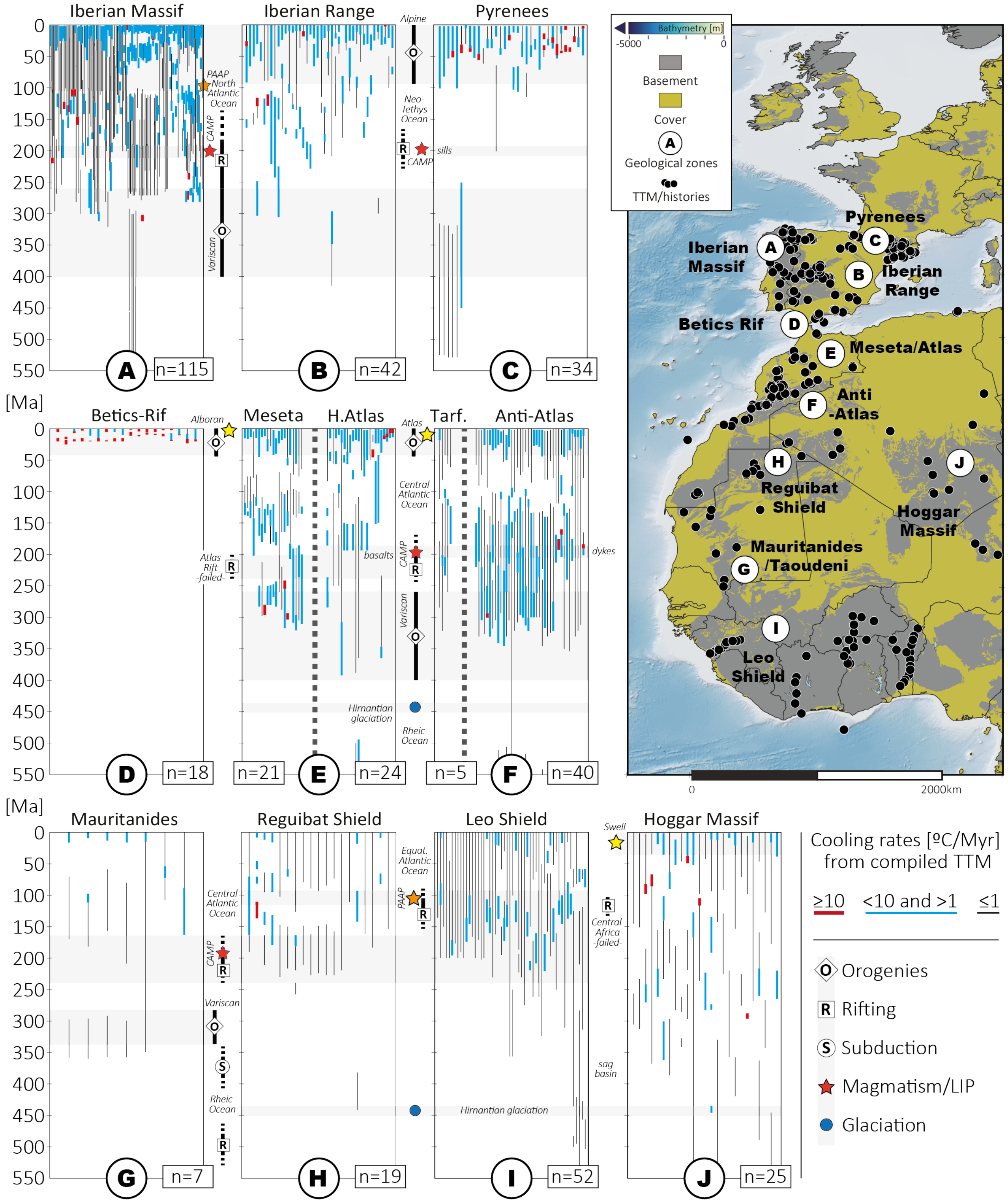

2461
2462 ***Figure A3*** | Time-temperature "cooling events" charts for Iberia (A, B, C, and D) and Northwest
2463 Africa (D, E, F, G, H, I, and J). See caption of ***figure A2*** for details.

Acknowledgments

The authors are deeply thankful to Mohamed Gouiza, Nicolas Pinet, Delphine Rouby, Kerry Gallagher, Francois Sapin, Giovanni Bertotti, and Alexis Derycke for conversations that steered this effort, their comments that improved it, and/or giving us access to material published but not fully available online. The North Africa Research Group (NARG; University of Manchester, UK) is thanked for supporting part of the digitalization of published data.

Publications to add to the text/database

Wildman, M., Brown, R., Ye, J., Chardon, D., Rouby, D., Kouamelan, A.N. and Dall'Asta, M., **2022**. Contrasting thermal evolution of the West African Equatorial and Central Atlantic continental margins. Gondwana Research, 111, pp.249-264. https://doi.org/10.1016/j.gr.2022.08.010

Nicholson, U., Bray, V.J., Gulick, S.P. and Aduomahor, B., **2022**. The Nadir Crater offshore West Africa: A candidate Cretaceous-Paleogene impact structure. Science advances, 8(33), p.eabn3096. https://doi.org/10.1126/sciadv.abn3096

Bryers, O., Bulot, L.G., Duval-Arnould, A., Hollis, C. and Redfern, J., **2022**. Kilometre-scale coral carpets on mixed carbonate-siliciclastic platforms; a sedimentological study from the Lower Cretaceous of northwestern Africa. Palaeogeography, Palaeoclimatology, Palaeoecology, 587, p.110792. https://doi.org/10.1016/j.palaeo.2021.110792

Jess, S., Enkelmann, E. and Matthews, W.A., **2022**. Why are the Appalachians high? New insights from detrital apatite laser ablation (U-Th-Sm)/He dating. Earth and Planetary Science Letters, 597, p.117794. https://doi.org/10.1016/j.epsl.2022.117794

Basler, L.C., Baughman, J.S., Fame, M.L. and Haproff, P.J., **2021**. Spatially variable syn-and post-Alleghanian exhumation of the central Appalachian Mountains from zircon (U-Th)/He thermochronology. Geosphere, 17(4), pp.1151-1169. https://doi.org/10.1130/GES02368.1

Bajolet, F., Chardon, D., Rouby, D., Dall'Asta, M., Loparev, A., Couëffe, R. and Roig, J.Y., **2022**. The sediment routing systems of Northern South America since 250 Ma. Earth-Science Reviews, p.104139. https://doi.org/10.1016/j.earscirev.2022.104139

Jian, H., Nedimović, M.R., Canales, J.P. and Lau, K.H., **2021**. New Insights Into the Rift to Drift Transition Across the Northeastern Nova Scotian Margin From Wide-Angle Seismic Waveform Inversion and Reflection Imaging. Journal of Geophysical Research: Solid Earth, 126(12), p.e2021JB022201. https://doi.org/10.1029/2021JB022201

Guan, H., Geoffroy, L. and Xu, M., **2021**. Magma-assisted fragmentation of Pangea: continental breakup initiation and propagation. Gondwana Research, 96, pp.56-75. https://doi.org/10.1016/j.gr.2021.04.003

Waldner, M., Bellahsen, N., Mouthereau, F., Bernet, M., Pik, R., Rosenberg, C.L. and Balvay, M., **2021**. Central Pyrenees mountain building: Constraints from new LT thermochronological data from the Axial Zone. Tectonics, 40(3), p.e2020TC006614. https://doi.org/10.1029/2020TC006614

Van Staal, C.R., Barr, S.M. and Murphy, J.B., **2012**. Provenance and tectonic evolution of Ganderia: Constraints on the evolution of the Iapetus and Rheic oceans. Geology, 40(11), pp.987-990. https://doi.org/10.1130/G33302.1

van Staal, C.R., Barr, S.M., Percival, J.A., Cook, F.A. and Clowes, R.M., **2012**. Lithospheric architecture and tectonic evolution of the Canadian Appalachians and associated Atlantic margin. Tectonic styles in Canada: The LITHOPROBE perspective: Geological Association of Canada Special Paper, 49, p.55.

van Staal, C.R., Barr, S.M., Waldron, J.W., Schofield, D.I., Zagorevski, A. and White, C.E., **2021**. Provenance and Paleozoic tectonic evolution of Ganderia and its relationships with Avalonia and Megumia in the Appalachian-Caledonide orogen. Gondwana Research, 98, pp.212-243. https://doi.org/10.1016/j.gr.2021.05.025

van Staal, C. and **Zagorevski**, A., **2020**. Accretion, soft and hard collision: Similarities, differences and an application from the Newfoundland Appalachian orogen. Geoscience Canada: Journal of the Geological Association of Canada/Geoscience Canada: journal de l'Association Géologique du Canada, 47(3), pp.103-118. https://doi.org/10.12789/geocanj.2020.47.161